doi : 10.17596/0003688

R/V Mirai Cruise Report
MR01-K02

May 14 – May 28, 2001

Japan Marine Science and Technology Center

(JAMSTEC)

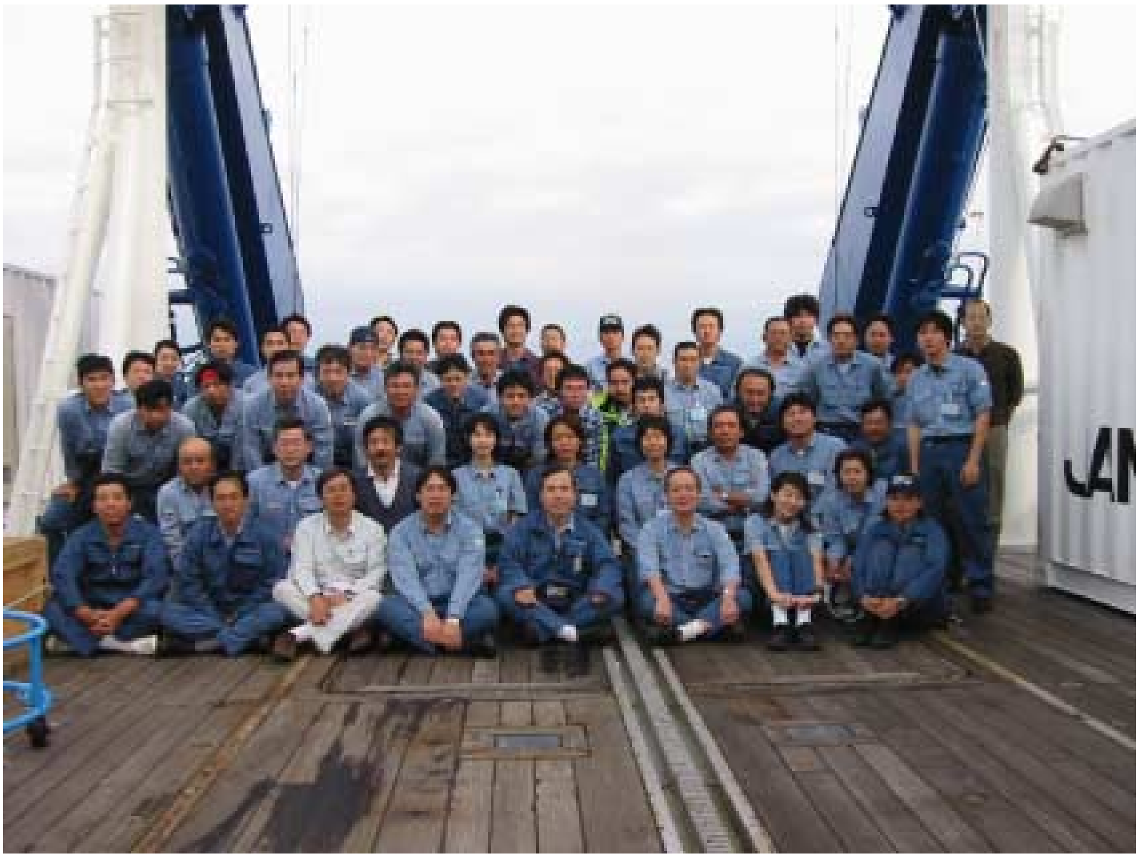

Contents

1．Summary

1. Cruise Title

Research on the Subtropical Gyre and the Subpolar Gyre in the North Pacific Ocean

Cruise code: MR01-K02
Ship: R/V Mirai
Captain: Masaharu Akamine (total 36 crew members)

2. Objectives

The Kuroshio in the western North Pacific is called as the Kuroshio Extension and forms the clear northern boundary of the sub-tropical gyre. The Kuroshio Extension is active and generates cold and warm eddies very frequently. There is a large possibility that these eddies play an important role in the meridional exchange of heat and freshwater across the Kuroshio Extension. But there has been no study to evaluate the role of these eddies. MR01-K02 was planned as one of activities to clarify the physical and dynamical structure of eddies along the Kuroshio Extension. In addition to the physical oceanographic research MR01-K02 was carried out as the joint cruise of variety of adopted subjects, such as the ocean lidar, sediments, and aerosol.

3. Period

From May 14, 2001 (departed Yokosuka, Kanagawa)
Through May 28, 2001(arrived at Sekinehama, Aomori)

4. Chief Scientist of the Cruise

Yasushi Yoshikawa / JAMSTEC

5. Overview

MR01-K02 cruise began on 14 May 2001, as department from the Yokosuka New Port. Cruise track was composed of four sections. The first section was a track from Yokosuka to 32-10N 152-30E. On this section, 41 XBT castings were carried out. Continuous aerosol monitoring by ACE-ASIA Group was also begun. CM-buoy was recovered at 32-09N 152-27E. The second section was from 32-10N 152-30E to 30-00N 146-25E. On the track 27 XBT castings were carried out. The third section was the main section in this cruise. On the meridional section from 30-00N to 38-00N along 146-25E, 28 CTD lowering with LADCP/RMS and 5 XCTD casts were carried out. Deployment of MMP buoy at 33-05N and deployments of two CM buoys at 34-15N and at 35-25N, were also carried out. Sediment was sampled by using piston core sampler at 33-05N. Meteorological observations using radiosonde release were carried out every 12 hours and the aerosol capture balloon was moored on deck. On the forth track from 38N 146-25E to Sekinehama port, 18 XCTD castings were carried out. The cruise was closed on 28th May at Sekinehama port. Though preliminary results will be reported in following sections in detail, here we would like to declare our great success on this cruise.

2．Cruise Track and Log

Cruise Track

R/V Mirai left for Kuroshio Extension area from Yokosuka-shin port in 14 July 2001. After observing and measuring the various parameters, R/V Mirai arrived at Sekinehama port in 28 July 2001. Cruise track of this cruise is shown in Figure 2-1.

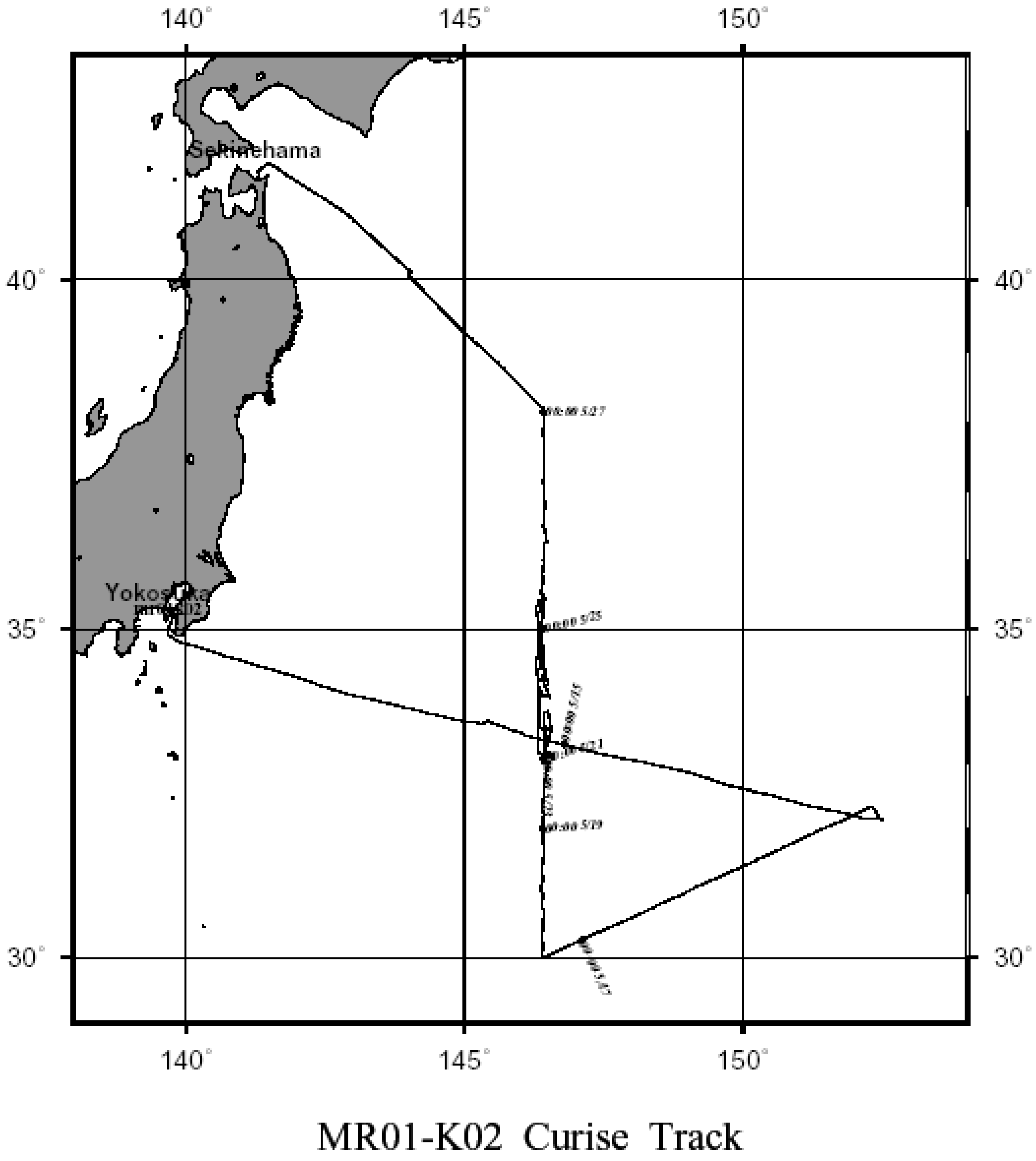

Figure 2-1 MR01-K02 Cruise Track

Cruise Log

(time)	(No.)	(content)

May 14, 2001 (Sunday)

08:45		Departure from Yokosuka-shin Port
11:30-		Start of continuous observation (Shipboard ADCP, Aerosols, pCO2, etc.)
10:30-11:00		Briefing for safety life on the ship
13:15-13:45		Boat Drill
14:00-16:00		Meeting on observations
16:45-17:00		Konpira-san
18:00	001	XBT (34-16.79N, 142-00.35E)
18:43	002	XBT (34-12.73N, 142-14.97E)
19:30		Start of environmental monitoring
19:30	003	XBT (34-08.29N, 142-30.11E)
20:15	004	XBT (34-04.23N, 142-45.07E)
21:01	005	XBT (34-00.81N, 143-00.08E)
21:47	006	XBT (33-58.08N, 143-15.06E)
22:35	007	XBT (33-51.18N, 143-30.08E)
23:23	008	XBT (33-51.91N, 143-45.08E)

May 15, 2001 (Monday)

00:10	009	XBT (33-49.04N, 144-00.09E)
00:58	010	XBT (33-45.77N, 144-15.09E)
01:44	011	XBT (33-42.71N, 144-30.19E)
02:28	012	XBT (33-39.86N, 144-45.10E)
03:11	013	XBT (33-37.41N, 145-00.10E)
03:51	014	XBT (33-35.84N, 145-15.12E)
04:47	015	XBT (33-35.90N, 145-30.11E)
05:35	016	XBT (33-31.27N, 145-45.20E)
06:23	017	XBT (33-26.96N, 145-59.96E)
07:14	018	XBT (33-22.64N, 146-15.11E)
08:03	019	XBT (33-19.34N, 146-30.03E)
08:52	020	XBT (33-16.90N, 146-45.04E)
09:41	021	XBT (33-13.81N, 147-00.05E)
10:29	022	XBT (33-10.75N, 147-15.03E)
11:16	023	XBT (33-07.65N, 147-29.99E)
12:02	024	XBT (33-04.92N, 147-45.16E)
12:48	025	XBT (33-02.56N, 148-00.00E)
13:35	026	XBT (32-59.98N, 148-15.01E)
14:24	027	XBT (32-57.14N, 148-30.00E)
15:15	028	XBT (32-54.25N, 148-45.01E)
16:07	029	XBT (32-51.35N, 149-00.05E)

17:01	030	XBT (32-47.72N, 149-15.02E)
17:54	031	XBT (32-43.42N, 149-30.02E)
18:50	032	XBT (32-39.29N, 149-45.04E)
19:43	033	XBT (32-36.31N, 150-00.04E)
20:36	034	XBT (32-33.06N, 150-15.05E)
21:30	035	XBT (32-30.13N, 150-30.04E)
22:25	036	XBT (32-33.09N, 150-45.01E)
23:20	037	XBT (32-23.28N, 151-00.01E)

May 16, 2001 (Wednesday)

00:15	038	XBT (32-20.11N, 151-15.04E)
01:07	039	XBT (32-17.57N, 151-30.04E)
01:59	040	XBT (32-14.83N, 151-45.04E)
02:52	041	XBT (32-11.46N, 152-00.03E)
04:00-07:30	042	Recovery ADCP buoy (32-09N, 152-27E)
10:35-12:20	043	CTD and water sampling (32-09N, 152-27E) 2000m
12:25	044	XBT (32-09.02N, 152-27.14E)
13:35	045	XBT (32-18.83N, 152-14.93E)
14:31	046	XBT (32-12.61N, 152-00.01E)
15:27	047	XBT (32-06.37N, 151-44.92E)
16:21	048	XBT (32-01.13N, 151-30.04E)
17:18	049	XBT (31-54.86N, 151-15.04E)
18:15	050	XBT (31-48.94N, 150-59.99E)
19:09	051	XBT (31-42.97N, 150-45.06E)
20:04	052	XBT (31-36.78N, 150-30.02E)
20:59	053	XBT (31-30.87N, 150-14.99E)
21:54	054	XBT (31-24.82N, 150-00.00E)
22:49	055	XBT (31-19.30N, 149-45.01E)
23:46	056	XBT (31-13.21N, 149-29.99E)

May 17, 2001 (Thursday)

00:42	057	XBT (31-07.88N, 149-15.01E)
01:40	058	XBT (31-01.36N, 149-00.02E)
02:38	059	XBT (30-55.13N, 148-45.01E)
03:36	060	XBT (30-49.30N, 148-30.01E)
04:35	061	XBT (30-43.00N, 148-15.01E)
05:36	062	XBT (30-37.16N, 148-00.00E)
06:35	063	XBT (30-31.47N, 147-44.99E)
07:32	064	XBT (30-25.87N, 147-29.97E)
08:30	065	XBT (30-20.03N, 147-14.99E)
09:28	066	XBT (30-14.20N, 146-59.99E)
10:26	067	XBT (30-07.94N, 146-45.03E)
11:23	068	XBT (30-01.72N, 146-30.02E)

12:02-12:18		Ocean Lidar
13:45-17:51	069	CTD, LADCP,WS(29-59.77N, 146-24.87E, 6070m)
19:23-23:06	070	CTD, LADCP,WS(30-14.72N, 146-24.34E, 5948m)
20:43	RS1712	Radiosonde released (30-14.18N, 146-23.79E)

May 18, 2001 (Friday)

00:58-05:07	071	CTD, LADCP,WS(30-30.43N, 146-25.02E, 6155m)
06:48-10:28	072	CTD, LADCP,WS(30-44.63N, 146-25.00E, ??m)
07:49-08:12		Captine Balloon (Kytoon)
08:31	RS1800	Radiosonde released (30-44.85N, 146-24.90E)
08:34-09:11		Captine Balloon (Kytoon)(30-44.86E, 146-24.90E, 600m)
09:22-0950		Captine Balloon(30-44.79E, 146-24.55E, 560m)
12:08-15:59	073	CTD, LADCP,WS(31-00.08N, 146-24.76E, 6158m)
12:42-13:13		Captine Balloon (Kytoon)(31-00.08N, 146-24.25E, 600m)
13:22-1400		Captine Balloon (Kytoon)(31-00.13N, 146-24.22E, 600m)
17:33-21:23	074	CTD, LADCP,WS(31-15.02N, 146-24.76E, 6078m)
20:27	RS1812	Radiosonde released (31-16.25N, 146-23.59E)
22:29-02:02	075	CTD, LADCP,WS(31-29.82N, 146-25.00E, 6091m)

May 19, 2001 (Saturday)

03:22-07:02	076	CTD, LADCP,WS(31-45.24N, 146-24.96E, 6180m)
05:04-06:15		Captine Balloon (Kytoon)(31-45.25N, 146-24.60E, 600m)
08:25-12:07	077	CTD, LADCP,WS(32-00.08N, 146-24.83E, 6014m)
08:33	RS1900	Radiosonde released (32-00.07N, 146-24.82E)
08:41-09:33		Captine Balloon (Kytoon)(31-59.98N, 146-24.55E, 1000m)
09:43-10:36		Captine Balloon (Kytoon)(31-59.76N, 146-24.55E, 1000m)
13:29-13:47		Ocean Lidar (32-14.91N, 146-24.87E, 100m)
14:07-17:53	078	CTD, LADCP,WS(32-14.96N, 146-24.63E, 5987m)
14:23-14:52		Captine Balloon (Kytoon)(32-14.88N, 146-24.17E, 1000m)
15:10-16:19		Captine Balloon (Kytoon)(32-15.23N, 146-23.96E, 1000m)
19:04-22:32	079	CTD, LADCP,WS(32-29.99N, 146-24.95E, 5884m)
	RS1912	Radiosonde released (32-30.35N, 146-24.29E)
23:47-03:14	080	CTD, LADCP,WS(32-44.91N, 146-24.98E, 5820m)

May 20, 2001 (Sunday)

04:35-08:04	081	CTD, LADCP,WS(33-00.04N, 146-29.10E, 5792m)
05:35-06:24		Captine Balloon (Kytoon)(32-59.91N, 146-30.56E, 800m)
06:30-07:24		Captine Balloon (Kytoon)(32-59.87N, 146-30.81E, 1000m)
08:35	RS2000	Radiosonde released (32-59.92N, 146-27.04E)
10:11-13:46	082	CTD, LADCP,WS(33-15.00N, 146-25.26E, 5778m)
10:26-11:15		Captine Balloon (Kytoon)(33-15.19N, 146-26.53E, 1000m)
11:21-12:16		Captine Balloon (Kytoon)(33-15.24N, 146-27.34E, 1000m)

15:06-15:25 Ocean Lidar(33-30.20N, 146-26.45E, 100m)
16:01-19:45 083 CTD, LADCP,WS(33-30.14N, 146-26.45E, 5851m)
RS2012 Radiosonde released (33-31.93N, 146-24.54E)

May 21, 2001 (Monday)

05:08-09:33 084 Sediment Sampling by Piston corer (33-05.00N, 146-24.97E, 5746m)
08:23 RS2100 Radiosonde released (33-05.01N, 146-25.02E)
12:11-14:24 085 Current Meter Buoy deployment (but, recovered tomorrow)
14:24 (let go sinker: 33-05.03N, 146-25.39E, 5755m)
18:40-22:18 086 CTD, LADCP,WS(33-44.80N, 146-25.52E, 5821m)
RS2112 Radiosonde released (33-45.48N, 146-28.01E)

May 22, 2001 (Tuesday)

05:14-08:09 087 Current Meter Buoy recovery (33-05.27N, 146-27.16E)
08:30 RS2200 Radiosonde released (33-07.13N, 146-29.09E)
12:12-14:25 088 Current Meter Buoy 're-'deployment
14:25 (let go sinker 33-05.49N, 146-26.90E, 5754m)
20:30 RS2212 Radiosonde released (34-16.06N, 146-21.45E)
19:16-22:26 Seabeam

May 23, 2001 (Wednesday)

05:40-07:43 089 ADCP buoy deployment
07:43 (let go sinker 34-15.36N, 146-27.04E, 5906m)
RS2300 Radiosonde released (34-24.51N, 146-23.94E)
14:00-15:50 090 ADCP buoy deployment
15:50 (let go sinker 35-24.69N, 146-26.74E, 5893m)
16:05 RS2306 Radiosonde released (35-25.18N, 146-24.85E)
16:48 RS2307 Radiosonde released (35-21.00N, 146-18.14E)
20:30 RS2312 Radiosonde released (34-41.19N, 146-18.05E)
23:28-23:47 091 test: CTD (34-00.33N, 146-25.54E, 200m)

May 24, 2001 (Thursday)

08:27 RS2400 Radiosonde released (34-00.56N, 146-25.24E)
11:50-15:23 092 CTD, LADCP,WS(34-00.43N, 146-25.56E, 5928m)
16:30-20:23 093 CTD, LADCP,WS(34-14.67N, 146-25.20E, 5983m)
20:33 RS2412 Radiosonde released (34-16.70N, 146-26.77E)
21:37-00:55 094 CTD, LADCP,WS(34-30.22N, 146-25.44E, 5916m)

May 25, 2001 (Friday)

02:02-05:51 095 CTD, LADCP,WS(34-45.37N, 146-24.78E, 5516m)

06:52-07:59	096*	CTD, LADCP,WS(35-00.03N, 146-24.61E, ??m), trouble
08:29	RS2500	Radiosonde released (35-00.97N, 146-22.59E)
11:04-14:54	096	CTD, LADCP,WS(35-00.56N, 146-23.94E, 5907m)
16:17-20:15	098	CTD, LADCP,WS(35-14.83N, 146-24.91E, 6020m)
20:29	RS2512	Radiosonde released (35-16.12N, 146-21.47E)
21:38-01:12	099	CTD, LADCP,WS(35-29.89N, 146-24.78E, 5972m)

May 26, 2001 (Saturday)

02:30-06:00	100	CTD, LADCP,WS(35-45.12N, 146-25.00E, 5882m)
07:18-10:48	101	CTD, LADCP,WS(35-59.62N, 146-24.79E, 5675m)
08:14-09:03		Captine Balloon (Kytoon)(35-59.40N, 146-25.45E, 1000m)
09:11-09:58		Captine Balloon (Kytoon)(35-59.35N, 146-25.47E, 1000m)
09:15	RS2600	Radiosonde released (35-59.36N, 146-25.49E)
10:04-10:15		Captine Balloon (Kytoon)(??N, ??E, 200m)
12:04-15:45	102	CTD, LADCP,WS(36-14.94N, 146-25.24E, 5627m)
18:44-22:30	103	CTD(Large), LADCP,WS(36-29.96N, 146-25.29E, 5662m)
20:35	RS2612	Radiosonde released (36-30.31N, 146-26.00E)
23:38-03:07	104	CTD(Large), LADCP,WS(36-44.83N, 146-25.33E, 5623m)

May 27, 2001 (Sunday)

04:31	105	XCTD (37-03.50N, 146-25.12E)
05:18	106	XCTD (37-15.05N, 146-24.99E)
06:19	107	XCTD (37-30.32N, 146-25.13E)
07:18	108	XCTD (37-45.00N, 146-24.96E)
08:23	109	XCTD (38-00.00N, 146-24.96E)
09:12	110	XCTD (38-10.35N, 146-24.93E)
09:29	111	XCTD (38-13.79N, 146-21.56E)
10:29	112	XCTD (38-25.27N, 146-06.73E)
11:29	113	XCTD (38-36.84N, 145-52.11E)
12:30	114	XCTD (38-47.21N, 145-38.98E)
13:30	115	XCTD (38-56.71N, 145-26.64E)
14:30	116	XCTD (39-05.96N, 145-13.85E)
15:30	117	XCTD (39-15.20N, 145-00.50E)
16:30	118	XCTD (39-24.58N, 144-47.34E)
17:40	119	XCTD (39-36.40N, 144-32.75E)
18:30	120	XCTD (39-44.22N, 144-23.21E)
19:30	121	XCTD (39-54.09N, 144-11.48E)
20:30	122	XCTD (40-03.68N, 144-00.66E)
21:30	123	XCTD (40-10.75N, 143-55.06E)
22:30	124	XCTD (40-19.97N, 143-41.35E)
23:30	125	XCTD (40-29.12N, 143-28.18E)

May 28, 2001 (Monday)

00:30	126	XCTD (40-38.32N, 143-15.49E)
01:30	127	XCTD (40-47.39N, 143-02.77E)
12:00		Arrival at Sekinehama

3．Participants List

R/V Mirai Scientists and Technical Staff during MR01-K02

Yasushi YOSHIKAWA	Chief Scientist	Ocean Observation and Research Department, JAMSTEC
Hirofumi YAMAMOTO	Scientist	Ocean Observation and Research Department, JAMSTEC
Takaki HATAYAMA	Scientist	Ocean Observation and Research Department, JAMSTEC
Humio MITSUDERA	Scientist	International Pacific Research Center
Akihiko MURATA	Scientist	Ocean Observation and Research Department, JAMSTEC
Takeshi KAWANO	Scientist	Ocean Observation and Research Department, JAMSTEC
Toshiya KANAMATSU	Scientist	Deep Sea Research Department, JAMSTEC
Nobuo SUGIMOTO	Scientist	National Institute of Environmental Studies
Ichiro MATSUI	Scientist	National Institute of Environmental Studies
Kazuhiko MIURA	Scientist	Science University of Tokyo
Takahito INABA	Scientist	Science University of Tokyo
Ryo ASHIKAWA	Scientist	Science University of Tokyo
Yuji FUJITANI	Scientist	Hokkaido University
Ippei NAGAO	Scientist	Nagoya University
Akihide KAMEI	Scientist	Communications Research Laboratory
Shungo KATO	Scientist	Research Center for Advanced Science and Technology, The University of Tokyo
Kazutake OHTA	Scientist	Ocean Research Institute, The University of Tokyo / Japan Science and Technology Corporation
Atsushi OOKI	Scientist	Ocean Research Institute, The University of Tokyo
Sou MATSUNAGA	Scientist	Hokkaido University
Takeo MATSUMOTO	Technical Staff	Marine Works Japan LTD.
Hiroshi MATSUNAGA	Technical Staff	Marine Works Japan LTD.
Kentaro HONDA	Technical Staff	Marine Works Japan LTD.
Naoko TAKAHASHI	Technical Staff	Marine Works Japan LTD.
Katsunori SAGISHIMA	Technical Staff	Marine Works Japan LTD.
Ai YASUDA	Technical Staff	Marine Works Japan LTD.
Taeko OHAMA	Technical Staff	Marine Works Japan LTD.
Kaori AKIZAWA	Technical Staff	Marine Works Japan LTD.
Yuichi SONOYAMA	Technical Staff	Marine Works Japan LTD.
Asako KUBO	Technical Staff	Marine Works Japan LTD.
Soichi MORIYA	Technical Staff	Marine Works Japan LTD.
Hiroaki MURAKI	Technical Staff	Marine Works Japan LTD.
Yutaka MATSUURA	Technical Staff	Marine Works Japan LTD.
Makoto SHIMOKAWARA	Technical Staff	Marine Works Japan LTD.
Masumi ISHIMORI	Technical Staff	Marine Works Japan LTD.
Masaki HANYU	Technical Staff	Global Ocean Development Inc.
Akinori UCHIYAMA	Technical Staff	Global Ocean Development Inc.
Shinya IWAMIDA	Technical Staff	Global Ocean Development Inc.
Shinichi KANEKO	Technical Staff	Marine Works Japan LTD.
Daisuke TERADA	Technical Staff	Marine Works Japan LTD.

Yuko ONO	Technical Staff	Marine Works Japan LTD.
Tokiko TAKABAYASHI	Technical Staff	Marine Works Japan LTD.

R/V Mirai Crew Members during MR01-K02

氏名	職名	Name	Rank
赤嶺　正治	船　長	Masaharu Akamine	Master
堂脇　幸男	一航士	Yukio Dowaki	Chief Officer
柴田　雄治	次一航	Yuji Shibata	1st Officer
丸山　博記	二航士	Hiroki Maruyama	2nd Officer
浅沼　充信	三航士	Mitsunobu Asanuma	3rd Officer
渡邉　陽一郎	機関長	Youichiro Watanabe	Chief Engineer
大野　晃照	一機士	Akiteru Ono	1st Engineer
鳴海　弘晃	二機士	Hiroaki Narumi	2nd Engineer
番匠　克己	三機士	Katsumi Bansho	3rd Engineer
東　興一	員外機機関士	Koichi Higashi	Engineer
宍戸　啓一郎	通信長	Keiichiro Shishido	C. R. Officer
森岡　直人	二通士	Naoto Morioka	2nd R. Officer
木下　洋一	甲板長	Hirokazu Kinoshita	Able Seaman
成尾　久司	甲板手	Hisashi Naruo	Able Seaman
山本　保行	甲板手	Yasuyuki Yamamoto	Able Seaman
川田　誠一郎	甲板手	Seiichiro Kawata	Able Seaman
表　国比己	甲板手	Kunihiko Omote	Able Seaman
堀田　一徳	甲板手	Kazunori Horita	Able Seaman
小国　久夫	甲板手	Hisao Oguni	Able Seaman
井上　祐治	甲板手	Yuji Inoue	Able Seaman
鈴木　勝	甲板手	Masaru Suzuki	Able Seaman
佐藤　剛	甲板手	Tsuyoshi Sato	Able Seaman
山本　伸海	甲板手	Nobuhiro Yamamoto	Able Seaman
岡田　雅重	甲板手	Masashige Okada	Able Seaman
本田　貞儀	操機長	Sadanori Honda	No.1 Oiler
吉川　利三	操機手	Toshimi Yoshikawa	Oiler
堀内　幸利	操機手	Yukitoshi Horiuchi	Oiler
井上　二三男	操機手	Fumio Inoue	Oiler
宮崎　隆	操機手	Takashi Miyazaki	Oiler
山下　一美	操機手	Kazumi Yamashita	Oiler
栗田　保隆	司厨長	Yasutaka Kurita	Chief Steward
秋田　天行	司厨手	Takayuki Akita	Cook
平石　初次	司厨手	Hatsuji Hiraishi	Cook
濱邊　竜弥	司厨手	Tatsuya Hamabe	Cook
大田　仁志	司厨手	Hitoshi Ota	Cook
吉澤　裕之	司厨手	Hiroyuki Yoshizawa	Cook

4．General Observations

4.1 Surface meteorological observation

(1) Personnel

Yasushi Yoshikawa (JAMSTEC): Principal Investigator
Kunio Yoneyama (JAMSTEC): (Shore-side participant)
Masaki Hanyu (GODI): Operation Leader
Shinya Iwamida (GODI)

(2) Objective

The surface meteorological parameters are observed as a basic dataset of the meteorology. These parameters bring us the information about temporal variation of the meteorological condition surrounding the ship.

(3) Methods

The surface meteorological parameters were observed throughout MR01-K02 cruise from the departure of Yokosuka on 14 May 2001 to the arrival of Sekinehama on 28 May 2001.

This cruise, we used 2 systems for the surface meteorological observation.

1. Mirai meteorological observation system
2. Shipboard Oceanographic and Atmospheric Radiation (SOAR) system

(3-1) Mirai meteorological observation system

Instruments of Mirai met system are listed in Table 4.1-1 and measured parameters are listed in Table 4.1-2. Data was collected and processed by KOAC-7800 weather data processor made by Koshin Denki, Japan. The data set has 6-second averaged every 6-second record and 10-minute averaged every 10-minute record.

Table 4.1-1: Instruments and their installation locations of Mirai met system

Sensors	Type	Manufacturer	Location (altitude from baseline)
Anemometer	KE-500	Koshin Denki, Japan	foremast (30m)
Thermometer	FT	Koshin Denki, Japan	compass deck (27m)
dewpoint meter	DW-1	Koshin Denki, Japan	compass deck (27m)
Barometer	F451	Yokogawa, Japan	weather observation room captain deck (20m)
rain gauge	50202	R. M. Young, USA	compass deck (25m)
optical rain gauge	ORG-115DR	SCTI, USA	compass deck (25m)
radiometer (short wave)	MS-801	Eiko Seiki, Japan	radar mast (33m)
radiometer (long wave)	MS-200	Eiko Seiki, Japan	radar mast (33m)
wave height meter	MW-2	Tsurumi-seiki, Japan	Bow (16m)

Table 4.1-2: Parameters of Mirai meteorological observation system

	Parameters	units	Remarks
1	Latitude	degree	
2	Longitude	degree	
3	Ship's speed	knot	Mirai log

4	Ship's heading	degree	Mirai gyro
5	relative wind speed	m/s	6 sec. / 10 min. averaged
6	relative wind direction	degree	6 sec. / 10 min. averaged
7	True wind speed	m/s	6 sec. / 10 min. averaged
8	True wind direction	degree	6 sec. / 10 min. averaged
9	barometric pressure	hPa	adjusted to the sea surface level 6 sec. / 10 min. averaged
10	air temperature (starboard side)	degC	6 sec. / 10 min. averaged
11	air temperature (port side)	degC	6 sec. / 10 min. averaged
12	dewpoint temperature (stbd side)	degC	6 sec. / 10 min. averaged
13	dewpoint temperature (port side)	degC	6 sec. / 10 min. averaged
14	relative humidity (starboard side)	%	6 sec. / 10 min. averaged
15	relative humidity (port side)	%	6 sec. / 10 min. averaged
16	Rain rate (optical rain gauge)	mm/hr	6 sec. / 10 min. averaged
17	Rain rate (capacitive rain gauge)	mm/hr	6 sec. / 10 min. averaged
18	down welling shortwave radiometer	W/m^2	6 sec. / 10 min. averaged
19	down welling infra-red radiometer	W/m^2	6 sec. / 10 min. averaged
20	sea surface temperature	degC	-5m
21	significant wave height (fore)	m	3 hourly
22	significant wave height (aft)	m	3 hourly
23	significant wave period (fore)	second	3 hourly
24	significant wave period (aft)	second	3 hourly

(3-2) Shipboard Oceanographic and Atmospheric Radiation (SOAR) system

SOAR system, designed by BNL (Brookhaven National Laboratory, USA), is consisted of 3 parts.

1. Portable Radiation Package (PRP) designed by BNL – short and long wave down welling radiation
2. Zeno meteorological system designed by BNL – wind, Tair/RH, pressure and rainfall measurement
3. Scientific Computer System (SCS) designed by NOAA (National Oceanographic and Atmospheric Administration, USA) – centralized data acquisition and logging of all data sets

SCS recorded PRP data every 6.5 seconds, Zeno/met data every 10 seconds.

Instruments and their locations are listed in Table 4.1-3 and measured parameters are listed in Table 4.1-4

Table 4.1-3: Instrument installation locations of SOAR system

Sensors	type	manufacturer	location (altitude from the baseline)
Zeno/Met			
Anemometer	05106	R. M. Young, USA	foremast (31m)
T/RH	HMP45A	Vaisala, USA	foremast (30m)
	with 43408 Gill aspirated radiation shield (R. M. Young)		
Barometer	61201	R. M. Young, USA	foremast (30m)
	with 61002 Gill pressure port (R. M. Young)		
Rain gauge	50202	R. M. Young, USA	foremast (30m)

Optical rain gauge	ORG-115DA	ScTi, USA	foremast (30m)
PRP			
Radiometer (short wave)	PSP	Eppley labs, USA	foremast (31m)
Radiometer (long wave)	PIR	Eppley labs, USA	foremast (31m)
Fast rotating shadowband radiometer		Yankee, USA	foremast (31m)

Table 4.1-4: Parameters of SOAR System

	Parameters	units	remarks
1	Latitude	degree	
2	Longitude	degree	
3	Sog	knot	
4	Cog	degree	
5	relative wind speed	m/s	
6	relative wind direction	degree	
7	barometric pressure	hPa	
8	Air temperature	degC	
9	relative humidity	%	
10	Rain rate (optical rain gauge)	mm/hr	
11	precipitation (capacitive rain gauge)	mm	reset at 50mm
12	down welling shortwave radiation	W/m^2	
13	down welling infra-red radiation	W/m^2	
14	defuse irradiation	W/m^2	

(4) Preliminary results

Wind (converted to U, V component, from SOAR), Tair (from SOAR) / SST (from EPCS), RH (from SOAR) / precipitation (from SOAR), solar radiation (from SOAR) and pressure (from Mirai/met) observed during the cruise are shown in Figure 4.1-1 and Figure 4.1-2. In the figures, accumulated precipitation data from SOAR capacitive rain gauge was converted to the precipitation amount in every minute and obvious noises were eliminated but not calibrated. Other figures are showing uncorrected data.

(5) Data archives

These raw data will be submitted to the Data Management Office (DMO) in JAMSTEC just after the cruise.

4.2 Ceilometer

(1) Personnel

Yasushi Yoshikawa (JAMSTEC):	Principal Investigator
Kunio Yoneyama (JAMSTEC):	(Shore-side participant)
Masaki Hanyu (GODI):	Operation Leader
Shinya Iwamida (GODI)	

(2) Objective

The information of the cloud base height and the liquid water amount around cloud base is important to understand the processes on the formation of the cloud. As one of the methods to measure them, the ceilometer observation was carried out.

(3) Methods

We measured cloud base height and backscatter profiles using CT-25K ceilometer (Vaisala, Finland) throughout MR01-K02 cruise from the departure of Yokosuka on 14th May to the arrival of Sekienehama on 28th May 2001.

Major parameters for the measurement configuration are as follows;

Laser source:	Indium Gallium Arsenide (InGaAs) Diode Laser
Transmitting wave length:	905 +/- 5 nm at 25 deg-C
Transmitting average power:	8.9 mW
Repetition rate:	5.57 kHz
Detector:	Silicon avalanche photodiode (APD)
	Responsibility at 905 nm: 65 A/W
Measurement range:	0 – 7.5 km
Resolution:	50 ft in full range
Sampling rate:	60 sec.

On the archived dataset, cloud base height and backscatter profile are recorded with the resolution of 30 m (100 ft).

(4) Preliminary results

The first, second and third lowest cloud base height which the ceilometer detected during the cruise are plotted in Fig. 4.2-1. Sometimes the ceilometer records calculated vertical visibility and the height of detected highest signal instead of the cloud base heights. But they are not plotted in the figure.

(5) Data archives

These raw data will be submitted to the Data Management Office (DMO) in JAMSTEC just after the cruise.

4.3 Surface temperature and salinity

(1) Personnel

Katsunori Sagishima	(MWJ) :Operation Leader
Kahori Akizawa	(MWJ)
Soichi Moriya	(MWJ)

(2) Objective

To monitor continuously the physical, chemical and biological characteristics of near-sea surface water.

(3) Methods

The *Continuous Sea Surface Water Monitoring System* (Nippon Kaiyo co., Ltd.) is located in the "*sea surface monitoring laboratory*" on R/V Mirai. It can automatically measure temperature, salinity, dissolved oxygen, fluorescence and particle size of plankton in the near-surface water every one- minute. Measured data are saved every one-minute together with time and the position of ship, and displayed in the data management PC machine. This system is connected to shipboard LAN-system and provides the acquired data for p-CO_2 measurement system, etc.

The uncontaminated seawater intake is 4.5m below the sea surface. Near-surface water was continuously pumped up about 200L/min from the intake to the laboratory and then flowed into *the Continuous Sea Surface Water Monitoring System* and p-CO_2 measurement system etc. through a steel pipe. The flow rate of surface water for this system was 12L/min, which controlled by some valves and passed through some sensors except with fluorometer (about 0.3L/min) through vinyl-chloride pipes.

The Continuous Sea Surface Water Monitoring System has six kinds of sensors, which TSG comprises of two SBE sensor modules. Sea surface temperature is measured by a ship bottom oceanographic thermometer situated on the suction side of the uncontaminated seawater supply in the forward hold. Specification and calibration date of the each sensor in this system of listed below.

a-1) Temperature and salinity sensors

SEACAT THERMOSALINOGRAPH

Model:	SBE-21, SEA-BIRD ELECTRONICS, INC.	
Serial number:	2118859-2641	
Measurement range:	Temperature -5 to +35 deg-C,	Salinity 0 to 6.5 S/m
Accuracy:	Temperature 0.01 deg-C/6month,	Salinity 0.001 S/m/month
Resolution:	Temperature 0.001 deg-C,	Salinity 0.0001 S/m
Calibration date:	09-Jan-01 (mounted on 27-Apr.-01 in this system)	

a-2) Ship bottom oceanographic thermometer (mounted at the back of the pump for surface water)

Model:	SBE 3S-A, SEA-BIRD ELECTRONICS, INC.
Serial number:	032175
Measurement range:	-5 to +35 deg-C
Initial Accuracy:	0.001 deg-C per year typical
Stability:	0.002 deg-C per year typical
Calibration date:	11-Jan.-01 (mounted on 27-Apr.-01 in this system)

b) Dissolved oxygen sensor

Model:	2127A, Oubisufair Laboratories Japan INC.
Serial number:	
Measurement range:	0 to 14 ppm
Accuracy:	±1% at 5 deg-C of correction range
Stability:	1% per month
Calibration date:	14-May-01

c) Fluorometer

Model:	10-AU-005, TURNER DESIGNS
Detection limit:	5 ppt or less for chlorophyll a
Stability:	0.5% per month of full scale

d) Particle size sensor

Model:	P-05, Nippon Kaiyo LTD.
Serial number:	P5024
Accuracy:	±10% of range
Measurement range:	0.02681mm to 6.666mm
Reproducibility:	±5%
Stability:	5% per week

e) Flowmeter

Model:	EMARG2W, Aichi Watch Electronics LTD.
Serial number:	8672
Measurement range:	0 to 30 L/min
Accuracy:	±1%
Stability:	±1% per day

The monitoring periods (UTC) during this cruise are listed below.

14-May.-‘01 11:00 to 27-May-‘01 23:27 (From Tokyo Bay to Sekinehama)

(4) Preliminary Result

(4-1) Salinity sensor

We cleaned the conductivity cell at Yokosuka port just before this cruise. We sampled every two days for salinity validation and in situ salinity calibration during this cruise. All salinity samples were collected from the course of the system while on station or from regions with weak horizontal gradients. All samples were analyzed on the Guildline 8400B.

The results were shown in Figure 4.3.-1.

(4-2) Dissolved Oxygen (D.O.) sensor

D.O. sensor of this system was calibrated before this cruise. To estimate of accuracy of the sensor, we collected the samples from the course of the system and analyzed by Winkler method. The standardization and pure water blank determination have been performed before the sample titration.

The results were shown in Figure 4.3-2. Precision of the sensor was different from the concentration and each calibration.

(5) Result

Preliminary data 10 minutes from Yokosuka port to Sekinehama. These data were compared with three part of YOKOSUKA (32-09.0N, 152-19.5E) to (29.60.0N, 146-24.3E), (29.60.0N, 146-24.3E) to (32-09N, 152-19.5E) to Sekinehama (shown in Fig. 4.3-3, Fig. 4.3-4, Fig. 4.3-5) . All salinity and dissolved oxygen data were not corrected.

(6) Note

We failed to input the calibration coefficient of Temperature sensor (SBE21). We corrected the Salinity value after this cruise.

(7) Other remarks

1. Equation was to obtain values of temperature (IPTS-68) converted into ITS-90 as follows.

$$T_{90} = 0.99976 * T_{68}$$

(8) Data archive

Format of raw data files was ASCII, calibration values of salinity and temperature (IPTS-68, ITS-90) were Microsoft excel files and ASCII format files, were stored on a magnetic optical disk (M.O.disk). All the data will be submitted to the DMO at JAMSTEC.

4.4 Shipboard ADCP

(1) Personnel

Yasushi Yoshikawa (JAMSTEC):	Principal Investigator
Masaki Hanyu (GODI):	Operation Leader
Shinya Iwamida (GODI)	

(2) Objective

The ocean current profiles are measured for the use of large fields of oceanography, as the basic dataset.

(3) Methods

We measured current profiles by VM-75 (RD Instruments Inc. U.S.A.) shipboard ADCP (Acoustic Doppler Current Profiler) throughout MR01-K02 cruise from departure of Yokosuka on 14th May to the arrival of Sekienehama on 28th May 2001. The E-W (East-West) and N-S (North-South) velocity components of each depth cell [cm/s], and echo intensity of each cell [dB] are measured.

Major parameters and the direct command setting for the measurement are as follows;

Frequency:	75kHz
Averaging:	every 300 sec.
Depth cell length:	800cm
Number of depth cells:	80
Ping per ADCP raw data:	60

Bottom track:

BAnnn	N/A
BCnnn	N/A
BDnnn	N/A
BEnnnn	N/A
BFnnnnn	N/A
BGnnn	N/A
BKn	N/A
BLmmm,nnnn,ffff	N/A
BMn	N/A
BPnnn	BP000
BRn	N/A
BXnnnn	N/A
BZnnn	N/A

Control:

CBnnn	default (411)
CFnnnnn	default (11010)
CGn	default (0)
CLn	default (1)
CPnnn	default (255)
CQnnn	default (8)
CTn	default (0)
CXn	default (0)

Environmental sensor:

EA+/-nnnnn	EA4500
EB+/-nnnnn	default (+0)
ECnnnn	default (1500)
EDnnnn	ED0065
EHnnnnn	default (0)
EP+/-nnnn	default (+0)

ER+/-nnnn	default (+0)
ESnn	ES35
ET+/-nnnn	default (+2500)
EXnnnnn	EX11000
EZnnnnnnn	EZ1020001
Performance and testing:	
PDnnn	default (0)
PInnnnnn	default (011111)
Speed log:	
SDa...r	SD1111111111111111
Timing:	
TEhhmmssff	default (00000000)
TPmmssff	TP000200
Water-track:	
WAnnn	default (255)
WBn	default (0)
WCnnn	default (64)
WDnnn nnn nnn	WD111111111
WEnnnn	WE5000
WFnnnn	WF800
WGnnn	WG001
WHnnn nnn nnn	default (111 100 000)
WIn	default (0)
WJn	default (1)
WLsss,eee	default (0,5)
WMn	WM1
WNnnn	WN080
WPnnnnn	WP00060
WQn	default (0)
WRnnn	default (12)
WSnnnn	WS0800
WTnnn	default (0)
WVnnn	WV999
WWnnn	default (4)
WXnnn	default (999)
WZnnn	default (10)

(4) Data archives

These raw data will be submitted to the Data Management Office (DMO) in JAMSTEC just after the cruise.

4.5 Geophysical Survey

(1) Personnel
Hirofumi Yamamoto (JAMSTEC): Principal Investigator
Takeshi Matsumoto (JAMSTEC): (Shore-side participant)
Masaki Hanyu (GODI): Operation Leader
Akinori Uchiyama (GODI)
Naoto Morioka (Mirai crew)
Shinya Iwamida (GODI)

4.5.1 Sea Bottom Topography Measurement

(1) Objective
To obtain the bathymetry data for the contribution of geophysical investigation.
To obtain the bathymetry data for the sea water sampling, core sampling and mooring ADCP buoys during the cruise.

(2) Methods
Bathymetry data was obtained by using SeaBeam2112.004 (SeaBeam, Inc., USA) 12kHz multi-narrow beam echo sounding system with 4kHz sub-bottom profiler.

(3) Data archives
This raw dataset will be submitted to the Data Management Office (DMO) in JAMSTEC just after the cruise by CD media.

4.5.2 Sea Surface Gravity Measurement

(1) Objective
To obtain gravity data for the contribution of geophysical investigation.

(2) Methods
The sea surface gravity data was obtained by using S-116 (LaCoste-Romberg, USA) gravity meter. For the calibration, the shore side gravity was measured at Yokosuka on the beginning of the cruise and Sekinehama on the end of the cruise by using CG-3M (Scintrex) portable gravity meter.

(3) Data archives
This raw dataset will be submitted to the Data Management Office (DMO) in JAMSTEC just after the cruise by CD media.
Remarks concerning about data quality are as follows;

4.5.3 Surface Three Component Magnetic Field Measurement

(1) Objective
To obtain surface 3-component magnetic field data for the contribution of geophysical investigation.

(2) Method
The surface 3-component magnetic field data was obtained by using 3-component magnetometer (Tera Technica, Japan) at the sampling rate 8Hz. We observed continuously through this cruise.

(3) Data archives
This raw dataset will be submitted to the Data Management Office (DMO) in JAMSTEC just after the cruise by CD media.

Remarks concerning about data quality are as follows;

1. Ship's motion data was stopped in the following period because of the Doppler radar INU alignment;
    1) From 25/0614UTC to 25/0634UTC May 2001

5. Oceanographic Observations

5.1 CTD observation

(1) Personnel
Yasushi Yoshikawa (JAMSTEC): Principal Investigator
Takaki Hatayama (JAMSTEC)
Humio Mitsudera (IPRC):
Masao Fukasawa (JAMSTEC): (Shore-side participant)
Takeo Matsumoto (MWJ):Operation leader
Hiroshi Matsunaga (MWJ)
Kentaro Honda(MWJ)
Naoko Takahashi (MWJ)
Motoki Matsuhashi (MWJ)
Daisuke Terada (MWJ)
Shinichi Kaneko (MWJ)
Tokiko Takahashi (MWJ)
Ohno Yuko (MWJ)

(2) Objectives
Investigation of the oceanic structure.

(3) Measured parameters
Temperature
Conductivity
Pressure
Dissolved Oxygen (below D.O.)

(4) Methods
We observed vertical profile of temperature and salinity by CTD / Carousel (Conductivity Temperature Depth profiler / Carousel Water Sampler).The sensor attached on CTD were temperature sensor, conductivity sensor , pressure sensor, and D.O.sensor, altimeter sensor. Salinity was calculated by measurement values of pressure, conductivity and temperature. The CTD/Carousel was deployed from starboard on working deck. Descending rate and ascending rate were kept about 1.2 m/s respectively.
The CTD raw data was acquired in real time by using the SEASAVE utility from SEASOFT software (ver.4.232) provided by SBE and stored on the hard disk of an IBM personal computer.
Water samplings were made during up-cast by sending a fire command from the computer.
CTD measurement at total in 31 stations(30°-00′N～36°-45′N along 146°-25′E and 32°-08′N 152°-26′E) have been carried out. (see Table. 5-1-1)
The CTD raw data was processed using SEASOFT (ver.4.232). Data processing procedures and used utilities of SEASOFT were as follows:

DATCNV: Converts the binary raw data to output on physical unit.
his utility selects the CTD data when bottles closed to output on another file.
SECTION: Remove the unnecessary data.
WILDEDIT: Obtain an accurate estimate of the true standard deviation of the data.
Std deviations for Pass 1:2
Std deviations for Pass 2:10
Points per block: 48
ALIGNCTD: ALIGNCTD aligns oxygen measurements in time relative to pressure.
Oxygen sensor relative to pressure = 3.0 seconds
CELLTM: Remove to conductivity cell thermal mass effects from the measured conductivity.
Primaly alpha = 0.03, 1/beta = 7.0

FILTER: Run a low-pass filter on one or more columns of data.
Filter A = 0.15sec
Variable to Filter: Pressure: Low Pass Filter A

LOOPEDIT: Marks scans bad by setting the flag value associated with the scan to badflag in input.cnv files that have pressure slowdowns or reversals.
Minimum Velocity Selection = Fixed Minimum Velocity
Minimum CTD Velocity [m/sec] = 0.0
Exclude Scan Marked Bad in LOOPEDIT = Yes

DERIVE: Calculates oceanographic parameters from the input.cnv file.

BINAVG: Calculation the averaged data in every 1db.

SPLIT: Splits the data made in CNVfiles into upcast and downcast files.

ROSSUM: Edits the data of water sampled to output a summary file.

Specifications of sensors are listed below.

(1) From Stn.043 to Stn.095
Under water unit: CTD 9plus (S/N 42423 Sea-bird Electronics, Inc.)
Calibrated Date: 17-May-1994
Temperature Sensor: SBE3-04/F (S/N 031359 Sea-bird Electronics, Inc.)
Calibrated Date: 27-Feb-2001
Conductivity Sensor: SBE4-04/0 (S/N 042240 Sea-bird Electronics, Inc.)
Calibrated Date: 27-Feb-2001
D.O. sensor: SBE13-04 (S/N 130540 Sea-bird Electronics, Inc.)
Calibrated Date: 06-Jun-2000
Altimeter sensor: Benthos 2110-2 (S/N 203 Benthos, Inc.)
Deck unit: SBE11 (S/N 11P8010-0308, Sea-bird Electronics, Inc.)
Carousel water sampler: SBE32 (S/N3221746-0278 Sea-bird Electronics, Inc.)

(2) From Stn.096 to Stn.103
Under water unit: CTD 9plus (S/N 79492 Sea-bird Electronics, Inc.)
Calibrated Date: 27-Oct-1999
Temperature Sensor: SBE3-04/F (S/N 031464 Sea-bird Electronics, Inc.)
Calibrated Date: 08-Jan-2001
Conductivity Sensor: SBE4-04/0 (S/N 041202 Sea-bird Electronics, Inc.)
Calibrated Date: 11-Jan-2001
D.O. sensor: SBE13-04 (S/N 130575 Sea-bird Electronics, Inc.)
Calibrated Date: 05-Jan-2001
Altimeter sensor: Benthos 2110-2 (S/N 203 Benthos, Inc.)
Deck unit: SBE11 (S/N 11P8010-0308, Sea-bird Electronics, Inc.)
Carousel water sampler: SBE32 (S/N 3221746-0278 Sea-bird Electronics, Inc.)

(5) Results

Time variations of the vertical profile of temperature and salinity, D.O. are shown in Fig 5-1-1～Fig5-1-15. Note that in these figures, the correction of salinity data by sampled water is not applied.

(6) Trouble

It was found that spike noises for temperature are generated on cast Stn.096. After that, we found that data from temperature sensor was not acquired. Therefore We exchanged Sensors , sensors is Temperature・Conductivity・D.O.・ Pressure, which S/N 031359, 042240, 130540 and 42423 for those which S/N is 031464, 041202, 130575 and 79492 respectively on next cast.

(7) Data archive

All raw and processed CTD data file were copied into magnetic optional disk (MO) and submitted to JAMSTEC Data Management Office (DMO) and will be under their control.

5.2 Water Sampling

5.2.1 Salinity

(1)Personnel

Yasushi Yoshikawa (JAMSTEC): Principal Investigator
Takeo Matsumoto (MWJ): Operation leader
Hiroshi Matsunaga (MWJ)
Kaori Akizawa (MWJ)

(2)Objectives

To check the quality of CTD salinity.

(3)Parameters

Salinity of sampled water

(4)Method

Seawater samples were collected with a bucket for the surface, 12-liter Niskin bottles for the deepest layer(6321db) and the other layers. They were stored in 250ml Phoenix brown glass bottles. The salinity measurements were carried out using “Guildline Autosal 8400B Salinometer”, which was modified by addition of an Ocean Scientific International peristaltic-type sample intake pump, with a bath temperature of 24deg-C. The instrument was operated in the “Autosal Room” of R/V Mirai. A double conductivity ratio was defined as a median of 31 readings of the salinometer. Data collection was started after 5 seconds and it took about 10 seconds to collect 31 readings by a personal computer. The salinometer standardizations were made with IAPSO Standard Seawater batch P137 whose conductivity is 0.99995(salinity 34.998). Sub-standard seawater was used to check the drift of the Autosal.

(5)Results

Analysis data of all samples were shown in Table.5.2.1. Salinity comparison between CTD data and AUTOSAL data sampled were shown in Fig.5.2.1.

(6)Data archive

The data of salinity sample will be submitted to the DMO at JAMSTEC.

Table 5.2.1-1 Analyzed sample

Station	Niskin Bottle	Sample Bottle	CTD Pressure(db)	CTD Temparature(deg-C)	CTD Salnity(PSU)	Bottle Salinity(PSU)	Diff(CTD-Btl)
69	2	1	6203.225	1.6244	34.6947	34.6958	-0.0011
69	5	2	5001.984	1.5103	34.6912	34.6910	0.0002
69	11	3	4000.989	1.4943	34.6820	34.6822	-0.0002
69	13	4	3001.966	1.5918	34.6626	34.6626	0.0000
69	15	5	2000.772	2.0041	34.5926	34.5922	0.0004
69	19	6	1002.032	4.0076	34.2528	34.2531	-0.0003
70	1	7	6124.915	1.6131	34.6948	34.6955	-0.0007
70	3	8	5502.701	1.5489	34.6934	34.6930	0.0004
70	5	9	5001.18	1.5146	34.6906	34.6904	0.0002
70	9	10	4001.439	1.4962	34.6820	34.6734	0.0086
70	11	12	3000.191	1.5950	34.6610	34.6606	0.0004
70	13	13	1500.693	2.6474	34.4868	34.4869	-0.0001
70	15	14	999.998	3.9593	34.2620	34.2582	0.0038
70	17	15	1999.708	2.0126	34.5916	34.5927	-0.0011
71	1	16	6290.885	1.6358	34.6948	34.6956	-0.0008
71	3	17	5498.692	1.5514	34.6931	34.6944	-0.0013
71	5	18	4999.93	1.5156	34.6907	34.6910	-0.0003
71	9	19	4000.058	1.5070	34.6812	34.6812	0.0000
71	11	20	3000.554	1.6078	34.6606	34.6609	-0.0003
71	13	21	2000.593	2.0126	34.5896	34.5889	0.0007
71	15	22	1500.897	2.6218	34.4783	34.4777	0.0006
71	17	23	999.753	4.1168	34.2357	34.2367	-0.0010
72	1	24	6313.29	1.6386	34.6948	34.6963	-0.0015
72	3	25	5499.969	1.5534	34.6929	34.6921	0.0008
72	5	26	5000.807	1.5137	34.6907	34.6907	0.0000
72	9	27	4000.134	1.4903	34.6824	34.6828	-0.0004
72	11	28	2999.948	1.6067	34.6605	34.6608	-0.0003
72	13	29	2000.582	2.0578	34.5833	34.5827	0.0006
72	15	30	1498.726	2.6950	34.4716	34.4727	-0.0011
72	17	31	1000.609	4.1679	34.2245	34.2249	-0.0004
73	1	32	6295.61	1.6369	34.6948	34.6958	-0.0010
73	3	33	5504.342	1.5557	34.6929	34.6934	-0.0005
73	5	34	5004.871	1.5183	34.6906	34.6908	-0.0002
73	9	35	4002.348	1.4998	34.6814	34.6813	0.0001
73	11	36	3001.624	1.6230	34.6568	34.6569	-0.0001
73	13	37	2001.7	2.0722	34.5788	34.5783	0.0005
73	15	38	1500.411	2.6734	34.4685	34.4695	-0.0010
73	17	39	1000.263	4.2015	34.2167	34.2199	-0.0032
74	1	40	6237.405	1.6294	34.6948	34.6960	-0.0012
74	3	41	5501.955	1.5529	34.6930	34.6928	0.0002
74	5	42	5001.167	1.5141	34.6908	34.6912	-0.0004
74	9	43	4001.317	1.4882	34.6824	34.6824	0.0000
74	11	44	3000.725	1.6051	34.6589	34.6586	0.0003
74	13	45	2000.432	2.0878	34.5747	34.5743	0.0004
74	15	46	1500.655	2.6776	34.4672	34.4683	-0.0011
74	17	47	1000.269	4.2956	34.2040	34.2042	-0.0002
75	1	48	6226.553	1.6274	34.6949	34.6956	-0.0007
75	3	49	5500.344	1.5485	34.6934	34.6932	0.0002
75	5	50	5000.581	1.5110	34.6912	34.6912	0.0000
75	9	51	4000.247	1.4810	34.6832	34.6839	-0.0007
75	11	52	2999.424	1.5792	34.6616	34.6617	-0.0001
75	13	53	2000.551	2.0684	34.5785	34.5791	-0.0006
75	15	54	1499.911	2.7227	34.4594	34.4602	-0.0008
75	17	55	1000.287	4.1689	34.2262	34.2269	-0.0007
76	1	56	6221.882	1.6266	34.6948	34.6960	-0.0012
76	3	57	5499.723	1.5506	34.6933	34.6933	0.0000
76	5	58	4999.543	1.5041	34.6917	34.6925	-0.0008
76	9	59	3999.528	1.4733	34.6838	34.6837	0.0001

Table 5.2.1-2 Analyzed sample

Station	Niskin Bottle	Sample Bottle	CTD Pressure(db)	CTD Temparature(deg-C)	CTD Salnity(PSU)	Bottle Salinity(PSU)	Diff(CTD-Btl)
77	1	64	6180.955	1.6226	34.6946	34.6960	-0.0014
77	3	65	5500.302	1.5421	34.6940	34.6940	0.0000
77	5	66	5000.493	1.5043	34.6916	34.6912	0.0004
77	9	67	3999.566	1.4774	34.6833	34.6831	0.0002
77	11	68	2999.576	1.5923	34.6602	34.6598	0.0004
77	13	69	2000.096	2.0874	34.5758	34.5750	0.0008
77	15	70	1500.443	2.7006	34.4619	34.4599	0.0020
77	17	71	1000.442	4.3524	34.2123	34.2139	-0.0016
78	1	72	6084.601	1.6069	34.6950	34.6960	-0.0010
78	3	73	5500.966	1.5474	34.6936	34.6938	-0.0002
78	5	74	5001.423	1.5086	34.6913	34.6924	-0.0011
78	9	75	4000.714	1.4993	34.6813	34.6817	-0.0004
78	11	76	3000.343	1.6180	34.6592	34.6589	0.0003
78	13	77	2000.564	2.0829	34.5804	34.5808	-0.0004
78	15	78	1500.556	2.7538	34.4630	34.4639	-0.0009
78	17	79	1000.037	4.5864	34.2276	34.2319	-0.0043
79	1	80	6015.315	1.6041	34.6944	34.6958	-0.0014
79	3	81	5500.935	1.5492	34.6933	34.6939	-0.0006
79	5	82	5000.724	1.5030	34.6919	34.6916	0.0003
79	9	83	4000.202	1.4806	34.6829	34.6836	-0.0007
79	11	84	3000.982	1.6061	34.6593	34.6593	0.0000
79	13	85	2000.957	2.0955	34.5753	34.5756	-0.0003
79	15	86	1499.679	2.6973	34.4657	34.4636	0.0021
79	17	87	999.77	4.6256	34.1955	34.1981	-0.0026
80	1	88	5944.661	1.6009	34.6938	34.6950	-0.0012
80	3	89	5501.409	1.5545	34.6928	34.6940	-0.0012
80	5	90	5000.209	1.5110	34.6910	34.6914	-0.0004
80	9	91	3999.695	1.4884	34.6819	34.6829	-0.0010
80	11	92	3000.164	1.6060	34.6579	34.6580	-0.0001
80	13	93	2000.623	2.1135	34.5694	34.5689	0.0005
80	15	94	1500.656	2.7663	34.4515	34.4518	-0.0003
80	17	95	1001.036	4.6198	34.2243	34.2276	-0.0033
81	1	96	5915.804	1.5946	34.6939	34.6944	-0.0005
81	3	97	5501.397	1.5496	34.6930	34.6930	0.0000
81	5	98	5001.57	1.5060	34.6916	34.6911	0.0005
81	9	99	4000.634	1.4783	34.6829	34.6833	-0.0004
81	11	100	3000.705	1.5909	34.6600	34.6593	0.0007
81	13	101	2000.086	2.0811	34.5750	34.5748	0.0002
81	15	102	1499.552	2.7147	34.4607	34.4606	0.0001
81	17	103	999.459	4.3200	34.2549	34.2569	-0.0020
82	1	104	5890.821	1.5967	34.6935	34.6945	-0.0010
82	3	105	5501.825	1.5556	34.6928	34.6927	0.0001
82	5	106	5002.68	1.5093	34.6912	34.6907	0.0005
82	9	107	4001.714	1.4859	34.6824	34.6838	-0.0014
82	11	108	3001.455	1.5873	34.6602	34.6599	0.0003
82	13	109	2001.739	2.0244	34.5848	34.5883	-0.0035
82	15	110	1501.741	2.6115	34.4838	34.4841	-0.0003
82	17	111	1001.395	4.2302	34.3337	34.3352	-0.0015
83	1	112	5943.985	1.6084	34.6931	34.6939	-0.0008
83	3	113	5503.073	1.5565	34.6927	34.6931	-0.0004
83	5	114	5003.141	1.5087	34.6914	34.6911	0.0003
83	9	115	4000.322	1.4819	34.6827	34.6823	0.0004
83	11	116	3001.674	1.5939	34.6599	34.6598	0.0001
83	13	117	2000.871	2.0280	34.5834	34.5842	-0.0008
83	15	118	1500.554	2.5297	34.4915	34.4917	-0.0002
83	17	119	1000.335	3.7325	34.3490	34.3481	0.0009
86	1	120	5930.668	1.6048	34.6937	34.6936	0.0001
86	3	121	5502.283	1.5552	34.6931	34.6921	0.0010

Table 5.2.1-3 Analyzed sample

Station	Niskin Bottle	Sample Bottle	CTD Pressure(db)	CTD Temparature(deg-C)	CTD Salnity(PSU)	Bottle Salinity(PSU)	Diff(CTD-Btl)
92	1	125	5921.445	1.6041	34.6936	34.6931	0.0005
92	3	126	5502.568	1.5570	34.6930	34.6919	0.0011
92	9	127	4000.771	1.4918	34.6821	34.6809	0.0012
92	13	128	2000.023	1.9725	34.5928	34.5915	0.0013
92	17	129	1000.454	3.3533	34.3624	34.3616	0.0008
93	1	130	5983.748	1.6141	34.6931	34.6929	0.0002
93	3	131	5498.089	1.5562	34.6927	34.6921	0.0006
93	9	132	4000.944	1.4929	34.6817	34.6807	0.0010
93	13	133	2000.01	1.9590	34.5947	34.5941	0.0006
93	17	134	999.911	3.1333	34.3961	34.3963	-0.0002
94	1	135	6003.823	1.6158	34.6933	34.6933	0.0000
94	3	136	5495.891	1.5519	34.6932	34.6936	-0.0004
94	9	137	3998.344	1.4674	34.6842	34.6844	-0.0002
94	13	138	1998.884	1.9532	34.5957	34.5949	0.0008
94	17	139	998.931	3.1850	34.3977	34.3975	0.0002
95	1	140	5631.011	1.5630	34.6934	34.6936	-0.0002
95	3	141	5501.495	1.5460	34.6937	34.6938	-0.0001
95	9	142	4000.427	1.4517	34.6856	34.6846	0.0010
95	13	143	2000.249	1.8939	34.6059	34.6056	0.0003
95	17	144	1000.248	3.2821	34.3775	34.3764	0.0011
96	1	145	5903.465	1.5994	34.6971	34.6933	0.0038
96	3	146	5502.017	1.5522	34.6966	34.6932	0.0034
96	9	147	4001.197	1.4600	34.6881	34.6840	0.0041
96	13	148	2002.159	1.9308	34.6023	34.5987	0.0036
96	17	149	1001.497	3.3537	34.3584	34.3545	0.0039
97	1	150	5990.825	1.6101	34.6987	34.6941	0.0046
97	3	151	5496.952	1.5558	34.6974	34.6934	0.0040
97	9	152	4000.542	1.4774	34.6875	34.6832	0.0043
97	13	153	2000.775	1.9785	34.5973	34.5943	0.0030
97	17	154	1001.103	3.5122	34.3348	34.3320	0.0028
98	1	155	5915.133	1.6000	34.6989	34.6942	0.0047
98	3	156	5492.311	1.5575	34.6976	34.6932	0.0044
98	9	157	4001.265	1.4899	34.6867	34.6824	0.0043
98	13	158	2000.897	2.0219	34.5895	34.5846	0.0049
98	17	159	999.707	3.6375	34.3155	34.3110	0.0045
99	1	160	5881.357	1.5924	34.6994	34.6952	0.0042
99	3	161	5500.419	1.5518	34.6984	34.6927	0.0057
99	9	162	4000.519	1.4762	34.6881	34.6835	0.0046
99	13	163	1999.545	2.0155	34.5913	34.5859	0.0054
99	17	164	999.86	3.7058	34.3076	34.3034	0.0042
100	1	165	5781.464	1.5798	34.6994	34.6941	0.0053
100	3	166	5501.317	1.5491	34.6987	34.6934	0.0053
100	9	167	4001.653	1.4711	34.6887	34.6838	0.0049
100	13	168	2001.05	2.0266	34.5887	34.5837	0.0050
100	17	169	1000.39	3.7529	34.3281	34.3234	0.0047
101	1	170	5744.377	1.5884	34.6986	34.6931	0.0055
101	3	171	5501.475	1.5620	34.6980	34.6932	0.0048
101	9	172	4000.24	1.4836	34.6876	34.6815	0.0061
101	13	173	2000.934	2.0515	34.5825	34.5777	0.0048
101	17	174	999.372	3.4613	34.3062	34.3031	0.0031
102	1	175	5741.635	1.5771	34.6996	34.6941	0.0055
102	3	176	5498.091	1.5608	34.6982	34.6923	0.0059
102	9	177	4000.819	1.4768	34.6884	34.6837	0.0047
102	13	178	1998.493	1.9874	34.5928	34.5868	0.0060
102	17	179	1000.591	3.3809	34.3709	34.3661	0.0048
103	1	180	5624.507	1.5567	34.7000	34.6943	0.0057
103	3	181	5500.944	1.5426	34.7000	34.6940	0.0060
103	9	182	4000.431	1.4604	34.6901	34.6841	0.0060

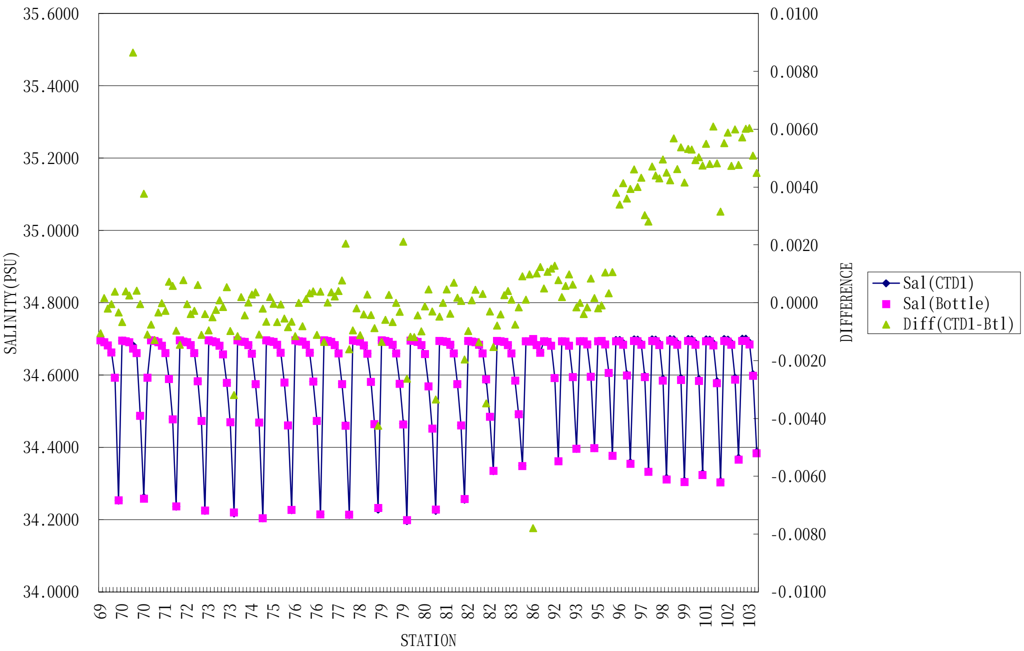

Fig.5.2.1 Salinity comparison between CTD data and AUTOSAL data

5.2.2 Dissolved oxygen

(1) Personnel

Yasushi Yoshikawa (JAMSTEC): Principal Investigator
Katsunori Sagishima (MWJ): Operation leader
Kahori Akizawa (MWJ)
Satoshi Moriya (MWJ)

(2) Objectives

Measurement of dissolved oxygen (D.O.) by the Winkler titration method following the WHP Operations and Methods (Cullberson, 1991)

(3) Parameters

D.O. in sea water down to Bottom –25m depth.

(4) Methods

(4-1) Instruments for D.O. analysis

D.O. Titrator:	Metrohm, Model 716 DMS Titrino/ 10ml of titration vessel
Detector:	Metrohm Pt Electrode/ 6.0408.100
Software	Data acquisition/ Metrohm, METRODATA/ 6.6040.100

(4-2) Sampling and analysis

The 12 Niskin water samplers sampled sea water during CTD up cast at each sampling stations. In each cast, several water samples for the Winkler titration were also sampled to calibrated BOD flasks (ca. 180ml) and glass stopper with long nipple, modified from the nipple presented in Green and Carritt (1966). Three times of bottle volumes of sample water were overflowed during of each sampling. During sampling, we measured the water temperature at the time of sampling for correction of the volume of sampling bottle. After the sampling, we analyzed D.O. with salinity correction within 30 to 60 minutes.

The samples for the titration method were analyzed by Metorhom piston burette of 10ml with Pt Electrode using Whole bottle titration in the laboratory under controlled temperature (ca 10-24 deg.-C). The standardizations and blank determination have been performed every day before the sample titration. Concentration of D.O. was calculated by equation (8) of WHP Operations and Methods (Culberson, 1991). The amount of D.O. in the reagents was reported 0.0017ml at 25.5 deg-C (Murray et al., 1968). However in this cruise, we used the value (=0.0027 ml at 21 deg-C) measured at 1995 WOCE cruise. D.O. concentrations we calculated were not corrected by seawater blank.

(5) Results

(5-1) Winkler Titration value

We prepared a 5 litter batch of 0.07N thiosulfate solution and 0.0100N standard KIO3 solution for Winkler method. We compared our KIO3 standard to CSK standard solution which is prepared by Wako pure chemical industries, Ltd. The results show that normality of our standard may be different 0.07 % from nominal normality.

65pairs of samples were analyzed as replicates taken by same Niskin bottle. The average and standard deviation (2 sigma) of difference was 0.001 ml/l and 0.018ml/l, respectively (Standard deviation corresponded to 0.34% of D.O. maximum (5.332) in this cruise).

(5-2) Vertical profiles

Vertical profiles of each stations in this cruise are shown in Fig.5.2.2-1.

5.3 **LADCP Observation of the flow field**

(1) Personnel
Yasushi Yoshikawa, Hirohumi Yamamoto, Masao Fukasawa (JAMSTEC)
Takeo Matsumoto, Hiroshi Matsunaga, Kentaro Honda, Naoko Takahashi (MWJ)

(2) Objectives
Objectives of the LADCP observations in this cruise are to study the physical and dynamical structure of eddies along the Kuroshio Extension. Deep and spatially dense LADCP lowerings with CTD/RMS system were planned along 146-25E, where the first trough of the KE meander would exist.

(3) Measured parameters
vertical profiles of current fields (u, v, w) from the surface to bottom of the sea

(4) Method
Vertical profiles of current fields were measured by LADCP lowered with CTD/RMS system. The LADCP we used was the RDI workhorse monitor (S/N 1512). The LADCP pinged a sound with frequency of 307.2kHz, and then received the Doppler-sifted one. Then currents of the water could be calculated. Parameters were set as follows. Depth cells were set as 24 bins where the length of each bin was 8m. Available data for one ping (every 1.2seconds) were expected less than length of 48m (8m by 6 bins). LADCP continued pings while the CTD/RMS system was lowered in the sea, from on deck, by way of near the ocean floor, and then to on deck. Consequently, vertical profiles of current fields from sea surface to the bottom could be obtained. In principle the descent and ascent speeds of CTD wire were set as 1.0m/s (0.5m/s in near sea surface and 0.8m/s in upper 1000m deep) and 1.5m/s, respectively. Detail note of the instrument and parameters we set was listed in table 5.3-1.

(5) Results
Twenty-eight LADCP casts lowering with CTD were carried out. It was a spatially dense, 25 minutes interval, full meridional section from 30-00N to 36-45N along 146-25E. The small type CTD/RMS system equipped at the starboard was mainly used for lowering except two casts (36-30N and 36-45N). In the northern two casts the large type CTD/RMS system equipped at the stern was used. In each casts the LADCP was lowered about 15m above the bottom of the sea.

(6) Data archive
The inventory information of the LADCP data obtained in this cruise will be submitted to Data Management Office of JAMSTEC. Original data will be archived at Ocean Observation and Research Department of JAMSTEC. (Contact to Dr. Y. Yoshikawa).

Table 5.3-1 notes of the instrument and parameters

Instrument
- S/N: 1512
- Frequency: 307200 HZ
- Configuration: 4 BEAM, JANUS
- Match Layer: 10
- Beam Angle: 20 DEGREES
- Beam Pattern: CONVEX
- Orientation: DOWN
- Sensor(s): HEADING TILT 1 TILT 2 TEMPERATURE
- Temp Sens Offset: -0.32 degrees C

Parameters
- WD = 111 100 000 Data Out (Vel,Cor,Amp; PG,St,P0; P1,P2,P3)

LN = 024	Number of depth cells (1-128)
LP = 00001	Lowered Pings per Ensemble (0-16384)
LS = 0800	Depth Cell Size (cm)
LV = 170	Mode 1 Ambiguity Vel (cm/s radial)
LZ = 030,220	Amp, Corr Thresholds (0-255)
TE = 00:00:00.00	Time per Ensemble (hrs:min:sec.sec/100)
TP = 00:01.20	Time per Ping (min:sec.sec/100)
EA = +00000	Heading Alignment (1/100 deg)
EB = +00000	Heading Bias (1/100 deg)
ED = 00000	Transducer Depth (0 - 65535 dm)
ES = 34	Salinity (0-40 pp thousand)
EX = 11111	Coord Transform (Xform: Type,Tilts,3 Bm,Map)
EZ = 1111111	Sensor Source (C,D,H,P,R,S,T)

5.4 XBT/XCTD Observation

(1) Personnel

Yasushi Yoshikawa (JAMSTEC): Principal Investigator
Takaki Hatayama (JAMSTEC)
Masaki Hanyu (GODI): Operation Leader
Naoto Morioka (Mirai crew)
Akinori Uchiyama (GODI)
Shinya Iwamida (GODI)

(2) Objectives

To investigate the oceanic structure and its time variation, vertical profiles of temperature or temperature and salinity were observed by the XBT/XCTD system on R/V Mirai.

(3) Parameters

Depth, Temperature for XBT
Depth, Temperature, Conductivity for XCTD

(4) Methods

Instruments;

XBT: Probe T-7, Converter MK-30N, Tsurumi Seiki Co., Ltd. Japan
XCTD: Probe XCTD-1, Converter MK-100, Tsurumi Seiki Co., Ltd. Japan

Specifications;

	Parameter	Range	Accuracy	Depth
XBT(T-7)	Temperature	-2.22 - +35.55 deg-C	+/- 0.2 deg-C	0–760m
XCTD	Conductivity	0 – 70 mS/cm	+/- 0.03 mS/cm	0–1,000m
	Temperature	-2 - +35 deg-C	+/- 0.02 deg-C	0-1,000m

(5) Results

Figure 5.4-1 shows XBT and XCTD casting locations. Table 5.4-1, 5.4-2 and 5.4-3 show the observation summary of XBT casting. Table 5.4-4 show the observation summary of XCTD casting.

(6) Data archives

The raw data is saved as a file such as “****.raw” and the 1-m interval data is saved as “****.xc1” for XCTD. The XBT data is saved as “***.xbt”.

All raw and processed data files of XCTD and XBT were copied onto CD-R and submitted to JASTEC Data Management Office (DMO) and will be under their control.

Table 5.4-1: Observation summary of XBT

No.	Station	Date	Time (UTC)	Latitude	Longitude	Probe Type	Max measured depth [m]	Sea floor depth [m]
1	X101	20010514	0900	34-16.7906N	142-00.3512E	T-7	788	9,201
2	X102	20010514	0943	34-12.7374N	142-14.9739E	T-7	788	7,826
3	X103	20010514	1030	34-08.2880N	142-30.1081E	T-7	788	5,966
4	X104	20010514	1115	34-04.2275N	142-45.0672E	T-7	788	5,617
5	X105	20010514	1201	34-00.8180N	143-00.0835E	T-7	788	5,157
6	X106	20010514	1247	33-58.0753N	143-15.0555E	T-7	788	5,430
7	X107	20010514	1335	33-55.1772N	143-30.0785E	T-7	788	5,216
8	X108	20010514	1422	33-51.9092N	143-45.0806E	T-7	788	4,102
9	X109	20010514	1510	33-49.0356N	144-00.0884E	T-7	788	5,707
10	X110	20010514	1558	33-45.7703N	144-15.0877E	T-7	788	5,708

Table 5.4-2: Observation summary of XBT (continued)

No.	Station	Date	Time (UTC)	Latitude	Longitude	Probe Type	Max measured depth [m]	Sea floor depth [m]
11	X111	20010514	1644	33-42.7120N	144-30.1936E	T-7	788	5,671
12	X112	20010514	1728	33-39.8589N	144-45.0959E	T-7	788	5,794
13	X113	20010514	1810	33-37.4130N	145-00.0957E	T-7	788	5,759
14	X114	20010514	1851	33-35.8437N	145-15.1187E	T-7	788	5,754
15	X115	20010514	1947	33-35.9036N	145-30.1108E	T-7	788	5,749
16	X116	20010514	2035	33-31.2731N	145-45.1982E	T-7	788	5,704
17	X117	20010514	2123	33-26.9554N	145-59.9647E	T-7	788	5,760
18	X118	20010514	2214	33-22.6388N	146-15.1149E	T-7	788	5,766
19	X119	20010514	2302	33-19.8379N	146-30.0275E	T-7	788	5,795
20	X120	20010514	2352	33-16.8963N	146-45.0409E	T-7	788	5,867
21	X121	20010515	0041	33-13.8058N	147-00.0455E	T-7	788	5,925
22	X122	20010515	0129	33-10.7530N	147-15.0332E	T-7	788	6,004
23	X123	20010515	0215	33-07.6457N	147-29.9944E	T-7	788	6,180
24	X124	20010515	0302	33-04.9173N	147-45.1621E	T-7	788	6,184
25	X125	20010515	0348	33-02.5590N	147-59.9997E	T-7	788	6,085
26	X126	20010515	0435	32-59.9824N	148-15.0118E	T-7	788	5,520
27	X127	20010515	0524	32-57.1424N	148-30.0036E	T-7	788	5,635
28	X128	20010515	0615	32-54.2485N	148-45.0065E	T-7	788	6,010
29	X129	20010515	0707	32-51.3511N	149-00.0463E	T-7	788	6,067
30	X130	20010515	0800	32-47.7155N	149-15.0233E	T-7	788	6,001
31	X131	20010515	0854	32-43.4219N	149-30.0240E	T-7	788	6,003
32	X132	20010515	0949	32-39.2883N	149-45.0400E	T-7	788	5,956
33	X133	20010515	1043	32-36.3148N	150-00.0440E	T-7	788	5,941
34	X134	20010515	1135	32-33.0928N	150-15.0473E	T-7	788	5,014
35	X135	20010515	1229	32-30.1301N	150-30.0381E	T-7	788	5,829
36	X136	20010515	1325	32-26.8429N	150-45.0082E	T-7	788	5,834
37	X137	20010515	1420	32-23.2804N	151-00.0222E	T-7	788	5,831
38	X138	20010515	1514	32-20.1089N	151-15.0354E	T-7	788	5,877

39	X139	20010515	1607	32-17.5689N	151-30.0403E	T-7	788	5,847
40	X140	20010515	1659	32-14.8323N	151-45.0360E	T-7	788	5,789
41	X141	20010515	1751	32-11.4642N	152-00.0338E	T-7	788	5,755
42	X201	20010516	0325	32-09.0153N	152-27.1399E	T-7	788	6,003
43	X202	20010516	0435	32-18.8317N	152-14.9274E	T-7	788	5,782
44	X203	20010516	0530	32-12.6098N	152-00.0104E	T-7	788	5,764
45	X204	20010516	0627	32-06.3702N	151-44.9240E	T-7	788	5,808
46	X205	20010516	0721	32-01.1276N	151-30.0355E	T-7	788	5,864
47	X206	20010516	0818	31-54.8643N	151-15.0373E	T-7	788	6,009
48	X207	20010516	0915	31-48.9391N	150-59.9932E	T-7	788	4,164
49	X208	20010516	1009	31-42.9732N	150-45.0573E	T-7	788	5,128
50	X209	20010516	1104	31-36.7760N	150-30.0210E	T-7	788	5,364
51	X210	20010516	1158	31-30.8655N	150-14.9916E	T-7	788	5,930
52	X211	20010516	1253	31-24.8184N	149-59.9967E	T-7	788	5,960
53	X212	20010516	1348	31-19.3028N	149-45.0126E	T-7	788	6,038
54	X213	20010516	1445	31-13.2284N	149-29.9907E	T-7	788	6,077

Table 5.4-3: Observation summary of XBT (continued)

No.	Station	Date	Time (UTC)	Latitude	Longitude	Probe Type	Max measured depth [m]	Sea floor depth [m]
55	X214	20010516	1541	31-07.8813N	149-15.0053E	T-7	788	6,085
56	X215	20010516	1639	31-01.3646N	149-00.0212E	T-7	788	6,205
57	X216	20010516	1738	30-55.1311N	148-45.0076E	T-7	788	6,209
58	X217	20010516	1836	30-49.2960N	148-30.0068E	T-7	788	6,178
59	X218	20010516	1935	30-42.9977N	148-15.0140E	T-7	788	6,147
60	X219	20010516	2036	30-37.1576N	147-59.9998E	T-7	788	6,190
61	X220	20010516	2135	30-31.4697N	147-44.9900E	T-7	788	6,375
62	X221	20010516	2232	30-25.8651N	147-29.9670E	T-7	788	6,245
63	X222	20010516	2330	30-20.0269N	147-14.9854E	T-7	788	6,221
64	X223	20010517	0028	30-14.2014N	146-59.9943E	T-7	788	6,259
65	X224	20010517	0125	30-07.9391N	146-45.0327E	T-7	788	5,591
66	X225	20010517	0223	30-01.7247N	146-30.0185E	T-7	788	6,124

Table 5.4-4: Observation summary of XCTD

No.	Station	Date	Time (UTC)	Latitude	Longitude	Probe S/N	Max measured depth [m]	Sea floor depth [m]
1	X301	20010526	1930	37-03.4986N	146-25.1185E	00113302	1100	5,565
2	X302	20010526	2018	37-15.0499N	146-24.9857E	00113300	1100	5,665
3	X303	20010526	2119	37-30.0157N	146-25.1253E	00113297	1100	5,647
4	X304	20010526	2218	37-45.0015N	146-24.8620E	00113299	1100	5,562
5	X305	20010526	2321	38-00.0031N	146-24.9604E	00113298	1100	5,420
6	X306	20010527	0029	38-13.7927N	146-21.5577E	00113304	935	5,324
7	X307	20010527	0129	38-25.2650N	146-06.7340E	00113303	947	5,290
8	X308	20010527	0229	38-36.8357N	145-52.1108E	00113306	942	5,303
9	X309	20010527	0329	38-47.2106N	145-38.9812E	00113360	1036	5,270

10	X310	20010527	0429	38-56.7128N	145-26.6373E	00113356	1036	5,252
11	X311	20010527	0529	39-05.9560N	145-13.8480E	00113357	1035	5,410
12	X312	20010527	0629	39-15.2013N	145-00.5048E	00113309	1035	5,569
13	X313	20010527	0729	39-24.5827N	144-47.3417E	00113308	1035	5,856
14	X314	20010527	0841	39-36.3990N	144-32.7474E	00113350	1041	6,395
15	X315	20010527	0929	39-44.2161N	144-23.2099E	00113349	1048	7,198
16	X316	20010527	1029	39-54.0947N	144-11.4812E	00113361	1037	6,586
17	X317	20010527	1130	40-03.6785N	144-00.6569E	00113351	1036	4,210
18	X318	20010527	1229	40-10.7520N	143-55.0604E	00113355	1035	3,953
19	X319	20010527	1330	40-19.9746N	143-41.3476E	00113354	1035	2,771
20	X320	20010527	1429	40-29.1154N	143-28.1779E	00113353	1035	2,235
21	X321	20010527	1529	40-38.3181N	143-15.4861E	00113352	1034	1,524
22	X322	20010527	1630	40-47.3884N	143-02.7738E	00113359	1035	1,325

5.5 Current Meter mooring

(1) Personnel

Takaki Hatayama (JAMSTEC) : Principal investigator
Hirofumi Yamamoto (JAMSTEC)
Yasushi Yoshikawa (JAMSTEC)
Masao Fukasawa (JAMSTEC) (Shore-side participant)
Takeo Matsumoto (MWJ)
Hiroshi Matsunaga (MWJ)
Kentaro Honda (MWJ)
Naoko Takahashi (MWJ)

(2) Objectives

The purpose is to get the knowledge of subsurface ocean circulation in the North Pacific Ocean. In the cruise(MR01-K02),we recovered one subsurface ADCP mooring at 32 ° 09.09N 152 ° 26.63E,and deployed three subsurface Current meter mooring.

(3) Parameters

Current profiles
Echo intensity

(4) Instrument

Recover ADCP

RDI NB-ADCP

Distance to first bin:	8m
Pings per ensemble:	16
Time per ping:	2.00s
Bin length:	8.00m
Sampling Interval:	3600s

Deployed ADCP

RDI NB-ADCP

Distance to first bin:	8m
Pings per ensemble:	16
Time per ping:	2.00s
Bin length:	8.00m
Sampling Interval:	3600s

(5) Recovery

We recovered one subsurface ADCP mooring at 32 ° 09.09N 152 ° 26E at 2000(MR00-K05).We monitored depth of acoustic releaser after we released the anchor.

(6) Deployment

Three Current meter mooring were deployed .The mooring was designed to moor the ADCP 400m.

Deployed position
33 ° 05.91N 146 ° 27.91E
34 ° 15.10N 146 ° 23.26E
35 ° 26.23N 146 ° 24.15E

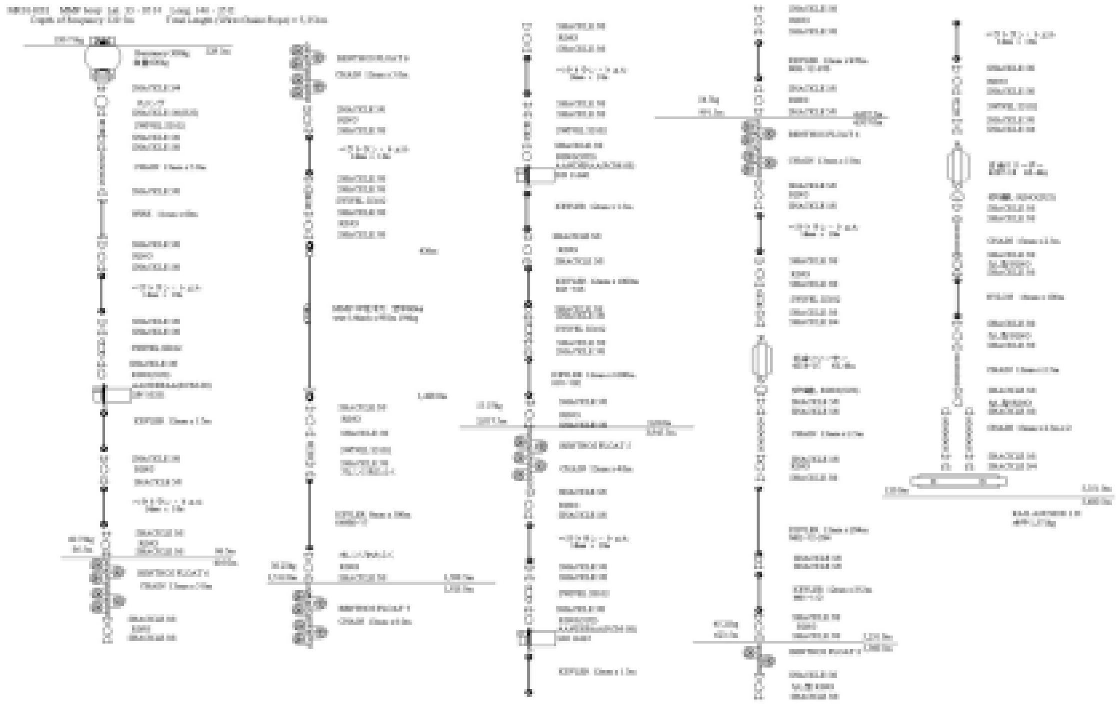

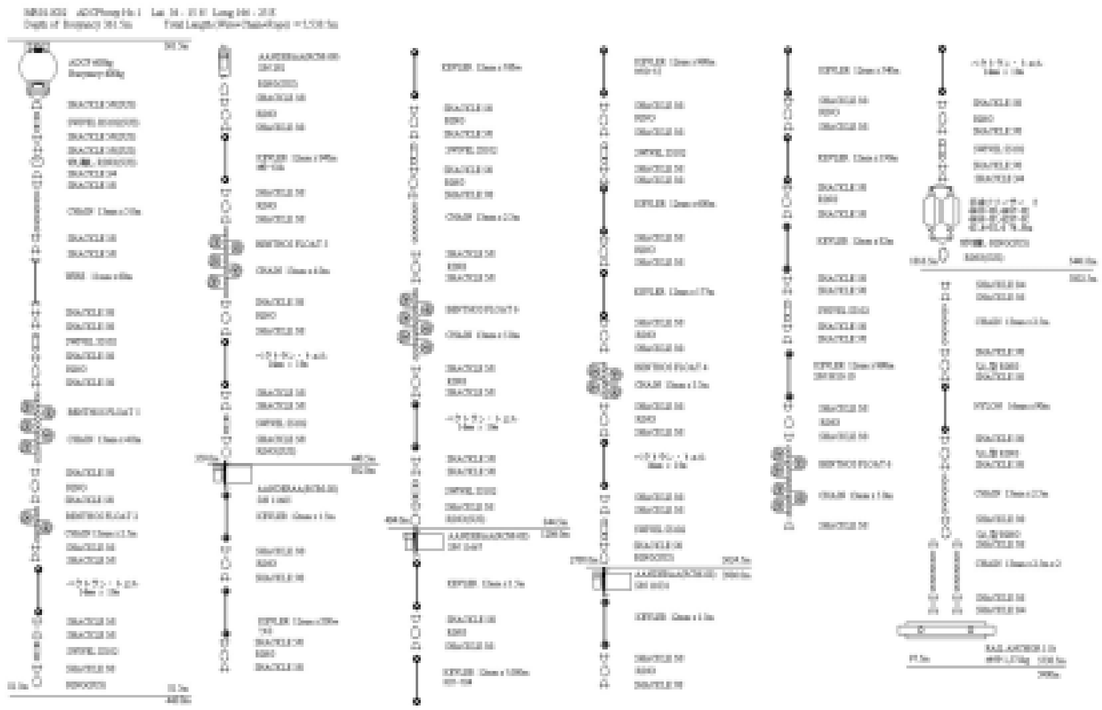

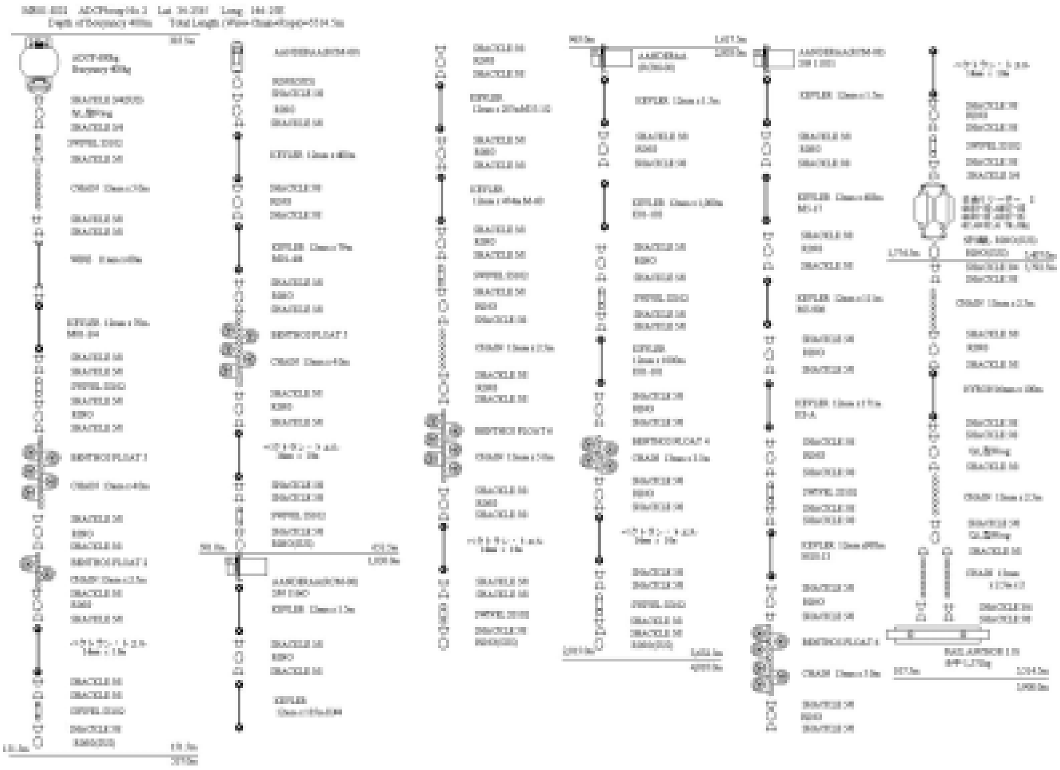

5.6 Ocean lidar

Personnel
Takeshi Kawano JAMSTEC, Ocean Research Department Principal Investigator
Ai Yasuda, MWJ
Yuichi Sonoyama, MWJ

1.Objectives

The LIDAR, laser radar, has been developed to detect a horizontal distribution of phytoplankton and a vertical distribution of suspended matters. In order to check the performance of the system and get the required parameters for the system, continuous measurements were made.

2.Method

(1) Ocean Lidar

The LIDAR operates a Nd.YAG laser, which emits a green pulse laser in 532 nm through KDP crystal as the second harmonic of Nd.YAG. Detectors in this system detects the laser–excited fluorescence from phytoplankton in the surface layer and the light scattered by particles from the depth of about 5O meters. A density of chlorophyll-a is estimated through the empirical equation, obtained by a least square method. A vertical distribution of phytoplankton will be estimated from the logarithm decrement of signal as a function of particles.

(2) Sea truth data

In order to compare the data from Ocean Lidar system, we made an observation as follows.

- Photosynthetic parameters

We made an P-I curve measurement in every 8 hours using a surface seawater. The bottles were spiked with 0.2 mmoles/mL of $NaH^{13}CO_3$ solution, and incubated for 3 hours at temperature-controlled bath in a laboratory. The light intensity was shown in table 5.6-1. Samples were filtered immediately after the incubation and the filters were kept to freeze till analyse of this cruise. After that, filters were dried on the oven of 45 degree C.

- PAR

In order to measure the photosynthetical available radiation, we made a continuous measurement using a PUV by Biospherical Instruments during the cruise.

-Chlorophyll-a

Surface seawater was sampled every 4 hours to measure Chlorophyll-a.

All the data and samples will be analyzed after the cruise.

Table. 5.6-1 Light Intensity of P-I measurements

Bottle No.	Light Intensity ($uE/cm^2/sec$)
1	1100
2	500
3	250
4	145
5	70
6	28
7	22
8	12

5.7 tCO2 and pCO2 measurements

(1) personnel

Akihiko Murata (JAMSTEC)
Taeko Ohama (MWJ)

(2) objective

To clarify spatial variations of TCO_2 and pCO_2 in surface seawater over Kuroshio Extension.

(3) measured parameters

Seawater TCO_2 and pCO_2 at nominal 4.5 m depth and atmospheric pCO_2.

(4) method

Concentrations of TCO_2 were measured during the entire cruise by a automated system with a coulometer (Model 5012, UIC Inc.). Seawater was collected in a nominal 250 ml glass bottle automatically. A volume of about 35 ml seawater was taken into a receptacle, and 2 ml of 10 percents (v/v) phosphoric acid was added. The CO_2 gas evolved was purged by 99.9999% N_2 gas for 12 minutes at a flow rate of 140 ml/min, and absorbed into an elctrolyte solution. Acids formed by the absorbed CO_2 in the solution were titrated with OH^-. Calibration of the coulometer was carried out using sodium carbonate solutions (0 – 2500 µmol/kg).

Partial pressures of CO_2 in the atmosphere and the sea surface were measured during the entire cruise by the automated system with a non-dispersive infra-red (NDIR) analyzer (BINOS™). It run on about 1.5 hour cycle during which four standard gases, an ambient air sample, and head space samples from the equilbrator are analyzed.

The ambient air sample taken from the bow is introduced into the NDIR through a mass flow controller which controls the air flow rate at about 0.5 L/min, a cooling unit, a parma pure dryer, and a desiccant holder ($Mg(ClO_4)_2$).

The equilibrator has a shower head space in the top through which surface seawater is forced to be showered at a rate of 5 – 8 L/min. Air in the head space is circulated with an air pump at 0.5 – 0.8 L/min in a closed loop through two cooling units, the perma pure dryer and the desiccant holder, which are the same ones used for air sample.

For calibration, compressed gas standards with nominal mixing ratios of 270, 330, 360, 410 ppmv in a synthetic air were used.

(5) data archive

All data will be submitted to JAMSTEC Data Management Office (DMO) and under its control.

6. Geographic Observation

6.1 Core Sampling

Personnel

Hirofumi YAMAMOTO *Ocean Research Dept, JAMSTEC**
Toshiya KANAMATSU *Deep Sea Research Dept., JAMSTEC**
Hiroaki MURAKI *Marine Geology Section, Dept. of Marine Science, MWJ***
Yutaka MATSUURA *Marine Geology Section, Dept. of Marine Science, MWJ***
Makoto SHIMOKAWARA *Marine Geology Section, Dept. of Marine Science, MWJ***
Masumi ISHIMORI *Marine Geology Section, Dept. of Marine Science, MWJ***

Japan Marine Science and Technology Center, ** Marine Works Japan Ltd.

Summary

We performed deep-sea sediment collection at the alternative site (33°05.00' N, 146°24.97' E, water depth 5758m) using a 20 m piston corer after the cancellation of coring at the original proposed site (32°09' N, 152°29' E) due to no sedimentary structure. Totally 1886 cm sediment was recovered, and sediment below 1050.1 cm from the top is considered as core inflow. The major lithology of the sediment is a mottled dark brown-gray clay, which is predominantly composed of siliceous bio-tests, and accompanied by glassy and lithic volcanic ashes. Measurements of magnetic susceptibility, gamma ray attenuation, and color reflectance, and soft-X ray photograph were performed as onboard routine work.

1. Objectives

The Kuroshio and Kuroshio Extension play an important role in the North Pacific Subtropic Gyre. Reconstruction of its pasts improves our understanding of the evolution of surface current system in the North Pacific area. We designed a series coring to recover sediment in the adjacent area of Kuroshio Extension.

The change of paleoceanographic conditions in the area will be studied with paleo-temperature analysis of seawater inferred from microfossil assemblage, and flux variation as a proxy of paleoclimate determined by environmental rock magnetic techniques. Paleomagnetostratigraphy and tephra chronology will contribute to age determination of deep-sea sediments.

2.Methods

Following devices and systems were used for sediment collection and onboard measurements

2-1. Coring equipment

Piston core sampler consists of 1200kg-weight, 20m-long duralumin pipe (consisted of 80mm inner diameter four 5 m pipes), and a pilot core sampler. We used a multiple core sampler called "Ashura" as a pilot corer, which is equipped with an 80kg-weight and three sub-tubes of 60cm in length and

73mm in diameter. The logger equipped with clinometers and a magnetic compass, was attached to the piston head to obtain information of attitude of core sampler during operation around subsurface of sea-floor.

2-2. Site survey system

Bathymetric data were collected by the multibeam survey system, SEA BEAM 2112. The system generates data which allows the production of wide-swath contour maps of the seafloor. The Subbottom Profiling Subsystem operated at 4 kHz is an additional option to the SEA BEAM System. The depth penetration of the subbottom profiling subsystem varies with bottom composition and may be as much as 75 m. The system is operated at forming a vertical beam of 45° athwartship and 5° fore/aft.

Global positioning system (GPS) of WGS84 were used to determine a geographic position.

2-3. Sampling procedures

After recovering of the piston corer, 5 m duralumin core barrels were cut into 1 m each, then sediment column were pushed out of barrels using an oil pressure extender. Whole-round sections were run through the multisensor (MST). After MST measurements, the cores were vertically split into two sections; working and archive halves. On this cruise, photograph and visual description were routinely performed on archive halves. Slabs sample for soft X-ray analysis was taken from archive halves. Colors scanning and personal sampling were made on working halves The residue sediments in working halves after sampling were packed in plastic bags for further studying. The flow chart of the sample treatment is shown in **Figure 6.1-1**

Sample curtain and shipboard sampling

As usually sediment stretch, length of sections are changed after a handling. In this cruise, the lengths of working halves are used for formal reports and post-cruise researches (**Table 6.1-2**). And also note that a difference between section lengths of working and archive halves from a same whole-core occasionally appear during splitting. Following continuous sub-samplings were performed. Plastic cube (22.4 x 22.4 x 22.4 mm) for paleomagnetic and rock magnetic analysis. Two sets of Kabuse (18 x 10 x 1000 mm), and ODP type u-channel (22.4 x 22.4 x 1000 mm) for radiolarian and diatom assemblage analysis and for father studies. Slab sample for soft X-ray photo (30 x 7 x 200 mm) for observation of texture and structure of sediments.

2-4. Visual core description

The color, texture and structure of sediment on each archive halves were described to identify lithologic features of recovered cores. Representative or distinct lithology in sections were sampled for smear slide observation. The details were recorded in the core description form (attached to Appendix), and a summarized lithology was illustrated in **Figure 4.**

2-5. Multi sensor core logging

Gamma-ray attenuation (GRA) and magnetic susceptibility (MS) were measured on whole-core section before splitting using the onboard GEOTEK multisensor core logger (MSCL). The MSCL have three sensors, Which is gamma-ray attenuation, P-wave velocity (PWV), and magnetic susceptibility. However, PWV sensor could not be measured, because there was always gap between the core liner and the core, which prevents PWV sensor transfer through the core. The principle of GRA is based on the facts that medium-energy gamma rays (0.1-1Mev) interact with the formation material mainly by Compton scattering, that the elements of most rock-forming minerals have similar Compton mass attenuation coefficients, and that the electron density measured can easily be related to the material bulk density. The 137 Cs source used transmits gamma rays at 660 KeV. A standard NaI scintillation detector is used in conjunction with a universal counter. GRA calibration assumes a two-phase system model for sediments and rocks, where the two phases are the minerals and the interstitial water. Aluminum has an attenuation coefficient similar to common minerals and is used as the mineral phase standard. Pure water is used as the interstitial-water phase standard. The actual standard consists of a telescoping aluminum rob (five elements of varying thickness) mounted in a piece of core liner and filled with distilled water. GRA measurement was carried on every 1 or 2-cm whole-core with 1-seconds counting. GRA data provide wet bulk density and fractional porosity for core thickness is constant (multiple core:74mm, piston core:80mm). MS was measured using Bartington MS2C system within the MSCL. The main unit is the widely used, versatile MS2 susceptometer for rapid measurements with a number of sensors. The unit has a measuring range of 1x10-5 to 9999x10-5(SI, volume specific). It has five front panel controls: on-off switch, sensitivity range switch, SI or cgs unit switch, zero button, measure button, and continuous measurement switch. The unit switch should always be on SI. This loop sensor has an internal diameter of 100mm. It operates at a frequency of 0.565 kHz and an alternating field (AF) intensity of 80 A/m (=0.1mT). MS data measurement was carried on every 1 or 2-cm whole-core with 1 second. MS data is used mostly as a relative proxy indicator for changes in composition that can be linked to paleoclimatic controlled depositional processes.

2-6. Color reflectance

Color reflectance was measured by using the Minolta Photospectrometer CM-2002. This is a compact and hand-held instrument, and can measure the spectral reflectance of surface sediment with a scope of 8 mm in diameter. High-speed and accuracy measurements of spectral reflectance in the range from 400-700 nm can be obtained by ltracompact spectral sensors, hybrid IC analog circuitry, and a 32-bit, 16MHz microcomputer. To ensure accuracy, the CM-2002 uses a double-beam feedback system, monitoring the illumination on the specimen at the time of measurement and automatically compensating for any changes in the intensity or spectral distribution of the light. Calibration was carried out with the zero and white calibration pieces (Minolta CM-2002 standard accessories) before the measurement of core samples. The color of working half core was measured on every 1 or 2-cm through crystal clear polyethylene wrap. The color reflectance data are indicated as color parameters of L*, a*, and b* (L*: black and white, a*: red and green, b*: yellow and blue; Additionally, the Munsell colors (H: hue, V: value, C: chroma) and spectral data were also obtained. Spectral data can be used to estimate the abundance of certain compounds

2-7. Soft X-ray photographs analysis

Onboard Soft X-ray photographs analysis system (Soft X), Pro-TEST 150 (SOFTEX), was used to observe the structure of sediment sample, especially to recognize coring disturbance of flow-in, fluidization or other possible deformation occurred during coring. Sediment slabs were sampled from archive cores using original plastic cases (200 x 30 x 7mm). X-ray photographs of samples through the plastic cased were taken in a standard power (50kVp, 2mA, in 200 seconds). In this cruise, total 67 samples were photographed in 13 nega-films. The developer is equipped on the ship, photographed films were developed on board.

3. Results

3-1. Site survey

We canceled coring at original proposed site (32°09’ N, 152°29’ E, water depth 6000+ m), because a subbottom record revealed no acoustic layering structure in the survey area, also suggested a hard surface of sea-floor. Alternatively, we changed the point to 30.05N, 146°25’ E. The surface of the area is smoothed **(Figure 6.1-2**), and subbotom profiling record show a clear acoustic opaque layering (**Figure 6.1-3**)

Table 6.1-1. Position of PC-1

Latitude	Longitude	water depth
30°05.00’ N	146°24.97’ E	5758m

3-2. Lithology of PL-01 and PC-01 (Figure 6.1-4)

PL-01: We recovered three multiple cores (Ashura) at the PC-01 site. The obtained core shows brown color and mottled texture, which contains much siliceous biogenic component of radiolarian, diatoms tests and sponge spicules.

PC-01: We recovered non-disturbed 10.50 m sediment. Below the horizon (80 cm in section 12), sections show inflow structure, which is characterized by a vertically flowed structure and absence of original sedimentary structure. The recovered sediment shows a dark brown - light gray color with moderately - severly mottled textures through all sections. Ash layers are frequently interbedded with a few - several cm thicknesses. Two types of volcanic ash were recognized. One is mostly composed of glass, clear layering; the other is dark colored mottle form, which is dominant in the lithic fragment with mixture of pelagic clay. The clay contains much biogenic siliceous tests such as radiolarian, diatoms, sponge spicules and silicoflagellates. Clay minerals and volcanic glass are other minor components. Preliminary microscopic inspection shows that diatom tests are most common components.

Ash layer and pumice pebbles

Nine glassy ash horizons were recognized in PC-01. Most ash layers are composed of fine grains. Several ash layers consist of not only single layer, but also various colored layers. Ash layers contain a large number of fresh glasses (transparent); babble wall and pipe vesicular shards are commonly observed. Texture of lithic fragments are unclear under micro-scope, but probably most are basltic fragments

Isolated pumice pebbles are common in 10-20 cm in section 6.

3-3. Results of Multi sensor core logging (Figure 6.1-5)

As the fractional porosity is calculated from attenuated gamma counts, the pattern shows mirror image of that of gamma density. Generally magnetic susceptibility and gamma ray attenuation are inversely correlated, and thus volumetric magnetic susceptibility and gamma bulk density are directly correlated to each other. Such pattern of profiles implies that high bulk density (low gamma ray attenuation) intervals are associated with high content of magnetic materials.

Generally sections involving mottles of litic volcanic ash show high magnetic susceptibility value. On the other side, magnetic susceptibility show quick drop at glassy ash layers. In undisturbed sections, fluctuating pattern of magnetic susceptibility and gamma attenuation are basically corresponding to changes of lithology. Sudden drops of magnetic susceptibility occur at glassy ash layers. Much higher magnetic susceptibility occurs at of litic volcanic ash layers and sediments including isolated pumiceous pebbles. At the sharp boundary of dull yellow and gray clays at the top of sec. 6, a drop of magnetic susceptibility was observed. The inflow sediment shows fairly smoothed pattern in magnetic susceptibility. We observed low Gamma ray attenuation value in the indurate layers, which usually accompanied by ash layers.

3-4. Results of color reflectance measurement

Depth profiles of reflectance parameters, L*, a*, and b* (**Figure 6.1-6**) are shown in similar pattern to MST data is identified in color parameter profiles of the flow-in sediment, which show rather constant values than upper undisturbed sediments. A general fluctuating pattern of parameter L* seems to be independent of parameters a* and b*. Variations of L* are generally corresponding to visible lithologic changes. Glassy ash layer, which usually shows white gray color, reveals high L* value, and severely mottled layer, more dark colored, show low L* value. Also fluctuation in L* is mostly synchronous to magnetic susceptibility fluctuation pattern. Thus it is expected that L* value is largely affected by terreginous inputs. On the other hand, fluctuation patterns of a* and b* are synchronized and seems more cyclic pattern. These large fluctuation patterns show meter order wavelength. It is impossible to consider that such long wavelength variations are caused from lithologic change, because lithologic change occur in centimeter order (see Visual Description). Origin is unclear but more long-term change such as change in oceanographic condition is a possible mechanism for the characteristic pattern.

4. Future Study

Following research plans have been proposed using sediments obtained during this cruise.

Radiolarian and Diatom assemblage analysis (JAMSTEC), Volcanic ash analysis (JAMSTEC), Paleomagnetic and Rock magnetic analysis (JAMSTEC).

Captions

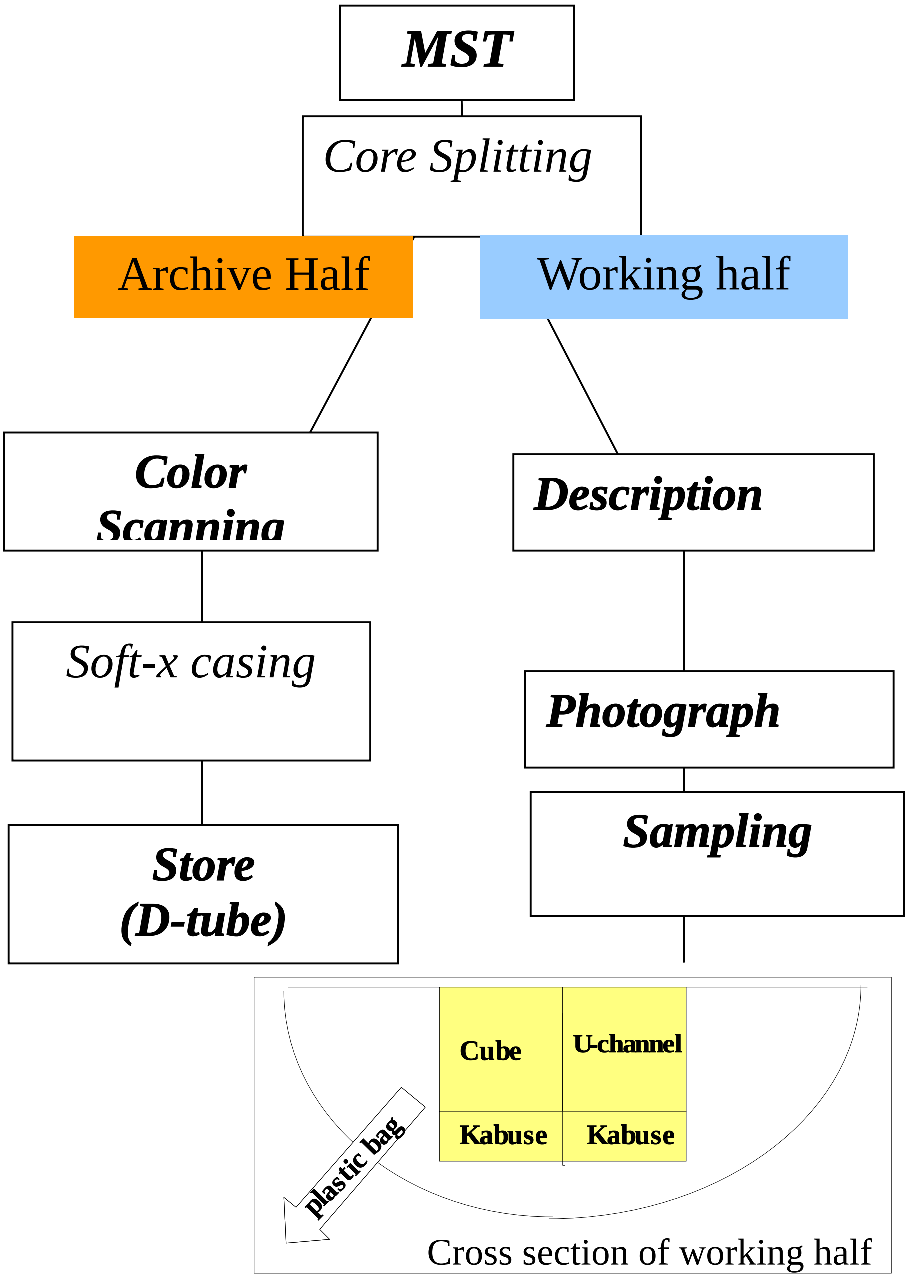

Figure 6.1-1. Chart flow of core sample treatment.

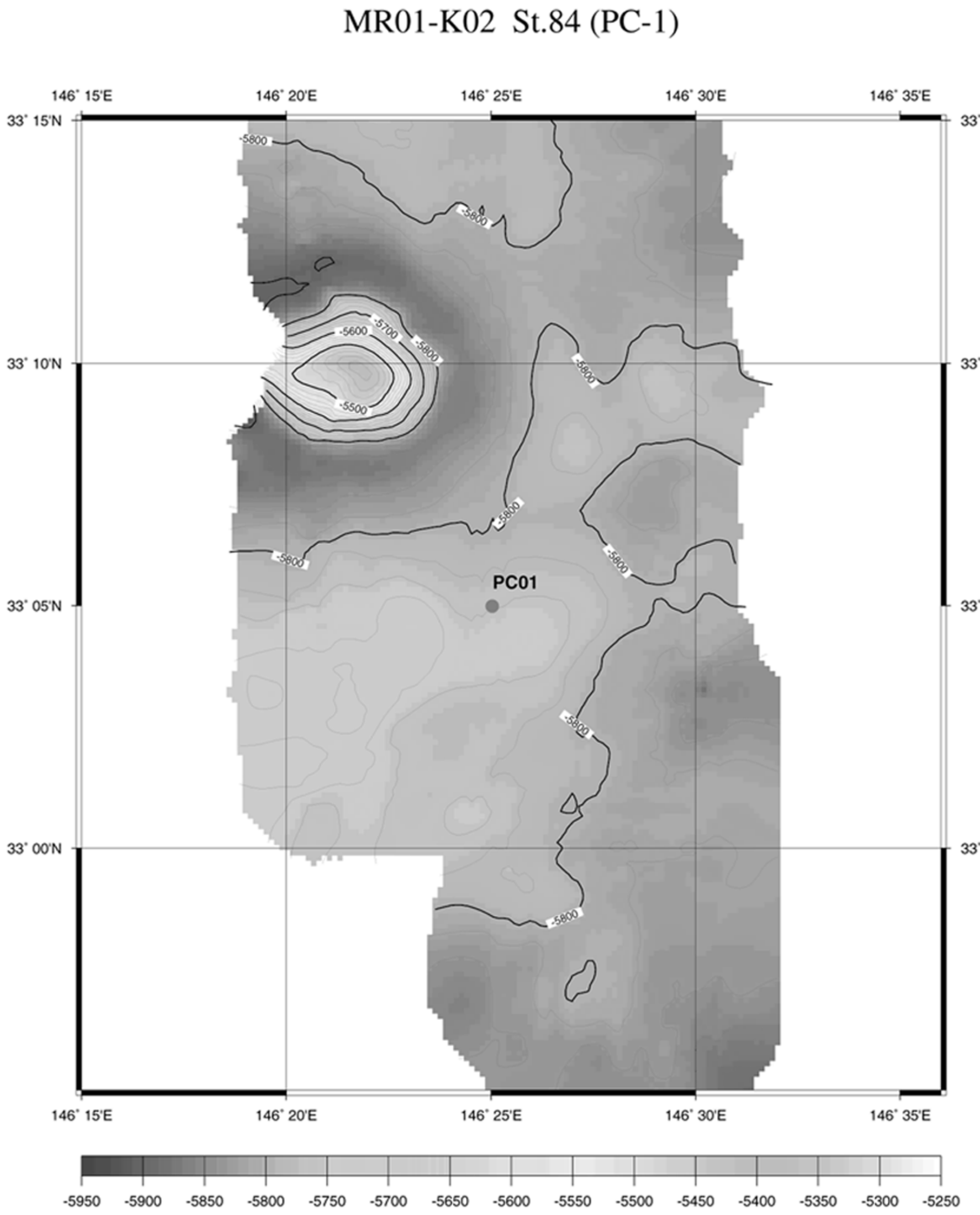

Figure 6.1-2. Topographic map in the adjacent are of PC-01 coring site.

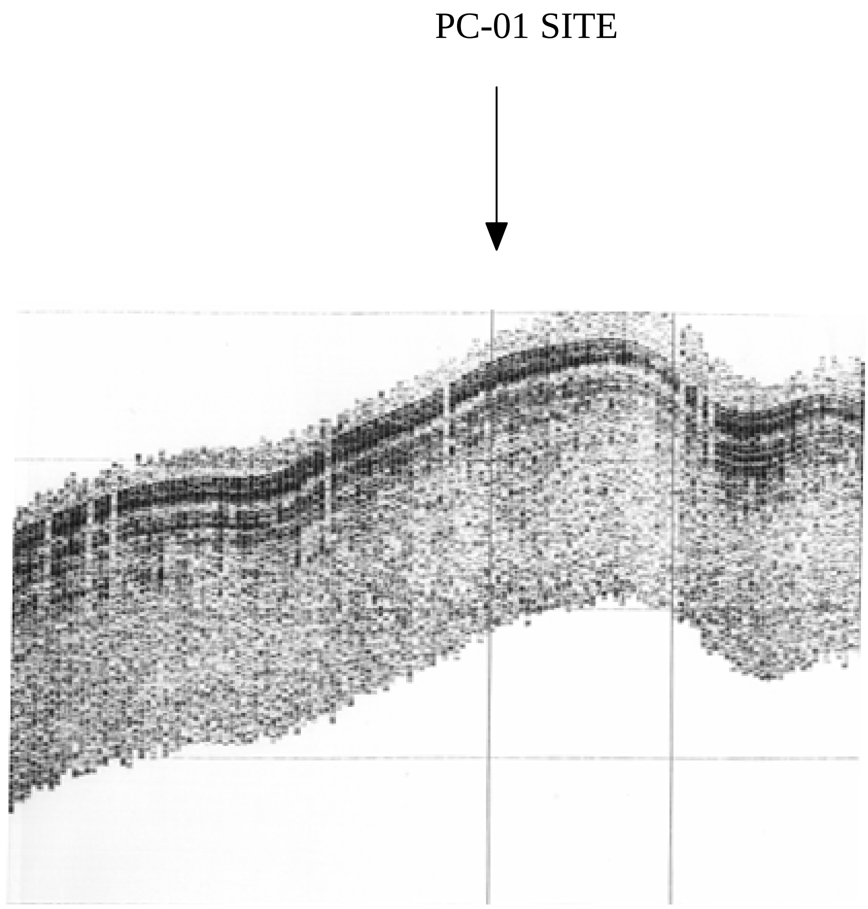

Figure 6.1-3. Subbottom profiling record across the PC-01 coring site.

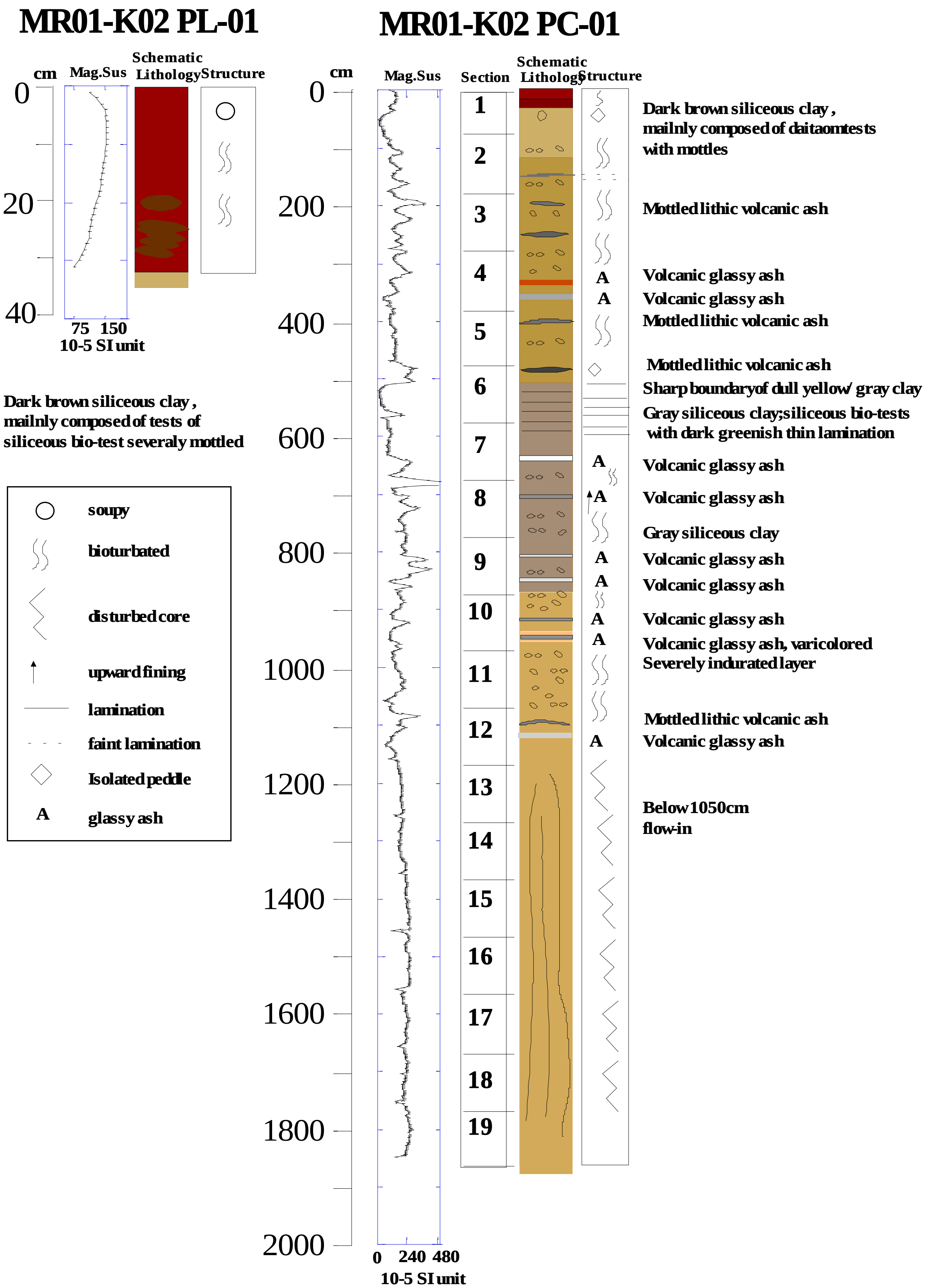

Figure 6.1-4. Summary of PL-01 and PC-01 lithology.

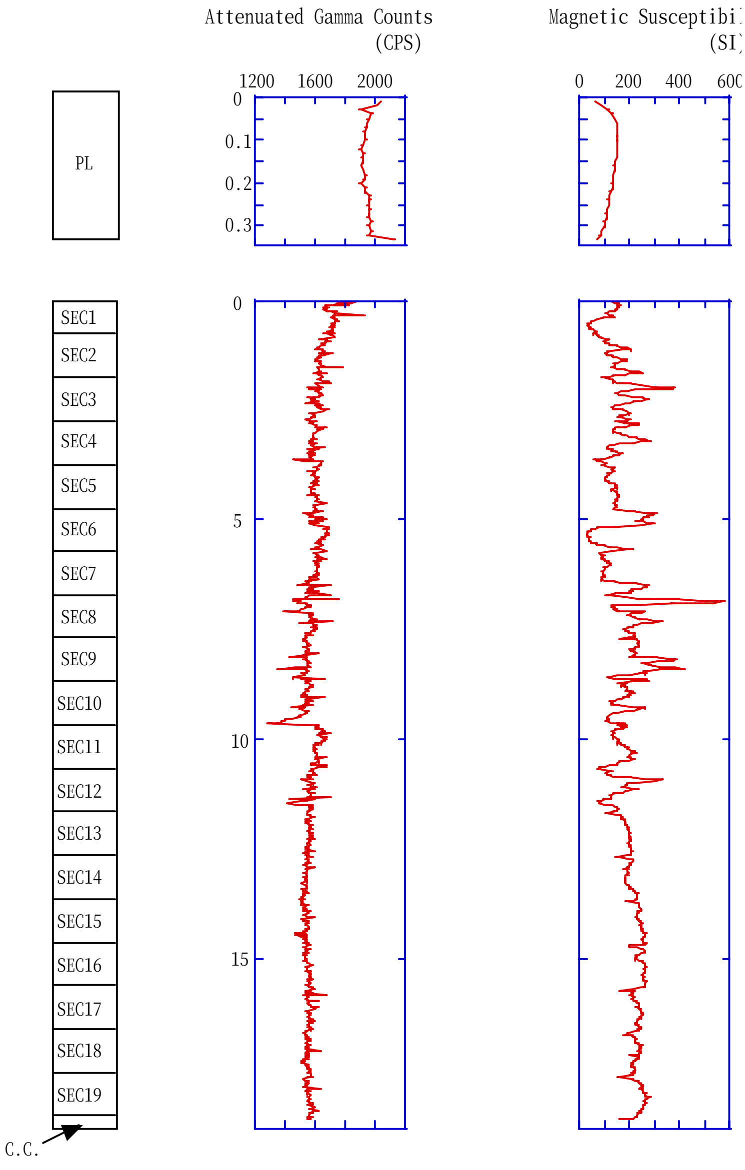

Figure 6.1-5. MR01-K02 PC01&PL01(HAND2) Physical Properties RAW DATA

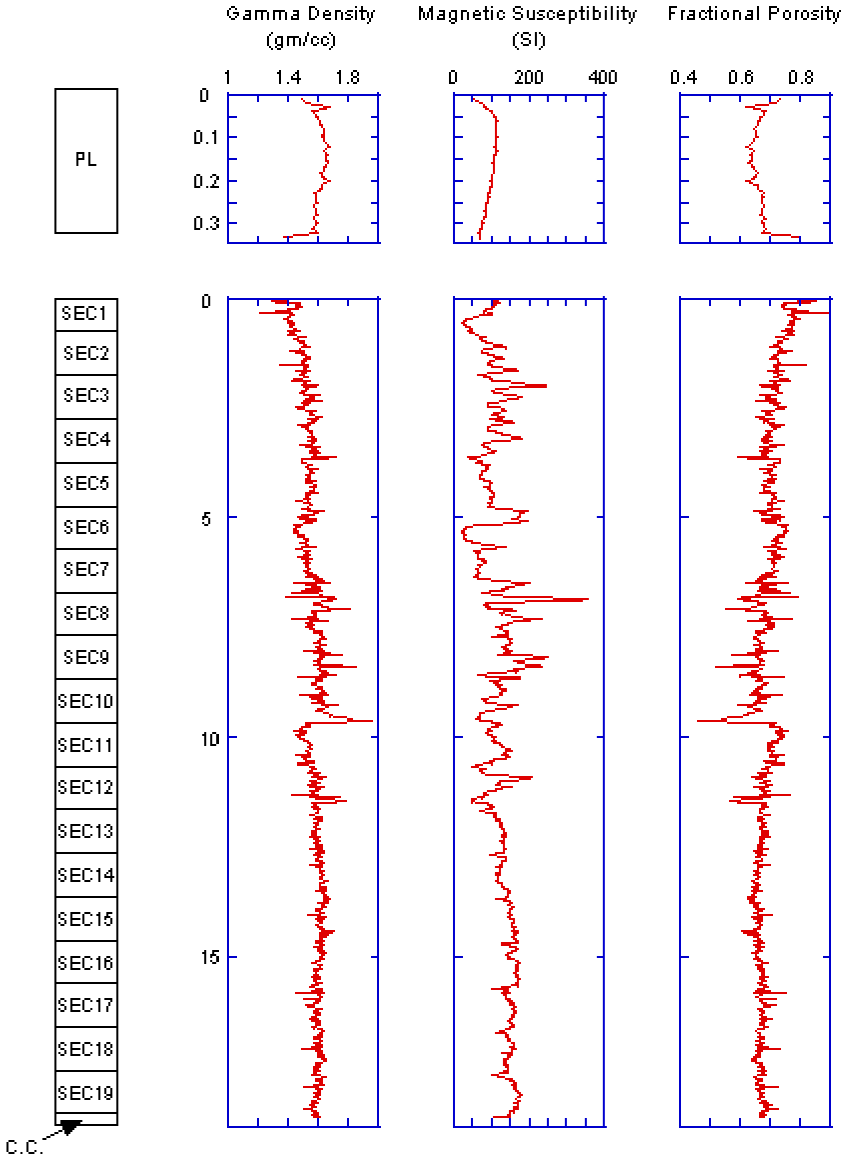

Figure6.1-6. MR01-K02 PC01&PL01(HAND2) Physical Properties

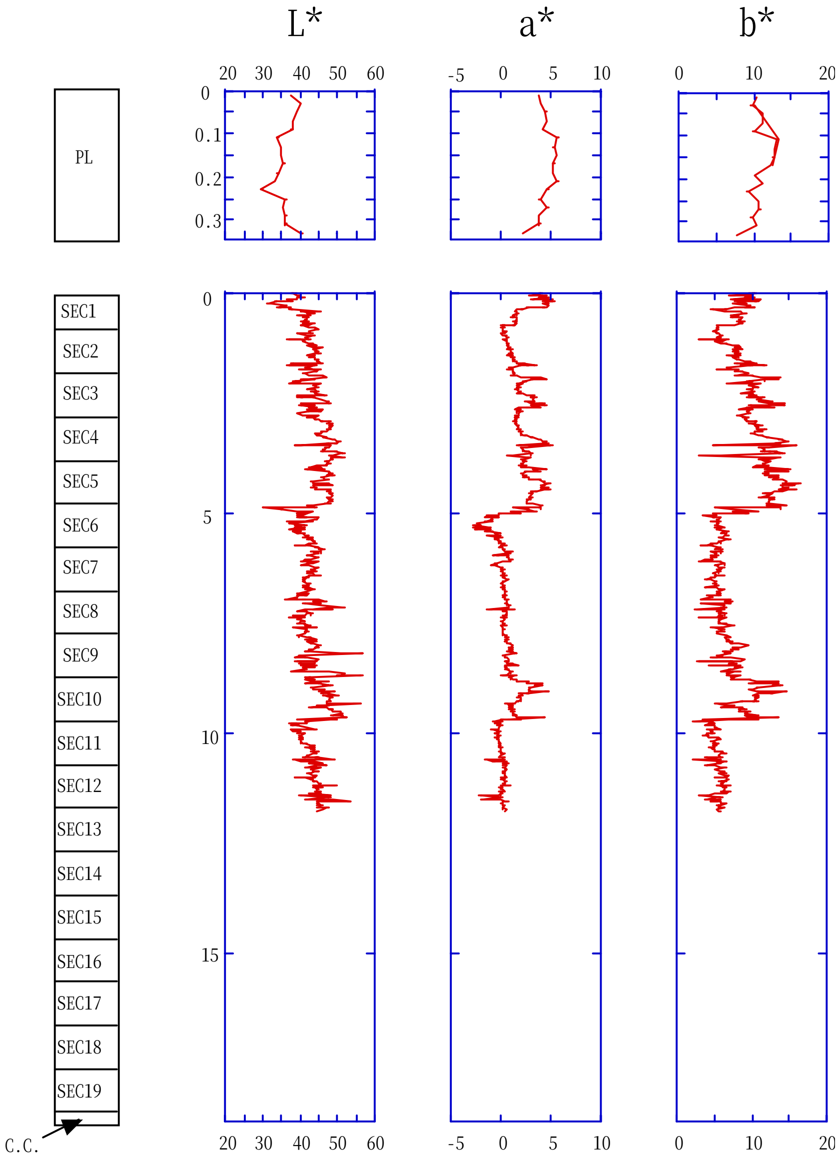

Figure 6.1-7. MR01-K02 PC01&PL01(HAND2) Physical Properties

(Color reflectance)

Table 6.1-2. Sample information

Sec. No.	Whole core length (cm)	Top of Section	Archive Hailf length (cm)	Working Half length (cm)	No. cube	No. soft-X case	No. U-channele	No. Kabuse	Plastic Bag 2cm interval
1	74	0	74.5	79	34	4	1	2	↑
2	102.2	74	101.2	101.2	45	6	1	2	
3	101	176.2	101	101	45	6	1	2	
4	101	277.2	100.5	98	45	6	1	2	
5	97.8	378.2	98	98	44	5	1	2	
6	97.5	476	97.5	97.5	43	5	1	2	
7	99.5	573.5	100	100	44	5	1	2	
8	97	673	97.5	97.5	43	5	1	2	
9	100	770	100	100	44	5	1	2	
10	100.1	870	100	100	44	5	1	2	
11	98	970.1	98	97.5	44	5	1	2	
12	99.5	1068.1	100	99	44	5	1	2	↓
13	100.3	1167.6	100	99.5	-	-	-	-	-
14	100.3	1267.9	100	99.5	-	-	-	-	-
15	100	1368.2	100	100.5	-	-	-	-	-
16	100.5	1468.2	100	100.5	-	-	-	-	-
17	101.2	1568.7	101	101.5	-	-	-	-	-
18	99	1669.9	99	99	-	-	-	-	-
19	96.4	1768.9	96.5	97	-	-	-	-	-
CC	19	1865.3	20	21	-	-	-	-	-
	total	1884.3							

PL	Whole core length (cm)	Top of Section	Archive Hailf length (cm)	Working Half length (cm)	NO. cube	No. soft-X case	No. U-channele	No. Kabuse	Plastic Bag 2cm interval
HAND1	27	-	28	27.5	-	2	-	-	↑
HAND2	34.5	-	36	33.5	15	2	1	2	
HAND3	32.5	-	35	35	-	2	-	-	↓

7. Meteorological Observations

7.1 Radiosonde

(1) Personnel
Humio Mitsudera (IPRC): Principal Investigator
Masaki Hanyu (GODI): Operation Leader
Shin'ya Iwamida (GODI)

(2) Objective
Atmospheric soundings over Kuroshio extension and Oyashio

(3) Parameters
Vertical profile of temperature, humidity and wind speed/direction

(4) Methods
Atmospheric sounding by radiosonde was carried out from 17th May to 28th May 2001 during MR01-K02 cruise. Mostly we observed twice (00Z and 12Z) a day and sometimes we launched additional radiosonde balloons. In addition to the regular observation in operational mode, we attached radiosonde to the aerosonde balloon and observed in research mode.

(5) Preliminary results
The log file of radiosonde launching is listed in Table 7.1-1 for research mode operation and Table 7.1-2 for operational mode respectively.
Profiles of temperature and dew point temperature are plotted on the thermodynamic chart (EMAGRAM) with wind profiles in Figure 7.1-1, 7.1-2 and 7.1-3.

(6) Data archives
Regularly observed data were sent to the world meteorological community by GTS through Japan Meteorological Agency immediately after the each observation. 23 reports were sent during the cruise.
Raw data is stored as ASCII format every 2 seconds during ascent and will be submitted to DMD JAMSTEC.

Table 7.1-1: Log of radiosonde observation with Aerosonde observation

No.	Time (UTC) YYMMDDHH	Log (degE)	lat (degN)	Press (hPa)	Temp (degC)	RH (%)	WD (deg)	WS (m/s)
1	2001051803	146.41	31.00	1012.6	25.6	47	10	6.8
2	2001051820	146.41	31.75	1014.6	19.6	65	66	2.4
3	2001051905	146.41	32.25	1013.3	20.4	63	114	2.8
4	2001051906	146.40	32.25	1012.9	19.6	65	170	2.0
5	2001051920	146.50	33.00	1014.2	18.9	73	247	1.2

Table 7.1-2: Radiosonde launch log

No.	Time (UTC) YYMMDDHH	log (degE)	lat (degN)	Press (hPa)	Temp (degC)	RH (%)	WD (deg)	WS (m/s)	Max Altitude (hPa)	(m)	Cloud Amount	Cloud Type
1	01051712	146.40	30.25	1008.9	20.4	79	333	8.6	41.0	21,969	10	-
2	01051800	146.42	30.75	1012.2	20.4	63	353	6.2	33.7	23,105	4	Cu
3	01051812	146.39	31.27	1013.2	18.5	62	35	5.5	45.2	21,296	2	-
4	01051900	146.42	31.98	1014.6	21.2	60	86	0.9	31.5	23,576	10	As,Cu
5	01051912	146.41	32.50	1013.6	18.8	68	201	5.1	48.3	20,861	0	—
6	01052000	146.49	33.00	1014.1	18.8	74	184	2.7	53.0	20,255	1-	Cu
7	01052012	146.47	33.52	1013.6	19.8	74	234	5.9	71.3	18,430	0	—
8	01052100	146.42	33.08	1014.8	19.9	75	235	5.2	57.6	19,767	2	Cu
9	01052112	146.46	33.76	1014.3	20.3	81	222	4.2	79.0	17,875	1	-
10	01052200	146.48	33.11	1013.7	21.0	79	145	7.9	65.3	19,050	10	As
11	01052212	146.33	34.20	1012.3	19.7	89	156	4.5	99.2	16,507	10	-
12	01052300	146.45	34.35	1007.4	18.3	92	103	13.0	40.2	22,116	10	Sc
13	01052308	146.33	35.39	1004.3	19.0	90	135	15.1	59.4	19,655	10	Sc
14	01052312	146.33	34.62	1003.6	18.9	95	109	11.4	51.9	20,517	10	-
15	01052400	146.42	34.01	1000.4	21.4	100	208	9.9	33.6	23,251	10	St
16	01052412	146.45	34.27	998.2	20.9	97	225	9.6	66.1	19,065	10	-
17	01052500	146.38	35.01	998.3	20.2	85	280	12.3	43.9	21,520	9	Cu
18	01052512	146.36	35.25	1006.8	19.1	79	307	11.1	61.5	19,500	0	—
19	01052600	146.43	35.99	1010.1	19.1	67	166	2.6	79.9	17,894	10	Cs
20	01052612	146.43	36.50	1008.0	20.0	85	219	9.1	59.4	19,681	0	—
21	01052700	146.42	38.14	1002.5	18.4	87	292	8.8	37.7	22,544	10	Sc
22	01052712	144.07	40.00	1004.8	11.1	93	40	4.2	61.2	19,455	10	-
23	01052800	141.38	41.54	1007.0	11.5	88	270	1.6	50.6	20,585	10	Sc

8. Aerosol Observations

8.1 Background of ACE-Asia

Kazuhiko Miura (Department of Physics, Science University of Tokyo)

Atmospheric aerosol particles affect the Earth's radiative balance directly by scattering or absorbing light, and indirectly by acting as cloud condensation nuclei (CCN), thereby influencing the albedo and life-time of clouds. The natural aerosol has been substantially perturbed by anthropogenic activities, particularly by increases of sulfates, nitrates, organic condensates, soot, and soil dust. The present day global mean radiative forcing due to anthropogenic aerosol particles is estimated to be between - 0.3 and -3.5 Wm^{-2}, which must be compared with the present day forcing by greenhouse gases of between +2.0 and +2.8 Wm^{-2} (IPCC, 1995).

Although aerosol particles have this potential climatic importance, they are poorly characterized in global climate models. This is a result of a lack of both comprehensive global data and a clear understanding of the processes linking aerosol particles, aerosol precursor emissions, and radiative effects. At this time, tropospheric aerosols pose the largest uncertainty in model calculations of the climate forcing due to man-made changes in the composition of the atmosphere. Clearly there is an urgent need to quantify the processes controlling the natural and anthropogenic aerosol, and to define and minimize the uncertainties in the calculated climate forcings. Among the largest sources of uncertainty is the climate forcing by Asian aerosols.

The Aerosol Characterization Experiments (ACE) , which are sponsored by the International Global Atmospheric Chemistry Program (IGAC), are envisioned as a series of international field studies aimed at understanding the combined chemical and physical processes that control the evolution of those aerosol properties that are relevant to radiative forcing and climate. The ultimate goal of this series of studies is to provide the necessary data to incorporate aerosols into global climate models and to reduce the overall uncertainty in the climate forcing by aerosols.

The strategy of ACE is to investigate the multiphase atmospheric system in key areas of the globe. ACE-1, conducted in late 1995, was aimed at the minimally polluted marine troposphere in the Southern Ocean near Tasmania. TARFOX, conducted in June of 1996, studied continental aerosol off the eastern coast of North America. ACE-2, conducted in June of 1997, focused on anthropogenic aerosols from the European continent and desert dust from the African continent as they move over the North Atlantic Ocean.

ACE Asia, of which intensive observations are planned in spring 2001 and 2003, will focus on the outflow of both desert dust and anthropogenic aerosol from Eastern Asia to the Pacific Ocean. The goal of ACE Asia is to determine and understand the properties and controlling factors of the aerosol in the anthropogenically modified atmosphere of Eastern Asian and the Northwest Pacific and to assess their relevance for radiative forcing.

The R/V Mirai is elected as the platform of Japanese shipboard observation. The MR00-K04 cruise was regarded as the pre-ACE Asia cruise by all Japan researchers. PIs and on board members of the pre-ACE Asia group were shown in Tables 8.1-1 and 8.1-2, respectively. The MR01-K02 cruise was regarded as the ACE Asia cruise. Pis and on board members of the ACE Asia group were shown in Tables 8.1-3 and 8.1-4, respectively.

Table 8.1-1 Participating Organizations of pre-ACE Asia group

Participating Organizations	PI
Institute of Low Temperature Science, Hokkaido University (ILTSa)	Kimitaka Kawamura
Institute of Low Temperature Science, Hokkaido University (ILTSb)	Tatsuo Endo
Faculty of Engineering, Hokkaido University (HU)	Sachio Ohta
Ocean Research Institute, University of Tokyo (ORI)	Mitsuo Uematsu
Faculty of Science, Science University of Tokyo (SUT)	Kazuhiko Miura
National Institute for Environmental Studies (NIES)	Nobuo Sugimoto
Japan Ocean Science and Technical Center (JAMSTEC)	Kunio Yoneyama

Table 8.1-2 On Board members of pre-ACE Asia group

Scientists
Mutsuhiro Mochida (ILTSa), Kiyoshi Matsumoto (ORI), Kazuhiko Miura (SUT),
Technicians
Ichiro Matsui (NIES)
Students
Masahiro Narukawa (ILTSa), Yuji Fujitani (HU), Takeshi Hara (SUT), Takeshi Ui (SUT), Takeshi Kishida (SUT)

Table 8.1-3 Participating Organizations of ACE Asia group

Participating Organizations	PI
Institute of Low Temperature Science, Hokkaido University (ILTSa)	Kimitaka Kawamura
Institute of Low Temperature Science, Hokkaido University (ILTSb)	Tatsuo Endo
Faculty of Engineering, Hokkaido University (HU)	Sachio Ohta
Ocean Research Institute, University of Tokyo (ORI)	Mitsuo Uematsu
Research Center for Advanced Science and Technology, University of Tokyo (RCAST)	Yoshizumi Kajii
Faculty of Science, Science University of Tokyo (SUT)	Kazuhiko Miura
Faculty of Environment, Nagoya University (NU)	Ippei Nagao
National Institute for Environmental Studies (NIES)	Nobuo Sugimoto
Communications Research Laboratory (CRL)	Hiroshi Kumagai
Japan Ocean Science and Technical Center (JAMSTEC)	Kunio Yoneyama

Table 8.1-4 On Board members of ACE Asia group

On Board (12 persons)
Scientists
Kazuhiko Miura (SUT), Shungo Kato (RCAST), Ippei Nagao (NU), Nobuo Sugimoto (NIES), Akihide Kamei (CRL)
Technicians
Kazutake Ohta (ORI), Ichiro Matsui (NIES)
Students
Sou Matsunaga (ILTSa), Yuji Fujitani (HU), Atsushi Ooki (ORI), Ryo Ashikawa (SUT), Takahito Inaba (SUT)

8.2 Gas measurements

Personnel

Shungo KATO, Jun Matsumoto, Yoshizumi Kajii (Research Center for Advanced Science and Technology, The University of Tokyo)

(2) Objectives

The polluted air emitted in East Asia is transported to the Pacific and would be affect the air quality in a remote place. The gas measurements on a ship in the western Pacific would contribute to elucidate of the long-range transport of polluted air from East Asia. Also, some gases emitted from the ocean were measured.

(3) Measured parameters

Carbon monoxide (CO), Ozone (O_3), Sulfur dioxide (SO_2), Nitric oxide (NO), Nitrogen oxides (NO_x), Hydrocarbons (HC).

(4) Method

CO was measured by an IR-Gas filter correlation analyzer (Thermo Environmental Instruments, Model 48C). O_3 was measured by an UV absorption analyzer (Thermo Environmental Instruments, Model 49C). SO_2 was measured by an UV-Fluorescence analyzer (Thermo Environmental Instruments, Model 43C Trace Level). NO and NO_x were measured by an Ozone-Chemiluminescence analyzer (Thermo Environmental Instruments, Model 42S). These gases were analyzed continuously on the ship and minutely average data was logged by a personal computer. The detection limits were estimated 10 ppbv, 1.0 ppbv, 0.1 ppbv, 0.05 ppbv, 0.05 ppbv for CO, O_3, SO_2, NO and NO_x, respectively. Zero gas was automatically injected for 15 minutes every hour for CO and SO_2, and manually injected twice times in a day for NO and NO_x. The air was taken through a 1/4 PFA tube from the side of the compass deck for these measurements. The air for hydrocarbon measurements was sampled into Silcosteel canisters (Restek) using a bellows pump and was analyzed by Pre-concentrator (Entech7000) and GC-FID (Hewlett Packard, HP6890) in the laboratory in The University of Tokyo.

(5) Results

In Figure 8.2-1, the results of CO, O_3, SO_2, NO and NO_x are shown against date. Before leaving Yokosuka (before May 14 morning), high concentrations of CO and SO_2 were observed. NO and NO_x were not measured when the ship was stayed at Yokosuka to keep clean condition in the analyzer, but very high concentration was expected there. O_3 concentration was high in daytime since photochemical production was enhanced in polluted urban atmosphere. But O_3 concentration decreased during night since O_3 decreased by the reaction with NO and no production reaction occurred without sunlight. After leaving Yokosuka, the air become clean gradually and CO, SO_2, NO and NO_x concentrations decreased. On May 15, only the concentration of SO_2 become increased, but the reason is unknown. In the afternoon on May 16, the air was affected by the exhaust form the ship itself, and high concentrations of SO_2, NO and NO_x were observed. O_3 was reacted with NO and decreased when the exhaust affected. On May 17, a low pressure passed and clean maritime air with low CO and O_3 concentrations were observed. During May 18 - 21, the air condition seems stable. After May 22, there are many peaks of NO, NO_x and SO_2. These spikes were caused by the exhaust from the ship itself. On May 24, low pressure passed and very clean maritime air were observed. O_3 decreased to about 10 ppbv, and CO also decreased. On May 27, polluted air from Japan transported and high O_3, SO_2, and NO_x were observed. High concentration of NO_x without involving high NO would be old air-mass: long-range transported polluted air. Because the lifetime of NO is short. And when high NO is observed, the air is freshly polluted and the pollutants emitted from near place.

The concentrations of hydrocarbons which mainly originated from human activity (ethane, propane, butane, pentane, acetylene, benzene etc.) changed similar as O_3 concentration, rather than CO. Low concentration appeared in May 17 and May 24. In the cases of ground-base measurements at other places, these hydrocarbons have good correlation with CO, but not with O_3. Ethane concentration is shown in Figure 8.2-2 compared with CO and O_3 concentrations. This difference is interesting, but there is no suitable explanation at this moment.

Some biogenic hydrocarbons were also measured. Ethylene (C_2H_4), which is originated from both anthropogenic and biogenic activity, show different trend from the anthropogenic hydrocarbons.

There should be a parameter which control the concentration of ethylene, if it mainly produced from biogenic activity in the Ocean, but the parameter is not identified at a moment. Isoprene is mainly emitted from the plants on land. But the life time of isoprene in the atmosphere is only a few hour and it is not probable to transport from the land to the ocean. It is suggested ocean also produce isoprene by biogenic activity. In this cruise observed isoprene concentration is almost lower than the detection limit , but high concentration were observed on May 19. The area where the ship traveled on May 19 would be a high biogenic activity, or the weather would be a favorable to biogenic activity (May 19 was sunny day).

(6) Data archives

The original data will be archived at RCAST, The University of Tokyo (Contact Shungo KATO).

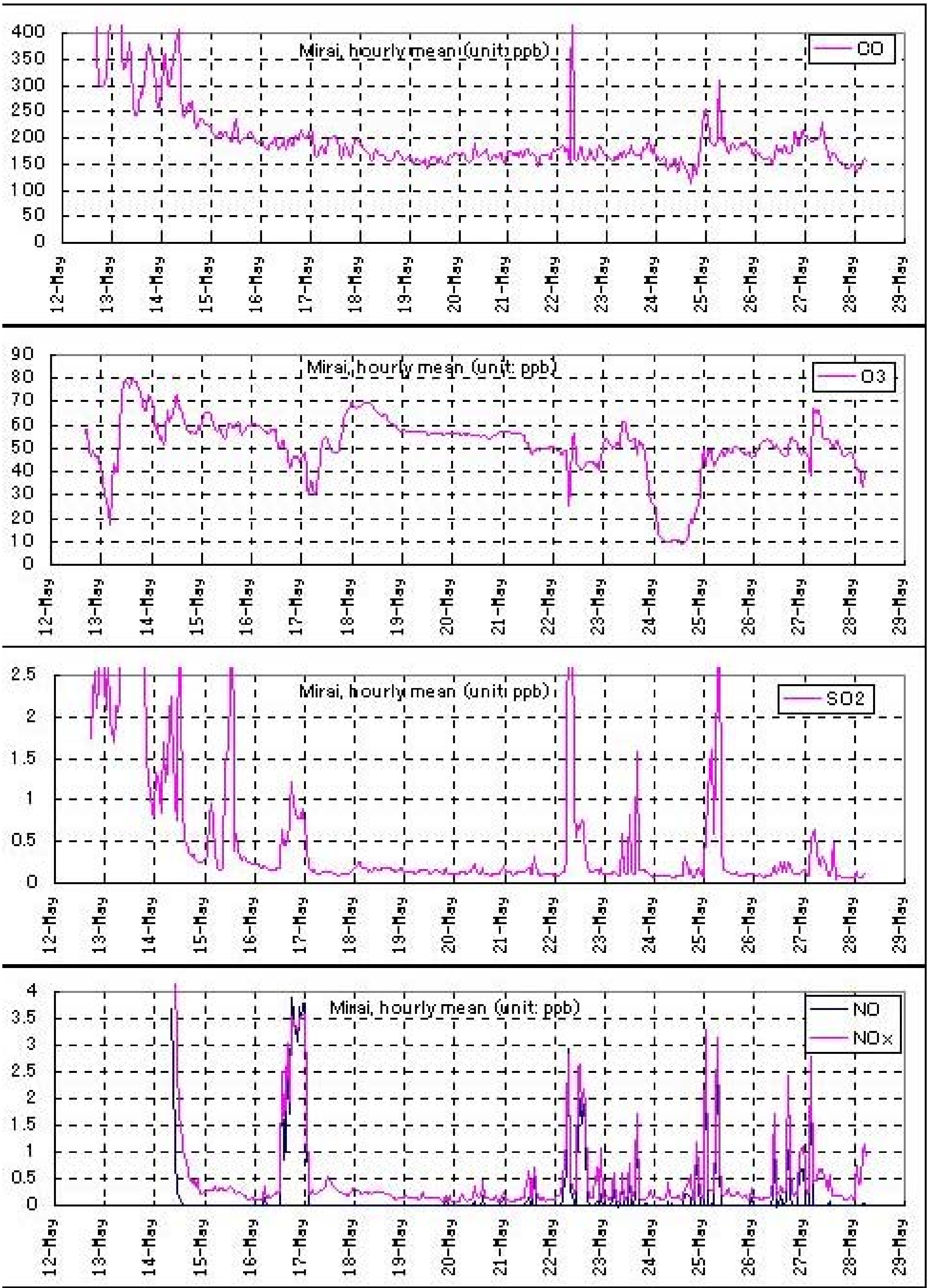

Figure 8.2-1 Concentrations of CO, O_3, SO_2, NO and NO_x.

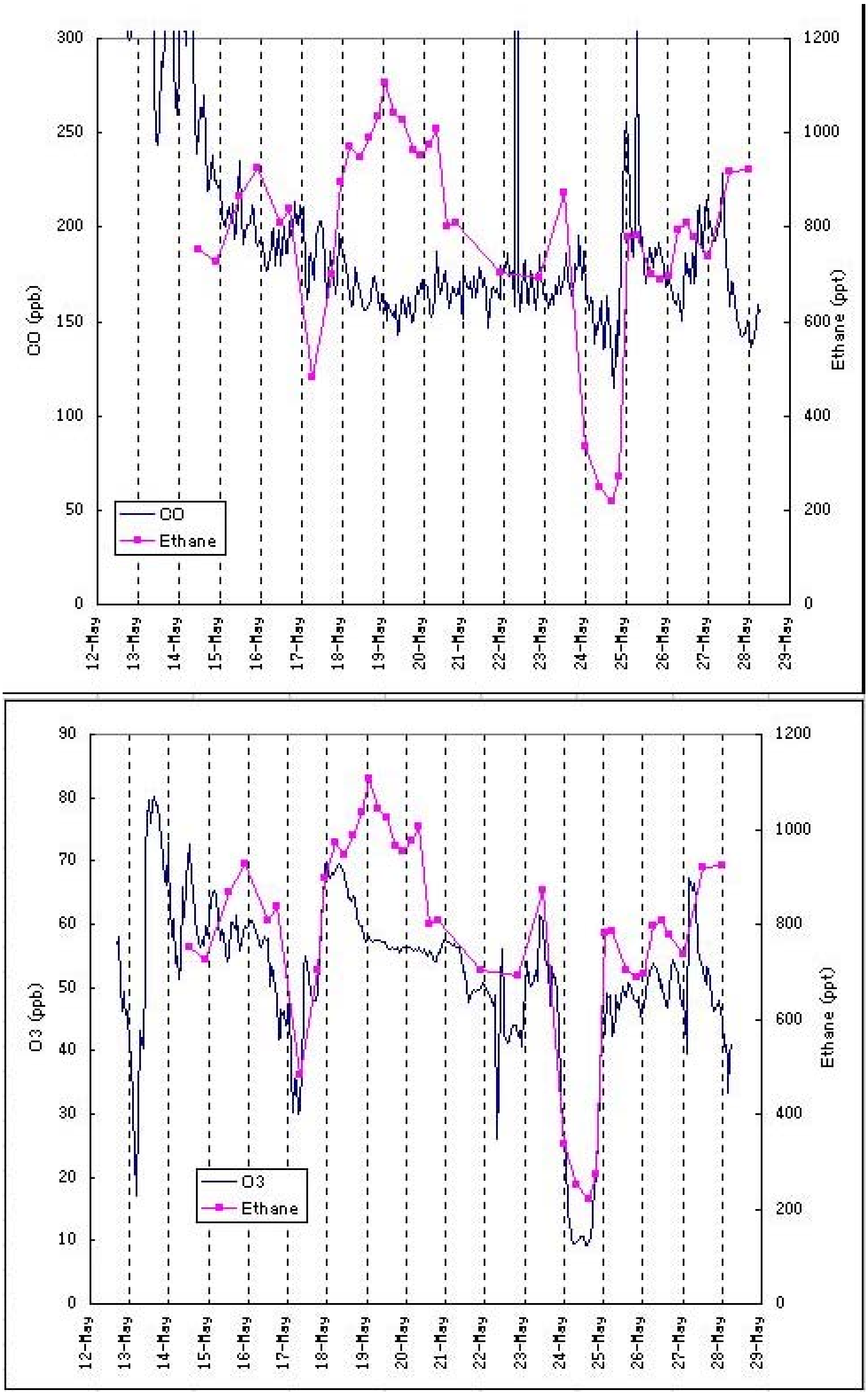

Figure 8.2-2 Comparison with ethane and CO, O_3 concentrations.

8.3 Distributions of atmosphere and seawater DMS

(1) Personnel

Ippei Nagao (Graduate School of Environmental Studies, Nagoya University,)

(2) Objectives

It is widely accepted that DMS is one of the major precursors of non-sea salt sulfate aerosols in the marine air and can contribute to the atmospheric sulfur cycle. DMS is produced by the phyto-plankton in the surface seawater and released to the atmosphere. The emission rate of DMS to the atmosphere can be partly dependent on the seawater DMS distribution.

Western North Pacific Ocean is a research field of Aerosol Characterization Experiment (ACE-Asia), and DMS is one of key parameters to this experiment. Objectives of the measurement on this cruise (MR01-K02) is to obtain the spatial distributions of DMS in the surface seawater and atmosphere, and to estimate the emission rate to the atmosphere in this area.

(3) Measured parameters

Continuous measurement of the atmospheric DMS concentration was automatically carried out during this cruise almost at every 90 min. except for the seawater DMS analysis. The seawater DMS concentration (at 10 m depth) was also measured at each CTD observation point along 146° 25′ E.

(4) Method

DMS was measured by Shimdzu GC-14B equipped with a flame photometric detector (GC/FPD) and β-β' ODPN glass column.

①Atmospheric DMS concentration

Air was introduced from the port side of the R/V Mirai with 5 m long Teflon-tube (ID is 12 mm). Sampling flow rate is set approximately at 85 ml L^{-1} and atmospheric DMS was cryotrapped in a U-shaped glass tube filled with Tenax-GR in cooled ethanol (approximately –60 ℃) after removing water vapor and oxidant. After 60 min. of sampling, DMS was desorbed by heating of the concentration tube at +140 ℃ within 3 min. and introduced to GC/FPD. During these steps, the air flow rate and temperature of the concentration tube were monitored and recorded by personal computer at every 10 seconds.

②Seawater DMS

Surface sea water was sampled by Rossett water sampler at 10m depth at almost every 15′ in latitude from 30° 00′ N to 36° 45′ N. Surface seawater was introduced to 100-mL pyrex vials. The water samples was immediately transferred to a 30 mL glass syringe, and 20 mL of sea water was introduced to a degasification vessel. Samples were sparged with N_2 gas (60 mL min^{-1}) for 20 min. The extracted gas was then dried by using a Nafion drier and cryotrapped in a U-shaped glass tube in cooled ethanol (approximately –60 ℃). This concentration tube was subsequently heated (approximately 140 ℃), releasing the extracted gas onto GC column. Two or three samples was analyzed to determine the seawater DMS concentrations at each point.

(5) Results

Fig. 1 shows the latitudinal distribution of the sea water DMS concentration along 146° 25′ E, ranging between 0.4 and 2.0 nmol l^{-1} except for the sample at 36° 45′ N. Taking into consideration of the location of the Kuroshio current, the seawater DMS concentration in the open sea is less than 2.0 nmol l^{-1}. Although the sample number was one, sharp increase of DMS concentration at 36° 45′ N was observed, suggesting that the seawater DMS concentration might be much higher in the coastal sea region than those in the open sea.

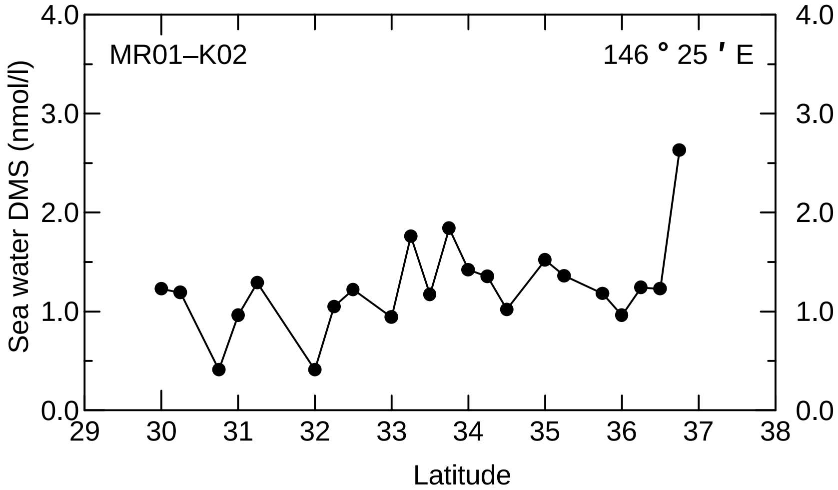

Fig. 1. Latitudinal distribution of DMS in the surface seawater along 146 ° 25 ′ E.

In order to make sure that the air sampling system operates successfully, time series of flow rates and temperature of the concentration tube was shown in Fig. 2. Cryogenic sampling and purge steps were repeated successfully. Atmospheric DMS concentration was determined from the sampling volume of air and the area of chromatogram calibrated by the DMS standard gas.

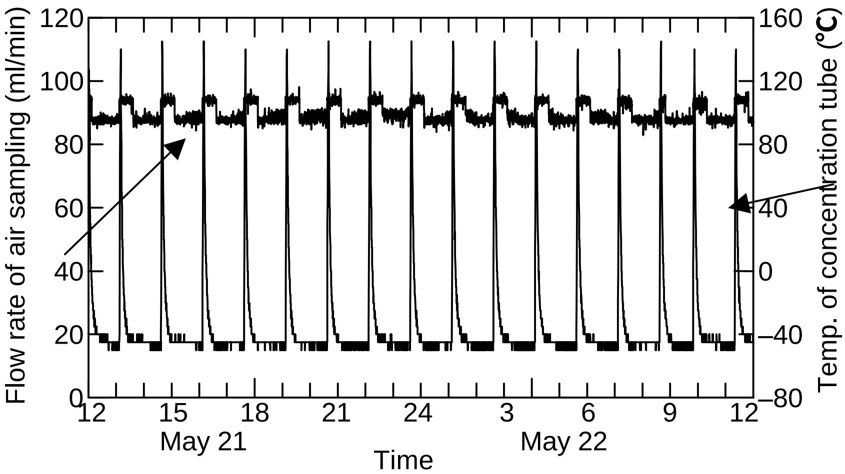

Fig. 2. Time series of sampling flow rate of air and temperature of the concentration tube.

Fig. 3 shows the atmospheric DMS concentration during this cruise. High concentration period (> 200pptv) was observed May 24 when maritime air mass was transported by the low-pressure system. Very low concentration was observed between May 18 to 20 showing less than the detection of this system (< about 8 pptv of DMS in the 5.1 liter of air).

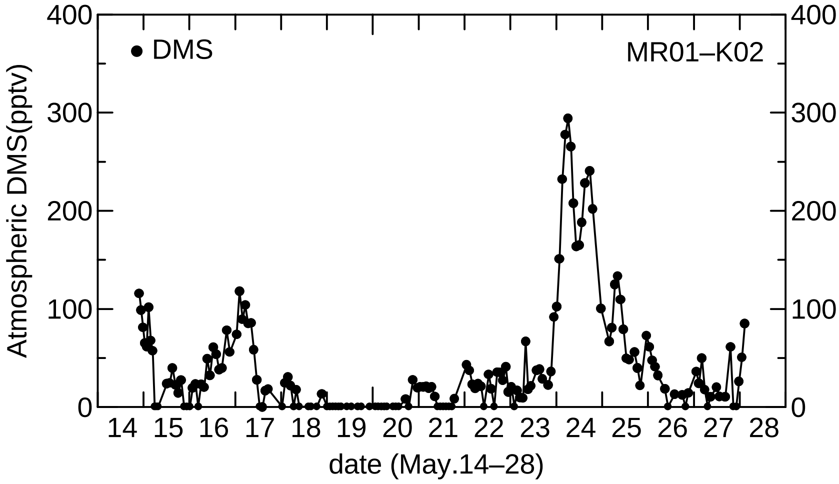

Fig. Time series of the atmospheric DMS concentration.

(6) data archive

All of raw and processed data will be submitted to JAMSTEC Data Management Office and will be under its control.

8.4 Studies on the aerosol formation from VOCs

(1) Personel

On board scientists:
Sou Matsunaga (Hokkaido University)

Co-workers not on board:
Kimitaka Kawamura (Hokkaido University)
Michihiro Mochida (Hokkaido University)
Takuya Saito (Japan Science and Technology Corporation, Hokkaido University)

(2) Objectives

Atmospheric chemical reactions between volatile organic compounds (VOCs) and atmospheric oxidants such as OH, ozone and nitrate radical in the existence of NOx causes production of tropospheric ozone. Tropospheric ozone is known as a greenhouse gas, but the oxidation products of VOCs are water soluble and are tend to transfer particle phase (aerosols).

Aerosols are thought to be directly and indirectly cooling the global climate. Biogenic VOCs such as isoprene which is derived from phytoplanktons in surface seawater are emitted from sea water to atmosphere. Isoprene is thought to be oxidized by OH, ozone and nitrate radical in the atmosphere and changes to unsaturated carbonyl compounds such as methacrolein and methylvinylketone. These oxidation products are also oxidized to hydroxycabonyl compounds such as hydroxyacetone and glycolaldehyde. In this study, we measured isoprene in surface seawater samples and ambient air samples *in situ* for calculating sea to air flux of isoprene, and collected the oxidation products of isoprene by annular denuder sampling system. And we also collected aerosol samples by MOUDI (micro orifice uniform deposit impactor) and high volume air sampler for clarify distributions of organic compounds in marine aerosols.

(3) Methods

Analysis of Isoprene:

Fourteen surface seawater samples and nine ambient air samples were *in situ* analyzed by GC/MS (Finnigan MAT GCQ) on R/V Mirai. Surface seawater samples (10m) were collected from niskin bottle into 600mL grass vial. Isoprene in the samples were immediately extracted by helium gas bubbling 40 min and analyzed by cryo focus GC/MS. Ambient air samples were collected into 6L stainless steel by canister using of an air compressor at compass deck of Mirai and analyzed by cryo focus GC/MS after approximately 1 hour of sampling.

Denuder Sampling:

Semi-volatile organic compounds (carbonyls and diacids) were collected by annular denuder sampling system. The compounds in the gas and particle phase were trapped on denuder and quartz fiber filters, respectively. Seven sets of samples were collected. One set of denuder sample includes one extract from denuder (gaseous compounds), one quartz fiber filter (paticulate compounds) and one extract from backup denuder (particulate compounds evaporated from filter). These extracts and filters were stored at -20 °C prior to analysis. Sampling flow rate were 4L/min (for carbonyls) and 10L/min (for diacids). These denuder samples will be determined by GC/FID.

High Volume Air Sampler and MOUDI:

Six and four aerosol samples were collected by high volume air sampler and MOUDI, respectively. These samples (quartz fiber filters and aluminum foils) were stored at -20 °C prior to analysis.

(4) Results

Follows are concentrations of isoprene in the seawater and air samples.

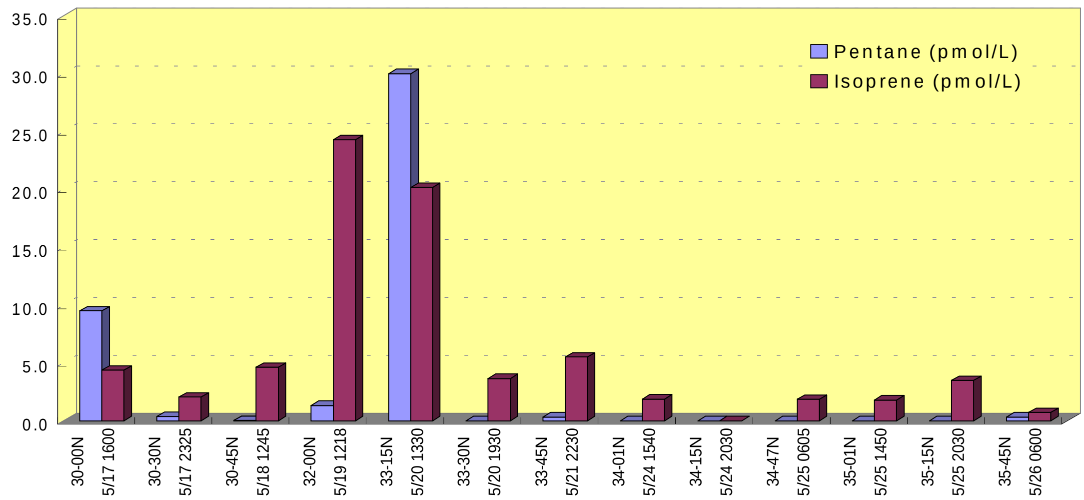

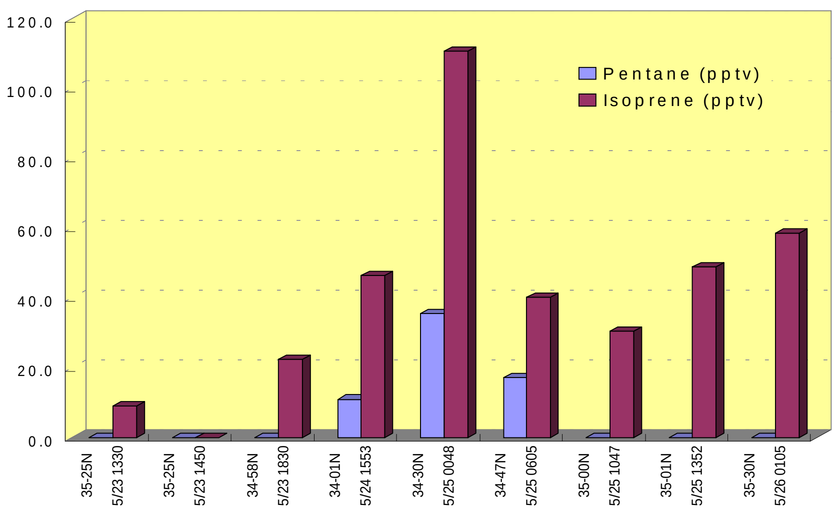

(5) Data Archive

All samples will be archived in Institute of Low Temperature Science, Hokkaido University. The inventory information of the samples is submitted to JAMSTEC DMO.

8.5 Chemical properties of aerosol

(1) Personnel

Mitsuo Uematsu (Ocean Research Institute, The University of Tokyo): Principal Investigator
Kazutake Ohta (Ocean Research Institute, The University of Tokyo / Japan Science and Technology Corporation)
Atsushi Ooki (Ocean Research Institute, The University of Tokyo)

(2) Objectives

In order to investigate the chemical properties of marine aerosols over the western North Pacific Ocean, measurements and sampling of atmospheric aerosols were carried out. Carbonecious aerosols occupy about 50% of total aerosol in continental air, however, field observations are not enough. Especially, few measurement of carbonecious aerosols in the marine atmosphere was carried out, so we tried to determine the spatial distributions of EC (elemental carbon) and OC (organic carbon) over the western North Pacific Ocean. Recently, sulfate aerosol in marine atmosphere has been measured in various locations, and meridional variability of sulfate became clear. Many specific characteristics of sulfate are, however, not clear. We conducted the size-fractionated aerosol sampling together with the particle number measurements, and examined the specific characteristics of sulfate aerosol in detail. In addition, the concentration of ozone was also measured simultaneously.

(3) Measured parameters

Carboneceous aerosol concentration: Organic carbon and Elemental carbon.

Bulk aerosol concentration (Hivolume aerosol sampler): MSA, Cl^-, NO_3^-, SO_4^{2-}, Na^+, NH_4^+, K^+, Mg^{2+}, and Ca^{2+}.

Bulk aerosol and acid gases concentrations (Filter pack system): MSA, Cl^-, NO_3^-, SO_4^{2-}, Na^+, NH_4^+, K^+, Mg^{2+}, Ca^{2+} , SO_2, and HNO_3.

Size-fractionated aerosol concentration (Low pressure impactor : 50% cut off diameter 0.06, 0.13, 0.22, 0.33, 0.52, 0.76, 1.25, 2.5, 3.9, 5.7, 8.5, and 12.1 μm, and back up filter) : Cl^-, NO_3^-, SO_4^{2-}, Na^+, NH_4^+, K^+, Mg^{2+}, and Ca^{2+}.

Size-fractionated aerosol concentration (virtual impactor): Trace metals.

Size-fractionated aerosol concentration (Low volume impactor): Organic nitrogen

Particle number concentration for large particle (RH50% humidity control): Particle number concentration (0.3, 0.5, 1.0, 2.0, and 5.0 μm in diameter range)

Particle concentration for large particle (in situ condition): Particle number concentration (0.3, 0.5, 1.0, 2.0, and 5.0 μm in diameter range)

Particle concentration for fine particle (in situ condition): Particle number concentration (0.1, 0.15, 0.2, 0.3, and 0.5 μm in diameter range)

Ozone concentration

(3) Methods

The concentrations of carbonaceous species (organic carbon and elemental carbon) in aerosols were measured for every 2 hours by using an Ambient Carbon Particulate Monitor (Rupprechet & Patashnick Co. Inc., Model 5400). The inlets of air were located on the compass deck (about 17m above the sea surface).

Bulk aerosol samples were collected for about 24 hours periods on cellulose acetate filters (Whatman 41) by a high-volume air sampler (Kimoto Electric Co. Inc., Model AS-810). Sample of bulk aerosol and acid gases samples were collected for 12 hours period by using a Nuclepore filter and an alkaline immersed filter by a filter pack system. Size-fractionated aerosols for trace metals were collected on polyflon filter (ADVANTEC PF040) by a high-volume virtual impactor PM2.5 (Kimoto Electric Co. Inc., Model AS 9) at 24 hours intervals, a low-volume impactor at 6 days intervals, and a low pressure 12 stages impactor (Tokyo Dylec, Model LP-20) at about 2 days intervals. In order to avoid contamination from ship exhaust, all aerosol samplers were automatically controlled by a wind sector to activate sampling only when the relative wind direction ranged from -90 ° to 90 ° of the bow and the relative wind speed was higher than 1.0m/s. The collections of aerosols were carried out on the compass deck.

After this cruise, the samples of aerosols and acid gases (SO_2 and HNO_3) will be analyzed for chemical components (major inorganic ions and organic species).

Particle number concentrations were measured for 2.5 minutes periods by optical particle counter. Sampling air flow was controlled at RH50% for large particle number measurements, and air flows were kept the same temperature as outside air for large and fine particle number concentrations.

The concentration of ozone was measured at 12 second intervals by using an ozone monitor (Dylec, Model 1150).

(4) Results

Carboneceous aerosol concentrations were obtained continuously.

Bulk aerosol concentrations (Hivolume aerosol sampler): 14 samples were obtained.

Bulk aerosol and acid gasese concentrations (Filter pack system): 24 samples were obtained.

Size-fractionated aerosol concentrations (Low pressure impactor): 8 samples were obtained.

Size-fractionated aerosol concentrations (virtual impactor): 12 samples were obtained.

Size-fractionated aerosol concentrations (Low volume impactor): 2 sampels were obtained.

Particle number concentrations for large particle (humidity control): Particle number concentrations were obtained continuously.

Particle number concentrations for large particle (in situ condition): Particle number concentrations were obtained continuously except for one day.

Particle concentrations for fine particle (in situ condition): Particle number concentrations were obtained continuously.

Ozone gas concentration was obtained continuously.

All of aerosols samples will be analyzed at Ocean Research Institute (ORI), the University of Tokyo.

(5) Data Archives

The data of the concentrations of aerosols and acid gases in this cruise will be archived at Ocean Research Institute (ORI), the University of Tokyo. The samples of aerosols and acid gases collected in this cruise will be stored at ORI, and then analyzed for chemical components.

8.6 Measurement of aerosol optical properties and chemical composition

(1) Personnel
On board scientists
Yuji Fujitani (Graduate school of Engineering, Hokkaido University) Graduate student of Doctor Course

Co-workers not on board
Tatsuo Endoh (Institute of Low Temperature Science, Hokkaido University): Associate Professor
Sachio Ohta (Graduate school of Engineering, Hokkaido University): Professor
Tamio Takamura (Center for Environmental Remote Sensing, Chiba University): Professor
Teruyuki Nakajima (Center for Climate System Research, University of Tokyo): Professor

(2) Objectives
It is necessary to measure spatial distribution and variation of optical properties and chemical species of the atmospheric aerosol to estimate the radiative forcing. But, there are no data available of aerosol properties on the western Pacific Ocean.
We, thus, measure the distribution of aerosol optical thickness, volume scattering coefficient, volume absorption coefficient, size distribution and chemical properties of atmospheric aerosols on the Pacific Ocean east of Japan.

(3) Measured parameters
Obtained parameters and samples inventory are shown in table 8-6-1 and in table 8-6-2.

Table 8-6-1 Obtained data inventory

Parameter	Period, Cycle	Instruments	Data Status / Data Format	comment
Optical thickness and size distribution	May14〜28 every 5min	Sky Radiometer (PREDE,POM-01MKII)	ASCII	measurement in clear sky
Aerosol size distribution	May14〜28 every 1min	Optical Particle Counter (RION,KC-01C)	ASCII	
Scattering coeffcient	May14〜28 every 1min	Intgrating Nephelometer (Radiance Research Model 903)	ASCII	
Absorption coefficient	May14〜28 every 1min	Particle Soot/ Absorption Photometer (Radiance Research)	ASCII	

Table 8-6-2 Obtained sample inventory

Parameter	Period, # of Samples	comments
Teflon filter	May14〜28 13 samples	After sampling kept in refregiator
Quartz fiber filter	May14〜28 9 samples	After sampling kept in refregiator

(4) Methods

Sky Radiometer (POM-01MKⅡ; PREDE), equipped on deck, measures direct and scattering solar radiation. The data provide optical thickness, Åangstrom exponent and size distribution of atmospheric aerosols.

Sample air is drawn through inlets 5m height on compass deck, to manifold in research room. Particle larger than 2 μm in diameter are removed by cyclone separators. From the manifold, the sample air is distributed to Particle Soot / Absorption Photometer (PSAP; Radiance Research), Integrating Nephelometer (IN; M903; Radiance Research) and Optical Particle Counter (OPC; KC-01C; RION). PSAP measures volume absorption coefficient, IN measures volume scattering coefficient and OPC counts number concentration of aerosols larger than 0.3, 0.5, 1.0, 2.0 and 5.0 μm in diameter. The aerosols are also collected on filter for chemical analysis by using another sampling system. The sampling system consists of three parts. One is Teflon filter sampling line (FP-500; 47mmφ; SUMITOMO DENKOH), the other is quartz fiber filter sampling line (2500QAT-UP; 47mmφ; Pallflex). And another is teflon and quartz fiber filters in tandem use line. Filter sampling is performed with the special cautions not to be contaminated by chimney exhaust. The filters are stored in the refrigerator. From the aerosols collected on Teflon filters, amounts of inorganic and metal components are analyzed by Ion chromatography and ICP-MS. From the sample on quartz fiber filters amounts of analyzed elemental and total carbons are determined by carbon analyzer.

(5) Results

The sky radiometer has been going well owing to more calm, silent condition and circumstances about shivering problems provided by the R/V Mirai, whose engines are supported by well defined cushions. Therefore, measured values will be expected to be considerably stable and provide good calculated parameters in higher quality. However, some noise waves were found to interfere the 16,13 and 12channel marine bands of VHF from sky radiometer. Fortunately the origin and source were identified by using a VHF wide band receiver and the interference waves were kept by fairly separating from two VHF antennae and decreased to recovery of 100%.

The volume scattering and absorption coefficients were, respectively, $1\sim3\times10^{-5}m^{-1}$ and $0.1\sim5\times10^{-6}m^{-1}$. Particle concentration larger than 0.3 μm was $3\sim150\times cm^{-3}$.

(6) Data archive

The data of PSAP, IN, OPC and skyradiometer are numerically analyzed and filter samples are chemically analyzed. All data are archived at Hokkaido University (Endoh and Ohta), University of Tokyo (Nakajima) and Chiba University (Takamura), and submitted to JAMSTEC within 3-years.

8.7 Study on the transport process and the modification of aerosols

(1) personnel

Kazuhiko Miura , Ryo Ashikawa, Takahito Inaba (Department of Physics, Science University of Tokyo)

(2) objectives

It is important to know aerosol profile in the lower troposphere for the process study of aerosol transport from continental to the remote ocean. There is no observation in the planetary boundary layer (PBL), however there are a few observations in the free troposphere (FT). In this work, we observed aerosol behaviors in the PBL by using kytoon system over the ocean.

Main purposes of our observation are as follows:

(a) Measuring the entire size distribution with three instruments
(b) Obtaining the residence time of aerosols with radon and thoron measurements
(c) Investigating the mixing condition of individual particles with TEM/EDX analysis
(d) Simultaneous sampling on surface and by kytoon system

(3) measured parameters

- size distribution
  scanning mobility particle sizer : 3936N25 (3085 + 3025A), TSI Inc. (44<d<168nm)
  optical particle counters : KC18 and KC01, Rion Co. Ltd.
  (d>100, 150, 200, 250, 300, 500, 1000, 2000, 5000 nm)
- total concentration of particles
  condensation nuclei counter : 3022A, TSI Inc.
- radon daughter concentration
  radon daughter monitor : ES-7269, JREC Co. Ltd.
- particle concentration profile with kytoon system
  kytoon : 10 m^3 in volume
  optical particle counter (d>300, 500, 700, 1000, 2000, 5000 nm) : KR12, Rion Co. Ltd.
- solar radiation
  portable sunphotometer (λ: 368, 500, 675, 778, and 862 nm) : MS-120(S), Eko Co.
- shape and elemental composition of aerosols
  sampling : cascade impactor : Model I-1L, PIXE Int. Corp.
  carbon-covered nitrocellulose film supported on an electron microscopic grid
  analysis : an energy dispersive X-ray spectrometer : Kevex Sigma

(4) method

In order to examine the transport process and the modification of aerosols, we measured the complete size distribution from 4.4 to 5000 nm in diameter with scanning mobility particle sizer (3936N, TSI Inc.) and two optical particle counters (KC18 and KC01D, RION Co. Ltd.) every five minutes. We also measured radon daughter concentration with radon daughter monitor (ES-7269, JREC Co. Ltd.) every four hours.

We also performed the kytoon observation up to 1000 m at eight stations (Table 8.7.1). Aerosol particles larger than 0.15 μm in radius were counted with the KR12 and temperature and relative humidity were measured for 1 min at every 50 m. Aerosol particles were collected directly on a carbon-covered nitrocellulose grid with two impactors for 10 min at the highest level and on the compass deck at the same time (Table 8.7.2). The electron micrograph will be obtained using a scanning electron microscope (Hitachi Co., H-9000). The elemental compositions in individual particles larger than 0.1 μm in radius will be analyzed with an energy dispersive X-ray spectrometer (Kevex Sigma).

(5) results

Variations of radon concentration (shown as peak counts) and total particle concentration are shown in Figs. 8.7.1 and 8.7.2, respectively. Radon and total particle concentration decreased as leaving the Japan Islands. The decreasing rate of particle was greater than that of radon.

An example of aerosol profile on 26 May 2001 with optical sonde on the kytoon system is shown in Fig. 8.7.3. This shows that there is a boundary at about 600 m in length and the concentration of smaller particles in the upper layer is higher than that in the under layer. The further analyses are in future work.

(6) data archive

The original data will be archived at Department of Physics, Science University of Tokyo (Contact Kazuhiko Miura).

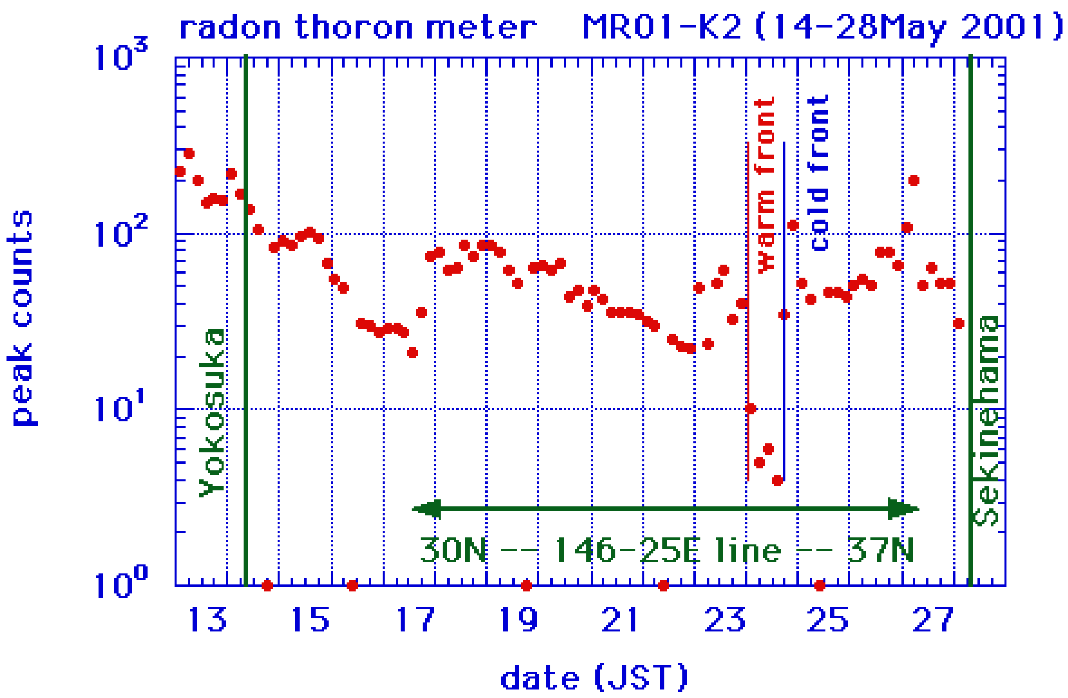

Fig. 8.7.1 Variation of radon concentration (peak counts).

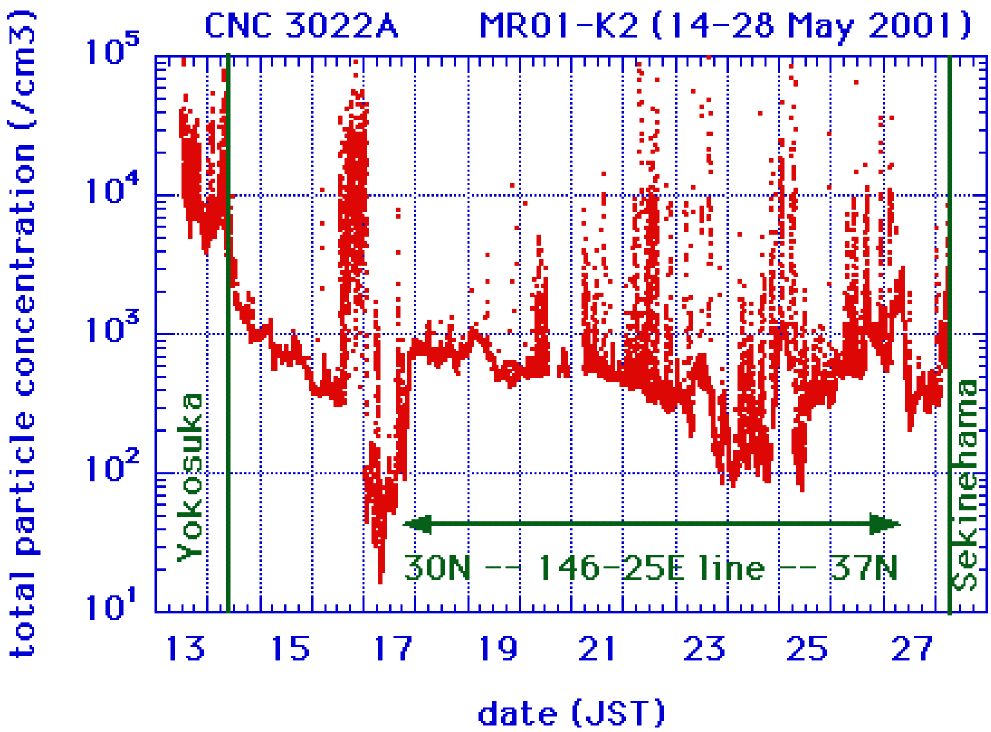

Fig. 8.7.2 Variation of total particle concentration.

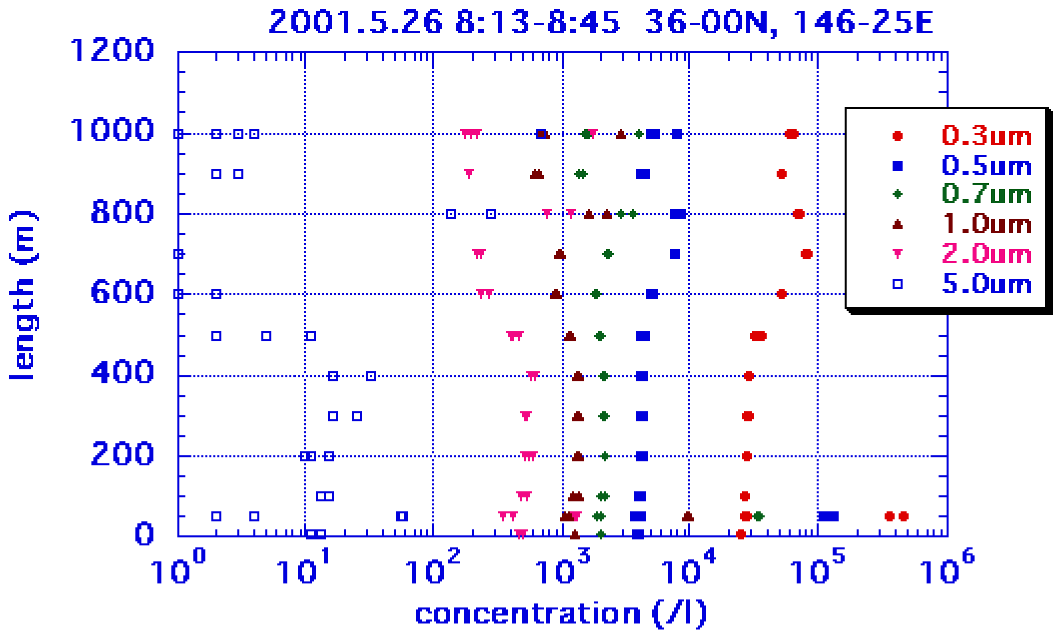

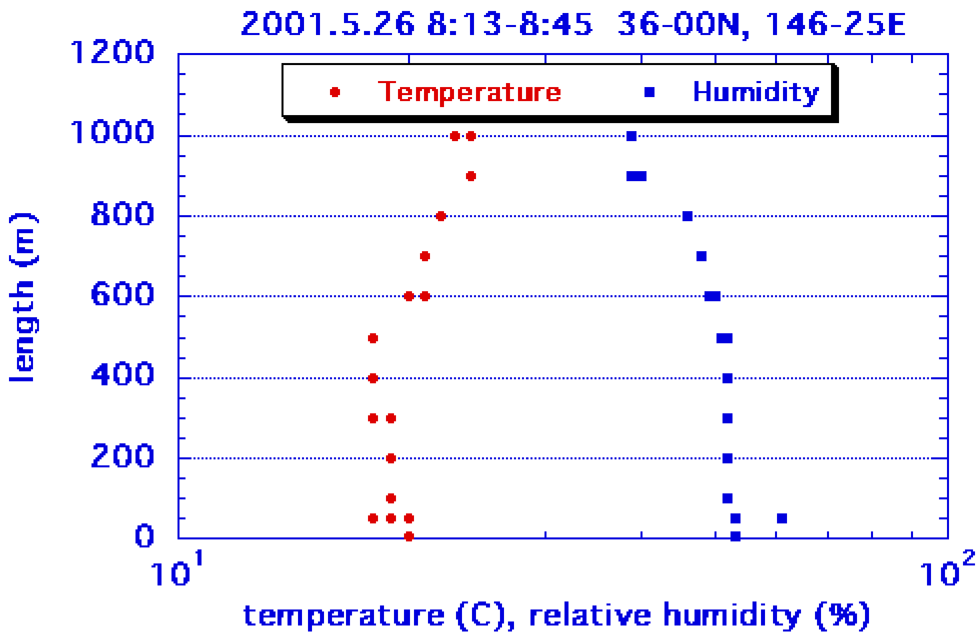

Fig. 8.7.3 Upper : An example of aerosol profile at 0813 to 0845 JST on 26 May 2001, at (36N, 146-25E) with optical sonde on the kytoon system.
Lower : Temperature and relative humidity profile measured at the same time.

Table 8.7.1 Measuring list of the number concentration profile with OPC on the kytoon.

No.	date	start time	stop time	max. length (m)	latitude	Longitude
1	2001.5.18	8:35	8:56	600	30-45N	146-25E
2	2001.5.18	12:40	13:02	600	31-00N	146-25E
3	2001.5.19	5:04	5:24	600	31-45N	146-25E
4	2001.5.19	8:41	9:14	1050	32-00N	146-25E
5	2001.5.19	14:23	14:53	1000	32-15N	146-25E
6	2001.5.20	5:35	6:06	1000	33-00N	146-25E
7	2001.5.20	10:26	10:57	1000	33-15N	146-25E
8	2001.5.26	8:13	8:45	1000	36-00N	146-25E

Table 8.7.2 Sampling list of the grid with two impactors.

No.	date(JST)	start time	stop time	latitude(N)	longitude(E)	Place	case No.
1	2001.5.13	11:05	11:15	35-16	139-40	Compass	1,31
2	2001.5.14	12:40	12:50	34-43	140-15	Compass	2,32
3	2001.5.14	20:09	20:19	34-08	142-30	Compass	3,33
4	2001.5.15	8:15	8:15	33-20	146-29	Compass	4,34
5	2001.5.15	13:22	13:32	33-01	148-07	Compass	5,35
6	2001.5.15	20:15	20:25	32-34	150-06	Compass	6,36
7	2001.5.16	7:03	7:13	32-07	152-28	Compass	7,37
8	2001.5.16	17:47	17:57	31-50	151-04	Compass	8,38
9	2001.5.17	8:32	8:42	30-20	147-16	Compass	9,39
10	2001.5.18	9:30	9:40	30-44	146-24	Compass	10,40
11	2001.5.18	9:30	9:40	30-44	146-24	600m	11,41
12	2001.5.18	13:38	13:48	31-00	146-24	Compass	12,42
13	2001.5.18	13:38	13:48	31-00	146-24	600m	13,43
14	2001.5.19	5:55	6:05	31-45	146-24	Compass	14,44
15	2001.5.19	5:55	6:05	31-45	146-24	600m	15,45
16	2001.5.19	10:07	10:17	31-59	146-24	Compass	16,46
17	2001.5.19	10:07	10:17	31-59	146-24	1050m	17,47
18	2001.5.19	15:50	16:00	32-15	146-23	Compass	18,48
19	2001.5.19	15:50	16:00	32-15	146-23	1050m	19,49
20	2001.5.20	6:55	7:05	32-59	146-30	Compass	20,50
21	2001.5.20	6:55	7:05	32-59	146-30	1000m	21,51
22	2001.5.20	11:45	11:55	33-15	146-27	Compass	22,52
23	2001.5.20	11:45	11:55	33-15	146-27	1000m	23,53
24	2001.5.23	8:47	8:57	34-31	146-22	Compass	24,54
25	2001.5.24	15:45	15:55	34-05	146-28	Compass	25,55
26	2001.5.25	15:25	15:35	35-05	146-21	Compass	26,56
27	2001.5.26	9:30	9:40	35-59	146-25	Compass	27,57
28	2001.5.26	9:30	9:40	35-59	146-25	1000m	28,58
29	2001.5.26	18:12	18:22	36-30	146-25	Compass	29,59
30	2001.5.27	8:20	8:30	37-59	146-24	Compass	30,60
31	2001.5.27	15:35	15:45	39-15	144-59	Compass	61,62

8.8 Lidar observations of aerosol and clouds

(1) Personnel

Nobuo Sugimoto, Ichiro Matsui, Atsushi Shimizu (National Institute for Environmental Studies), Kazuhiro Asai (Tohoku Institute of Technology)

(2) Objectives

Objectives of the observations and experiments in this cruise are

- to study distribution and optical characteristics of dust and other aerosols using a two-wavelength dual polarization lidar,
- to study microphysical parameters of ice clouds and thin water clouds with the combination of the lidar and the cloud profiling radar,
- to study a new polarization bistatic lidar method for measuring cloud particle size of lower water clouds.

(3) Measured parameters

- Vertical profiles of backscattering coefficient at 532 nm and 1064 nm.
- Vertical profile of depolarization ratio at 532 nm.

(4) Method

Vertical profiles of aerosols and clouds were measured with a two-wavelength dual polarization lidar. The lidar employs a Nd:YAG laser as a light source which generates the fundamental output at 1064 nm and the second harmonic at 532 nm. Transmitted laser energy is typically 100 mJ per pulse at 1064 nm and 50 mJ per pulse at 532 nm. The pulse repetition rate is 10 Hz. The receiver telescope has a diameter of 25 cm. The receiver has three detection channels to receive the lidar signals at 1064 nm and the parallel and perpendicular polarization components at 532 nm. An analog-mode avalanche photo diode (APD) is used as a detector for 1064 nm, and photomultiplier tubes (PMTs) are used for 532 nm. The detected signals are recorded with a digital oscilloscope and stored on a hard disk with a computer. The lidar system was installed in a 20-ft container with the cloud profiling radar (CPR) of the Communications Research Laboratory (CRL). The container has a glass window on the roof, and the lidar was operated continuously regardless of weather.

The experiment on the bistatic lidar method was performed with an additional receiver installed at a distance of 14 m from the lidar transmitter. The bistatic receiver detects backscatter from the lower clouds at a scattering angle of about 179 deg. Clouds particle size is derived from the ratio of signal intensity of two polarization components.

(5) Results

Figure 8.8-1 shows the quick-look time-height indication of the range-corrected signal during the cruise.

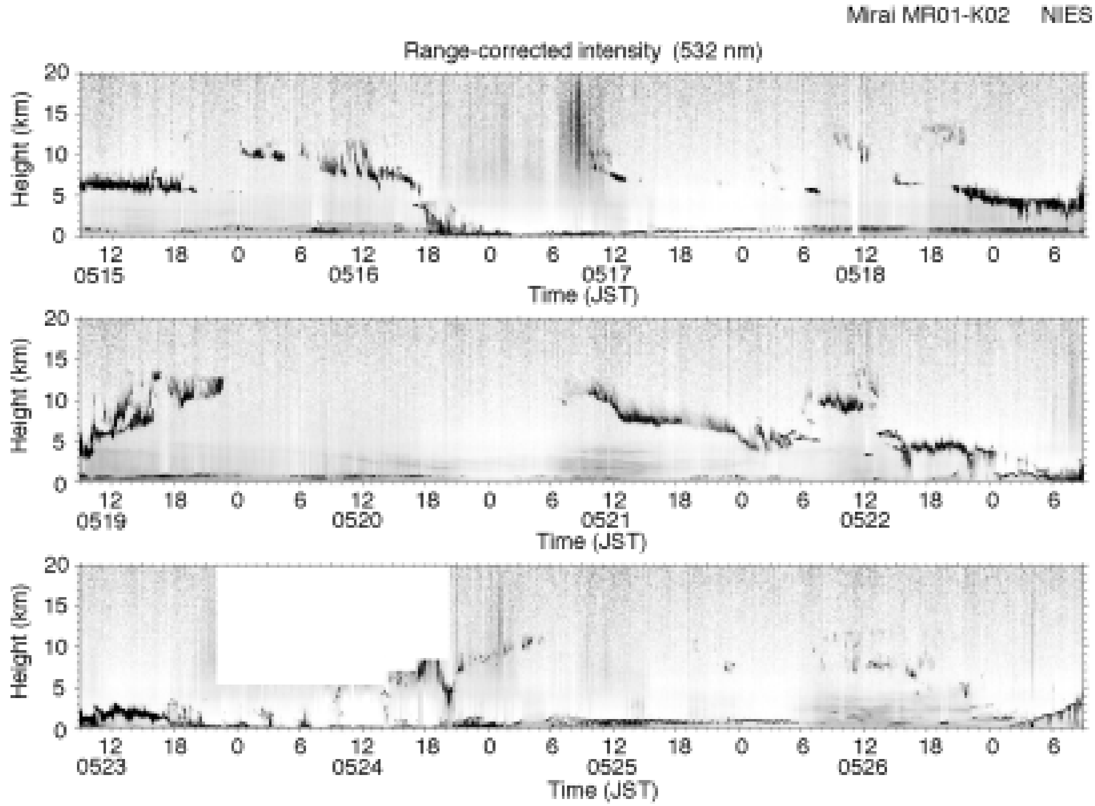

Figure. 8.8-1 Range-corrected signal at 532 nm.

Various types of clouds are observed. Structures accompanied by warm front and cold front are seen on May 22-23 and 24, respectively. Rain from the melting layer at about 4 km altitude is seen on May 22 and 24.

Notable features about aerosols are the layers observed during May 19-22, and on May 26. The depolarization and two-wavelength data show that the upper part (> 2km) of the plume observed during 8:00-15:00 of May 21 is mostly dust aerosols. The lower part is mostly sulfate or other small spherical aerosols. The aerosol layers observed on May 26 are mostly dust. But the high-density part observed at 10:00-14:00 below 2 km is not dust.

The experiment on the bistatic lidar was performed on May 19, 20 and 25. The result of the preliminary analysis shows that there is difference between convective cumulus and stratus in spatial distribution of particle size in the cloud.

(6) Data archive

- raw data
  - lidar signal at 532 nm (parallel polarization)
  - lidar signal at 532 nm (perpendicular polarization)
  - lidar signal at 1064 nm
  - period 05140738-05272400 (UTC), continuous
  - temporal resolution 10 sec.
  - vertical resolution 6 m.
- processed data
  - cloud base height, apparent cloud top height, cloud phase
  - cloud fraction
  - boundary layer height (aerosol layer upper boundary height)
  - backscatter coefficient of aerosols

depolarization ratio

8.9 Observation of clouds by 95GHz cloud profiling radar (CPR)

Akihide Kamei1), Hajime Okamoto2), Hiroaki Horie1), Sachiko Mutsuga1), Hiroshi Kuroiwa1), and Hiroshi Kumagai1)
1) Communications Research Laboratory, 2) Tohoku University

Objectives

Clouds are known to affect primarily the energy and water cycle in the climate system. However, their interactions with aerosols, with many chemical particles in the atmosphere, and with the radiative energy transfer are still not understood. For Mirai MR01-K02 cruise, we work for studying vertical distribution and microphysics of clouds and aerosols by using cloud profiling radar (CPR) of Communications Research Laboratory (CRL) in collaboration with the lidar systems of National Institute for Environmental Studies (NIES). One of the great advantages in the active remote sensing is that these sensors provide cloud boundaries with high accuracy. The basic elements of observations are cloud boundaries, cloud microphysics such as effective radius and ice/liquid water content (IWC/LWC), fall velocity of the cloud particles, depolarization (non-sphericity), and vertical distribution of aerosols. In addition, for this cruise, we expect to study longitudinal and latitudinal distribution of clouds and aerosols over Pacific Ocean near Japan. These data sets will also contribute to the APEX project directed by Prof. Teruyuki Nakajima (University of Tokyo) in a way that comparing these data sets with the modeling and satellite data should bring a breakthrough for the cloud-aerosol interaction studies.

Measured parameters

CRL has developed an airborne W-band CPR named SPIDER operating at 95GHz. For the cruise of Mirai vessel, the CPR system was modified to be suitable for shipborne measurements (Fig. 8.9-1). The CPR was operated in the vertical pointing mode and measured backscattering intensity of cloud particles by dual polarization. The radar measurements provide radar reflectivity factor, Doppler velocity, and linear depolarization ratio (LDR) in the vertical direction. (The lidar measurements provide backscattering coefficients in the vertical direction.) The microwave radiometer with dualfrequencies (23.8GHz and 31.4GHz) was also installed. This provides water vapor amounts and liquid water paths of water clouds.

Method

The CPR and the lidar system were co-located inside the same container on the upper deck of Mirai. Thus it is possible to perform radar/lidar algorithm to retrieve vertical profiles of effective radius and ice/liquid water content of ice and thin water clouds. The combination of the CPR and the microwave radiometer is used to retrieve cloud droplet effective radius and liquid water content of thick water clouds. Since the lidar instrument has a capability to detect aerosol signals, we might expect to study cloud-aerosol interactions. These studies will bring significant progress in our understandings of a role of clouds in relation to the cloud feedback processes and climate impact of anthropogenic aerosols through the cloud-aerosol interaction processes.

Results

Figure 8.9-2 shows a time-altitude cross-section of the received power observed by the CPR on 22 May 2001. The vertical axis indicates altitude between 0 and about 12km with every 82.5m range resolution. The horizontal axis denotes time (JST). Mirai was on a voyage to the north around 33oN and 146oE at that time.

Data archive

The CPR operation started from 14 May 2001 and has continued almost all day to 28 May 2001 unless it was clear sky or bad weather (Fig. 8.9-3). The basic operating parameters for CPR measurements are listed in Table 1. Observation data will be available after the data reduction for level 1 products.

Fig. 1: 95GHz cloud profiling radar for shipborne measurement.

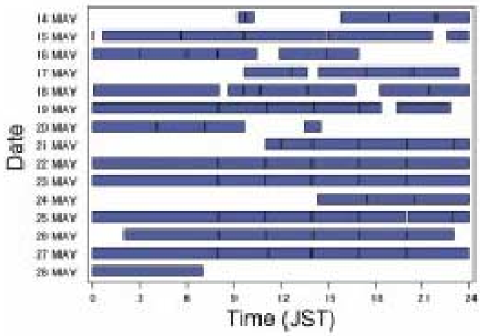

Fig. 3: Circumstance of data acquisition by CPR observations.

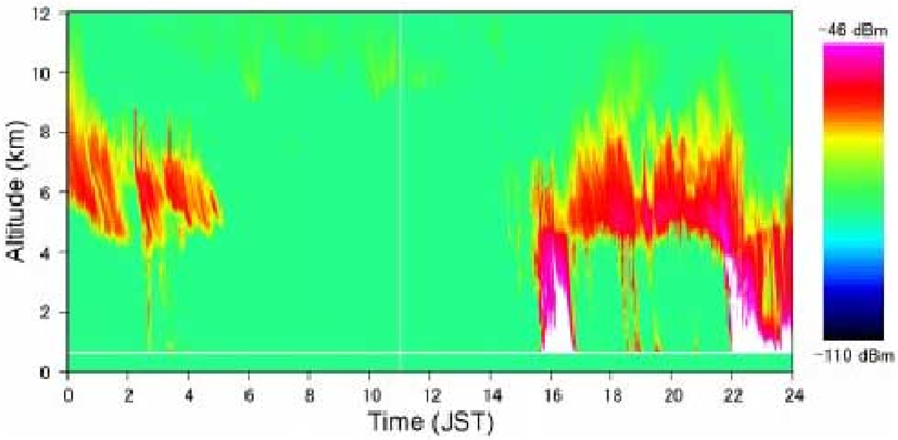

Fig. 2: The radar signals scattered from clouds for CPR observations on 22 May 2001.

Table 1. Basic operating parameters for CPR measruements

Mode	PPMAG4	PPMAG4
Pulse Width (nsec)	1100	2125
Filter (MHz)	1.0	0.5
Polarized Wave	HHVV	HHVV
Doppler	cc, cc, cc	cc, cc, cc
Pulse Spacing Time (μsec)	110, 110, 110, 7670	220, 220, 220, 4340
Number of Noise Samples	8	8
Number of Range Gates	144	73
Gate Spacing (m)	82.5	162.5
Range Gate Delay (m)	150	150
Maximum Range (m)	12030.0	12012.5
Average Number	56	108
External Average	1	1
Acquisition Time (msec)	448	540